PH.D DISSERTATION

Multiple Antenna-based GPS Multipath Mitigation using Code Carrier Information

By
Jin Ik Kim

August 2013

DEPARTMENT OF ELECTRICAL AND COMPUTER ENGINEERING
SEOUL NATIONAL UNIVERSITY

Multiple Antenna-based GPS Multipath Mitigation using Code Carrier Information

코드 케리어 정보를 이용한 다중 안테나 기반 GPS 다중경로오차 감쇄

지도교수 최 진 영

이 논문을 공학박사 학위논문으로 제출함

2013 년 8 월

서울대학교 대학원

전기공학부

김 진 익

김진익의 공학박사 학위논문을 인준함

2013 년 8 월

위 원 장 : _____

부위원장 : _____

위 원 : _____

위 원 : _____

위 원 : _____

공학박사학위논문

Multiple Antenna-based GPS Multipath Mitigation using Code Carrier Information

코드 케리어 정보를 이용한 다중 안테나 기반 GPS 다중경로오차 감쇄

2013 년 8 월

서울대학교 대학원

전기공학부

김 진 익

Multiple Antenna-based GPS Multipath Mitigation using Code Carrier Information

Jin Ik Kim

Ph.D. Dissertation

Department of Electrical
& Computer Engineering
Seoul National University

August 2013

To my parents

Abstract

Multiple Antenna-based GPS Multipath Mitigation using Code Carrier Information

Jin Ik Kim

Department of Electrical and Computer Engineering
Seoul National University

Although hundreds of millions of receivers are used all around the world, the performance of location-based services(LBS) provided by GPS is still compromised by interference which includes unintentional distortion of correlation function due to multipath propagation. For this reason, the requirement for proper mitigation techniques becomes crucial in GPS receivers for robust, accurate, and reliable positioning.

Multipath propagation can easily occur when environmental features cause combinations of reflected and diffracted replica signals to arrive at the receiving antenna. These signals which are combined with the original line-of-sight (LOS) signal

can cause distortion of the receiver correlation function and ultimately distortion of the discrimination function; hence, errors in range estimation occur. Therefore, multipath error in the satellite navigation system to improve location accuracy is an important issue to be addressed.

Recently, interference mitigation techniques utilizing multiple antennas have gained significant attention in GPS navigation systems. Although at the time of this dissertation, employing multiple antennas in GPS applications is mostly limited to academic research and possibly complicated military applications, it is expected that in the near future, antenna array-based receivers will also become widespread in civilian commercial markets. Rapid advances in antenna design technology and electronic systems make previously challenging problems in hardware and software easier to solve. Furthermore, due to the significant effort devoted to miniaturization of RF front-ends and antennas, the size of antenna array based receivers will no longer be a problem.

Given the above, this dissertation investigates multiple antenna-based GPS the interference suppression and multipath mitigation. Firstly, a modified spatial processing technique is proposed that is capable of mitigating both high power interference and coherent and correlated GPS multipath signals. The use of spatial-temporal processing for GPS multipath mitigation is studied. A new method utilizing code carrier information based on multiple antennas is proposed to deal with highly

correlated multipath components and to increase the signal to noise ratio of the beamformer by synthesizing antenna array processing.

In order to verify the proposed method, a software defined GPS receiver is used. Software-based GPS signal processing technique has already produced benefits for prototyping new equipment and analyzing GPS signal quality. Not only do such receivers provide an excellent research tool for GPS algorithm verification, they also improve GPS receiver performance in a wide range of conditions.

In this dissertation, the enhancement of the proposed method is presented in terms of the simulations and software defined GPS receiver using simulated IF data. From the result, the proposed method is robust to interference suppression, and multipath mitigation, and shows a strong possibility for use in improving location accuracy. Thus, this method can be employed to mitigate interference signals in vehicular navigation applications.

Keywords: Global Positioning System, Multipath, Code carrier information, Multiple antennas, Beamformer, Software-defined GPS receiver

Student Number: 2008-30220

Acknowledgements

I wish to express my deepest gratitude to my mentor, *Prof. Jang Gyu Lee*, who have supervised me and showed me the marvelous world of navigation. My special thanks go to the dissertation committee members, who made this work possible, namely *Prof. Jin-Young Choi*, *Prof. Kwang-Bok Lee*, *Prof. Kyoung-Mu Lee*, *Prof. Gyu-In Jee*, *Prof. Hyung-Keun Lee*. Finally, I would like to thank all of the NGC laboratory members for sharing good and bad times during my doctoral study.

Contents

List of Figures

List of Tables

Chapter 1
Introduction

1.1 Introduction

Despite the continually increasing demand for accurate and reliable global positioning system (GPS) dependent services, one of the main drawbacks of GPS signals is their susceptibility to interference. Interference ranges from unintentional distortion due to multipath propagation. Generally, the multipath decreases the effective signal-to-noise ratio (SNR) of received satellite signals such that a receiver may not be able to measure the true values of pseudoranges and carrier phases. Therefore, even a low-level multipath signal can easily reject GPS services.

Interference can generally be detected and suppressed by using time, frequency and spatial domain processing or a combination of these. Time/frequency narrowband multipath detection and suppression methods have been widely used and reported in the GPS research. However, their performance degrades when dealing with wideband interference or rapid changes of interference center frequency. On the other hand, interference mitigation techniques utilizing an antenna array can effectively detect and suppress both narrowband and wideband interfering signals regardless of their time and frequency characteristics.

Rapid advancements in electronic systems and antenna technology are facilitating powerful antenna array based solutions to further enhance the performance of GPS receivers in terms of signal to interference-plus-noise ratio (SINR). This chapter begins with a brief introduction of the GPS multipath and interference, mitigation strategies, and multiple antenna-based processing. These constitute the motivation for this research. The chapter then discusses the objectives and contributions of this dissertation and finally provides an outline for the dissertation.

1.2 Background and Motivation

Positioning and timing systems such as GPS are widely used in our everyday lives. Currently, most mobile phones and vehicle applications are equipped with GPS receivers. GPS applications can be found in rescue service, tracking of animals and vehicles, air navigation, marine and ground transportation, criminal offender surveillance, police and rescue services, timing synchronization, surveying, electrical power grids, space installations, and agricultural services etc. In fact, GPS now affect many aspects of our daily lives. However, GPS signals are vulnerable to interference because the received signals are extremely weak. For instance, GPS includes satellites orbiting at approximately 20,000 km above the earth, transmitting signals which are received on the earth's surface with a power of approximately -158.5 dBW for L1 C/A

and -160 dBW for L2 (Kaplan & Hegarty 2006). Such signals have spectral power densities far below that of the thermal noise (for L1 C/A signal, 16.5 dB below the noise floor for a receiver with a 2 MHz bandwidth). Even though the despreading process performed in both the acquisition and tracking operations raises these signals above the background noise, they are still susceptible to interference. The spread spectrum technique applied in the GPS signals provides a certain degree of protection against interference for narrowband interfering signals and the multipath (Pickholtz et el 1982); however, the spreading gain alone is not sufficient to avoid interference when the power of the interference is much stronger than the GPS signal power or to mitigate non-resolvable multipath components.

GPS interference can be classified into two groups: intentional and unintentional interference. Intentional interference can be generated by GPS jammers (e.g. by a transmission of a strong continuous wave (CW) signal or a strong Gaussian noise in GPS frequency bands). Unintentional interference can be generated by a variety of electronic devices working in their non-linear region (in order to emit strong electromagnetic signals in GPS frequency bands) or from broadband communication systems such as television and radio broadcasting stations which also have harmonics in GPS frequency bands (Borio 2008). Considering bandwidth, interfering signals can be categorized into narrowband and wideband. In the case of narrowband interference, only a small portion of the GPS frequency bands is affected whereas wideband

interference almost occupies the entire frequency band. For example, CW interference is a narrowband interfering signal and Gaussian noise jammers produce wideband interfering signals.

Significant advances in electronic technology have been made over the past few decades. However, these rapid changes have also generated a number of drawbacks that influence GPS. In recent years, low cost GPS jammers such as personal privacy devices (PPDs) have become available. The main target of these devices is to disturb GPS receivers within a radius of a few meters; however, this is not always possible due to the poor quality of the electronic elements used in PPDs. For example, it has been observed that these jammers can dangerously affect the GPS receivers and wide area augmentation systems (WAASs) employed in air navigation (Grabowski 2012). Therefore, interference not only degrades the performance of GPS receivers, but can also seriously risk the security and safety of human life. This makes GPS interference detection and mitigation a high research and development priority in the navigation field. The different types of interference that adversely impact GPS are presented in Table 1.1.

From the perspective of this dissertation, the interfering signals shown in Table 1.1 are categorized into three groups: “strong narrowband and wideband interference”, “multipath”, and “spoofing signals”. The first group includes any high power interfering signal that is not correlated with GPS signals such that it is spread during

the acquisition and tracking stages in a GPS receiver.

Therefore, this type of interference can be more conveniently detected and mitigated before despreading. On the other hand, multipath signals are inherently correlated with the GPS signals. Although long-delay or resolvable multipath signals are essentially suppressed during the despreading process, non-resolvable or short delay signals may significantly degrade the performance of receivers. The last group encompasses spoofing signals that mimic the authentic GNSS signals.

Table 1.1 Types of Interference and Typical Sources (Kaplan & Hegarty 2006)

Types of Interference		**Typical sources**
Narrowband	Continuous wave	Intentional sinusoidal jammers or near-band unmodulated transmitter's carriers
	Swept continuous wave	Intentional CW jammers or frequency modulation (FM) transmitter's harmonics
	Phase/frequency modulation	Intentional chirp jammers or harmonics from an amplitude modulation (AM) radio station, citizens band radio or amateur radio transmitter
Wideband	Band-limited Gaussian	Intentional matched bandwidth noise jammers
	Phase/frequency modulation	Television transmitter's harmonics of near-band microwave link transmitters
	Matched spectrum	Intentional matched spectrum jammers or nearfield of pseudolites
	Wide-band-pulse	Any type of burst transmitters such as radar or ultra wide band (UWB)
	Multipath	Reflection, diffraction and diffusion of signals off nearby objects
	Spoofing signal	spoofer structured to resemble a set of counterfeit GNSS signals to mislead receivers

They are therefore correlated with the GPS signals as well as the multipath. However, their navigation bits differ and their ranges are intelligently controlled. A spoofing signal includes several counterfeit pseudo random noise (PRN) codes which carry false time and position solutions to deceive receivers.

The main objective of this dissertation is to introduce new methods for suppressing interference and multipath signals based on multiple antennas processing. The mitigation approaches currently studied in the literature are briefly introduced in the following subsections.

1.2.1 Strong Narrowband and Wideband Interference

Generally, interference can be suppressed using either time, frequency, or spatial domain processing, or a combination of these. Interference suppression methods based on time and frequency processing have been broadly studied in the literature; however, the performance of these methods degrades when they encounter wideband interference (e.g. Gaussian jammers or harmonics from television transmissions) or when interfering signals change rapidly in time or frequency. On the other hand, interference mitigation techniques utilizing multiple antennas can effectively suppress narrowband and wideband interference signals independent of their time and frequency characteristics. Herein, strong narrowband and wideband interference is referred to as

any unnecessary radio frequency (RF) signal such as tones, swept waveforms, pulse and broadband noise, and any other multi-frequency and time-varying version thereof (Poisel 2004). Such narrowband and wideband interference is referred to as ‘strong’ when they have sufficient power to adversely affect on the receiver performance even after despreading and Doppler removal. In fact, in the context of array processing, all these interfering signals are considered as narrowband plane waves, provided the reciprocal of a maximum propagation delay across the array is much greater than the signal bandwidth (Van Trees 2002). This is explained in the following chapter. Therefore, regardless of the characteristics of these interfering signals, they can be suppressed by applying a proper spatial filter.

1.2.2 Multipath

Another type of interference in GPS applications is caused by multipath propagation. This phenomenon in outdoors environments is mostly caused by the reflection and diffraction of the signals off nearby objects such as buildings, mountains, trees and so on. Such a phenomenon can occur in outdoor situations as those depicted in Fig. 1.1. Although the spread spectrum technique is also resistant to multipath, it is only able to mitigate the resolvable multipath components of which the delays are more than 1.5 chip duration. The multipath may cause significant errors in pseudorange

measurements (e.g. for L1 C/A, up to 100 m). When the multipath results in one or more additional propagation paths which always have longer propagation time than the line of sight (LOS) signal and are the same as the LOS signal, their power density is far below the noise floor. This leads to the distortion of the correlation ambiguity function (CAF) and produces negative or positive biases on the pseudorange and carrier phase measurements depending of the received phases of the multipath components (Frrell 1999 & Kaplan 2006).

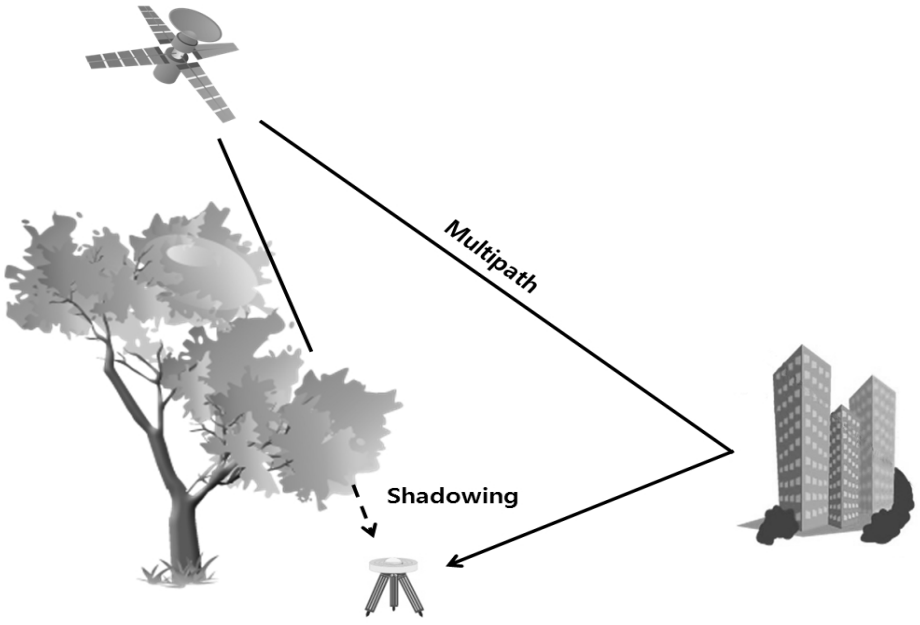

Figure 1.1 Outdoor multipath situations

Multipath propagation is generally modeled as specular or diffuse. In diffuse multipath scattering environments such as indoor settings, the magnitudes of the signals arriving by the various paths can be approximately modeled by a Rayleigh distribution (Rensburg & Friedlander 2004). On the other hand, in the specular multipath model, the multipath can be assumed as several deterministic replicas of the LOS signal with unknown delays and attenuation factors. This dissertation only focuses on mitigation strategies for specular multipath environments. Multipath signals should be considered as wideband interference since their power is dispread over the GPS frequency bands. However, due to the high correlation between these multipath signals and the LOS signal, in the acquisition and tracking stages, these signals are also despread, which causes the distortion of CAF and degradation of the receiver's performance. They may thus induce significant errors in pseudorange measurements. Therefore, the multipath should generally be mitigated after the despreading process. Multipath effects can be reduced in hardware, software or both parts of a GPS receiver. In hardware, the multipath can be mitigated by using a special antenna design such as a choke-ring to disguise the low elevation multipath signals and prevent the reflected signals from below the local horizon from reaching the antenna, or employing right hand circularly polarized (RHCP) antennas to at least suppress those multipath components that are reflected once. In term of the software, a large number of studies have been published that describe time-frequency domain algorithms; the most well-

known of these that have been widely implemented in commercial GPS receivers are correlation-based multipath mitigation methods (Irsigler & Eissfeller 2003, McGraw & Braasch 1999, Van Dierendonck et al 1992). Correlation-based methods that have been developed and studied over the years include the double-delta technique (Irsigler & Eissfeller 2003), the strobe correlator (Garin & Rousseau, 1997), the high resolution correlator (HRC) (McGraw & Braasch 1999), and the multipath estimation delay locked loop (MEDLL) (Van Nee 1992, Townsend et al. 1995). Although correlation-based techniques achieve much better results than the conventional standard delay locked loop (DLL) in terms of multipath timing bias, they may fail to mitigate the effect of closely spaced multipath components or may fail to detect when a multipath component is stronger than the LOS signal. In these situations, the performance of GPS receivers degrades significantly and the timing synchronization may fail (Closas et al 2006). In general, the important shared property between most of these correlation-based techniques is that their stable lock point is at the maximum power of the correlation function (Townsend & Fenton 1994), regardless of how much this peak has been shifted with respect to the peak that corresponds to the actual LOS. On the other hand, multipath mitigation methods based on spatial processing are theoretically able to mitigate multipath components stronger than the LOS signal, regardless of how close the multipath components are to each other and to the LOS signal. Section 1.3.2 briefly reviews the research conducted on GPS multipath mitigation employing

multiple antennas.

1.3 Antenna Array Processing in GPS

A large and growing body of literature has investigated antenna array processing as a powerful tool for GNSS interference suppression (Lorenzo 2007 & Daneshmand 2013). This section provides a background on multiple antenna-based methods for mitigating GPS interference introduced in the previous section. Some previous work and associated limitations for interference mitigation using multi-antenna processing are briefly described.

1.3.1 Interference Suppression

Multi-antenna processing in GPS applications has been widely used for interference suppression (Amin & Sun 2005, Amin et al 2004, Fante & Vaccaro 2000, Brown & Gerein 2001, e.g. Fante & Vaccaro 1998a, Fante & Vaccaro 1998b, Zoltowski & Gecan 1995). Zoltowski & Gecan (1995) suggest utilizing minimum power distortionless response (MPDR) beamforming for GPS applications to reject interference signals of which the power is significantly higher than that of GPS signals, these being below the noise floor. Amin & Sun (2005) and Sun & Amin (2005a) exploited the periodicity of

GPS signals and highlighted the usefulness of eigenvector beamformers for GNSS applications. In their proposal, instead of the conventional subspace beamformer, which projects the received signal onto the signal subspace, the received signal is projected onto the noise-plus-GPS signal subspace. Received signals will then be enhanced such that the beamformer maximizes the desired signal to interference-plus-noise ratio (SINR). Despite the effectiveness of multiple antenna-based methods, they suffer from hardware is very complex. Considering that the number of antennas determines the number of undesired signals that can be mitigated, the limitation on the number of antennas, and size and shape of the array can be considered as the main problem for these methods. To deal with this problem, techniques employing both time/frequency and spatial domain processing such as space-time adaptive processing (STAP) and space-frequency adaptive processing (SFAP) previously employed for radar and wireless applications have been studied and developed for GPS as well in the literature (e.g. Gupta & Moore 2004, Fante & Vaccaro 2002, Myrick et el 2001, Hatke 1998). These methods combine spatial and temporal filters to suppress more radio frequency interfering signals by increasing the degree of freedom without physically increasing the antenna array size. However, a number of considerations are required in designing a space-time filter in order to prevent distortions in pseudorange and carrier phase measurements. The term “adaptive” is employed as opposed to “deterministic” and means that the filter follows the changes in the environment and constantly adapts

its own pattern by means of a feedback control. While studying adaptive methods is outside the scope of this dissertation, moving antenna arrays and synthetic array processing are other solutions to increase the degree of freedom (DOF) without increasing the number of physical antenna elements (Daneshmand 2013). Recently, antenna motion in the form of synthetic antenna array processing has been utilized to augment the correlation matrix for the purpose of angle of arrival estimation, multipath mitigation, and other applications (Daneshmand et al. 2013b, Broumandan et al. 2008, Draganov et al. 2011).

1.3.2 Multipath Mitigation

Much work has been carried out in the context of multipath mitigation using multi-antenna processing in GPS applications, Seco-Granados et el. (2005) and Brown (2000) studied the maximum likelihood (ML) criterion in order to mitigate multipath components. Seco-Granados et el. (2005) modeled an equivalent zero-mean Gaussian noise that includes the contribution of all undesired signals such as reflections, interferences, and thermal noise and then applied the ML function to this model. Therefore, a simple model for interference is obtained at the expense of a mismatch with the actual interface model. Brown (2000) applied the ML function to estimate the amplitude, delay, and direction of multipath components. Sahmoudi & Amin (2007)

developed the Capon beamformer to deal with the multipath when the steering vector, delay, and amplitude of multipath components are known. These assumptions may not be realistic in practice for some applications. Another group of methods first finds the direction of multipath components by direction finding (DF) methods such as the multiple signal classification (MUSIC) algorithm and then places nulls in these directions (e. g. Moelker 1997), which may be computationally complex in some applications. The most significant difficulty for multipath mitigation is the high degree of correlation between the LOS signal and multipath components; the conventional antenna array processing techniques therefore fail to cope with multipath propagation. The correlation between the LOS signal and the undesired signals causes the signal cancelation phenomenon and the rank deficiency of the temporal correlation matrix (Van Trees 2002). In other words, steering the beam pattern in the direction of the LOS signal and simultaneously suppressing the highly correlated multipath components in other directions requires special considerations. To deal with this problem, code carrier information has been included in the literature. These methods can be used with a serial subspace projection method to estimate multipath signal spatial signature vectors. This is explained later in the following chapter.

1.4 Software-Defined GPS Receiver

The design of a hardware receiver has limited flexibility. Once the receiver is designed, the user has limited options in the radio frequency (RF) tuning and digital signal processing (DSP) portions. This limitation can be overcome by the utilization of software-based receivers. The application of the software receiver approach (also known as the software-defined radio approach) on GPS receivers has definite advantages for the algorithm designer, and the receiver architect when testing the performance of various implementations. The advantage of the ease and flexibility of their reprogramming means they can be produced more rapidly and the debugging and hardware costs are reduced. The software radio approach applied to GPS receivers was first presented in 1996, by Thor and Ako.

Nowadays, GPS software receivers can be grouped into three main categories as shown in Fig. 1.2. The majority of receivers are definitely found in the post-processing subgroup “algorithm prototyping”, which refers to the sometimes countless number of small software tools or lines of code that are developed to test a new algorithm. If the algorithm were tested with a real (or realistic) signal, one could already possibly speak of a software receiver. Another typical application of a postprocessing software receiver is GPS signal analysis, such as that used to investigate GPS satellite failures or to decrypt unpublished GPS codes. However, the GPS software receiver boom actually

started with the development of real-time processing capability. This was first accomplished on digital signal processing (DSP) and later on a conventional personal computer (PC). Today DSPs have been partially replaced by specialized processors for embedded applications, that have different features (Lachapelle & Korniyenko 2008).

The third category of GPS software receivers, FPGA-based receivers, is sometimes also programmed in a C-like language. As they can be reconfigured in the field, they can also be referred to as software receivers. Their overall design significantly differs to other PC-based and embedded GPS software receivers. In this dissertation, the performance of the proposed interference and multipath mitigation method will be verified by using a software-defined GPS receiver.

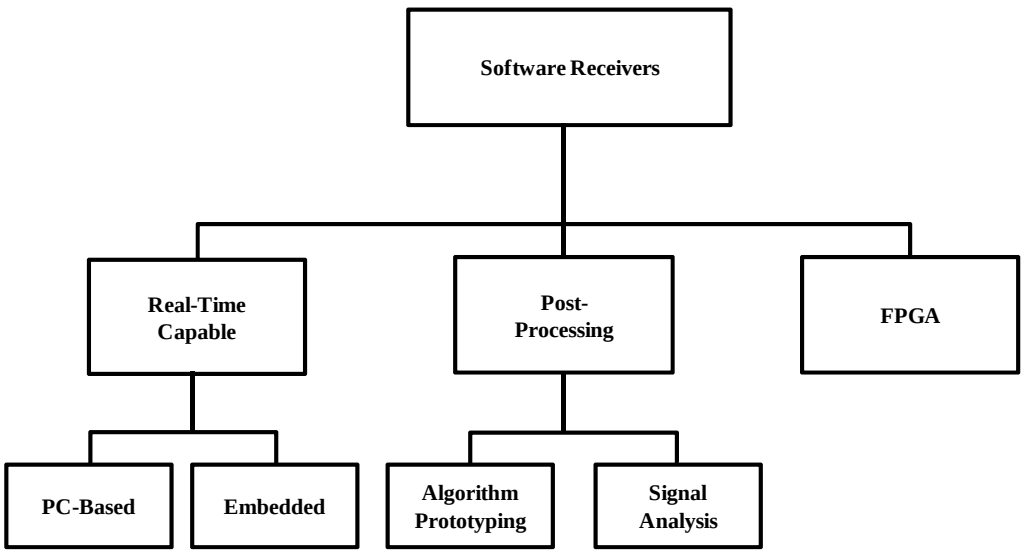

Figure 1.2 Different categories of software receivers

1.5 Objective and Contribution

The main goal of this dissertation is to investigate the use of multiple antenna-based processing to suppress different types of interferences. Herein, interference refers to strong narrowband and wideband interfering signals, which are GPS multipath components. This dissertation examines how spatial processing can be employed to deal with the interfering signals that are correlated with the LOS signal such as multipath signal components.

Given the primary objective, the main contributions of this dissertation are as follows:

1. A general scheme of a beamformer for dealing with both high power interference and multipath signal is proposed.

2. In order to mitigate interference and the multipath, a serial subspace projection that is based on the code carrier information is proposed.

3. In the suggested method, the code carrier information is applied to estimate the multipath signal spatial signature vectors.

4. Afterwards, in a constraint optimization problem, an optimal gain vector is

obtained to maximize the SNR of the desired signal, whereby it suppresses the interference and multipath signals.

5. As a software receiver analysis tool, the proposed beamformer is very helpful to estimate the interference and multipath subspace and completely nullify the interference and multipath signals.

6. For comparison with the proposed beamformer, the conventional MVDR beamformer and eigen-vector beamformer are considered under realistic environments.

With these contributions, the proposed beamforming methodology has a good structural advantage in interference suppression and multipath mitigation. Thus, this method can be employed in vehicular navigation applications operating in urban environments.

1.6 Dissertation Outline

This dissertation consists of six chapters and two appendices.

Chapter 1 states the problem to be investigated and researched during the course of this dissertation. It describes the relevant background of the research to position the current research topic within the current field, and briefly discusses some of the important relevant literature. The objective of this dissertation is then described.

Chapter 2 briefly describes the Global Positioning System and explains its different components. The GPS concept and position determination is then reviewed and the various error sources in GPS measurements are discussed.

Chapter 3 introduces background knowledge for the antenna array processing technique and the signal model received by an antenna array in the presence of interference. This is followed by a brief review on conventional optimization methods for designing a beamformer. Finally, space-time processing is introduced as an approach for enhancing interference mitigation capability of an antenna array.

Chapter 4 describes the core algorithm leading to interference suppression and multipath mitigation for the code and carrier using multiple closely-spaced antennas. It derives the formulation of a mitigation algorithm; a serial subspace projection is employed. In order to estimate multipath signal spatial signature vectors, code carrier information is introduced. A beamforming algorithm is applied to maximize the signal

to noise ratio. Numerous simulations are carried out and described to analyze the receiver's synchronization capability, correlation ambiguity function (CAF) and RMS error using a two-ray model.

Chapter 5 briefly introduces GPS software-defined receiver (SDR) methodology. To verify the performance of the proposed method, a realistic GPS IF data which consists of GPS C/A-code signals as well as interference and multipath signals is generated and applied to a software-defined GPS receiver. The performance verification is expressed by SNR loss, height error and 2-dimensional positioning errors. For comparison with the proposed method, a conventional MVDR deamformer, an eigen-vector beamformer and the proposed beamformer method are described.

Chapter 6 summarizes the research described in the earlier chapters of this dissertation. The drawbacks of the developed technique are then identified and recommendations for further research are presented.

Chapter 2
Global Positioning System

2.1 GPS System Overview

GPS consists of three major segments, including control, and user segments. The space segment consists of GPS satellites. The GPS operational constellation comprises 24 satellites arranged in 6 orbital planes with 4 satellites per plane. The orbits are nearly circular with inclination angles of 55 degrees and radii of approximately 20,200 km. The six orbits are equally spaced around the equator, resulting in 60 degree separation. This constellation ensures that a user located anywhere on the globe has a direct line of sight to at least four satellites at any time.

The control segment is responsible for monitoring the health and status of the space segment. The control segment consists of a system of tracking stations located around the world, including six monitor stations, four ground antennas, and a master control station, as given in Table 2.1. The ground monitoring stations measure signals from the SVs that are transmitted to the master control station. The master station determines the orbital model and the clock-correction parameters for each satellite. These parameters are related to the ground antennas for transmission to the satellites for broadcasting to the user segment (Strang, Gilbert 1997 & Kaplan 2006).

The user segment consists of antennas and receiver-processors that measure and decode the satellite transmissions to provide positioning, velocity, and precise timing information to the user. Since the user receiver operates passively (i.e., it does not transmit any signals), the GPS space segment can provide service to an unlimited number of users. It is important to note that the GPS system is a line-of-sight system. If the path between the receiver and a satellite is obstructed, then the satellite signal will not be received.

Each GPS satellite transmits ranging codes and navigation data by using code-division-multiple-access (CDMA) on the same two carrier frequencies, L1 (1575.42

Table 2.1 Location of the Components of the Operation Control Segment

Master control station	Falcon Air Force Base, Colorado Springs
Master control station(backup)	Gaithersburg, MD
Monitoring station	Falcon Air Force Base, Colorado Springs
Remote monitoring station	Canaveral, FL
Remote monitoring station	Hawaii
Remote monitoring station	Ascension Island
Remote monitoring station	Diego Garcia
Remote monitoring station	Kwajalein
Ground antenna	Canaveral, FL
Ground antenna	Ascension Island
Ground antenna	Diego Garcia
Ground antenna	Kwajalein

MHz) and L2 (1227.60 MHz). The carrier frequencies are modulated by speared-spectrum signals to carry information to the user. Three pseudorandom noise (PRN) ranging codes are associated with each satellite. The C/A code modulates the L1 carrier phases. This code has a length of 1023 chips and a 1.023 MHz chip-rate, resulting in a period of 1 ms. A different C/A PRN code is used for each satellite and each C/A PRN code is nearly orthogonal to all other C/A PRN codes. Although all satellites broadcast on the same two frequencies, a GPS receiver is able to lock on to a particular satellite and discriminate between satellites by correlating an internally generated version of the C/A code of a satellite with the received signal, Since the C/A codes for each satellite are unique and nearly orthogonal, the cross-satellite interference is small. The GPS space vehicles are often identified by their unique PRN code number.

The precise (P) code modulates both the L1 and L2 carrier phases. The P code is very long, at 10.23 MHz PRN. In the anti-spoofing (AS) mode of operation, the P code is encrypted into the Y code. The encrypted Y code requires a classified AS module for each receiver channel and can only be used by authorized users with cryptographic keys.

The navigation message also modulates the L1 C/A code signal. The navigation message is a 50 bit/s signal consisting of data a bit decoded by a GPS receiver decodes into satellite orbit, clock correction, and other system parameters.

The GPS provides two levels of services: a standard-positioning service (SPS) and a

precise-positioning service (PPS). SPS is a positioning and timing service based on only the C/A code, which is available to all GPS users on a continuous, worldwide basis with no direct charge. This level of service is provided on the L1 frequency, which contains the C/A code and a navigation-data message. Predicable accuracy of the SPS is ~100 m (2 drms) horizontal, 156 m (95%) vertical, and 350 ns (95%) time (Kaplan 2006).

PPS is a more accurate positioning, velocity, and timing service which is only available only to a user authorized by the U.S. government. Access to this service is controlled by two techniques known as AS and selective availability (SA). SA is implemented by replacing the P code with the classified Y code. SA is implemented by purposefully degrading the satellite clock and ephemeris data available to the non-authorized user. The authorized user has the ability to access the Y code and remove the effect of SA. Predicable accuracy of PPS is 22 m (2 drms) horizontal, 27.7 m (95%) vertical and 200 ns (95%) time (Strang, Gilbert 1997 & Kaplan 2006). Full PPS operational capability was achieved in the spring of 1995.

2.2 Basic Concept of GPS

The position of a certain point in space can be found from the distance measured from this point to some known positions in space. Various examples to explain can be used to explain this point. In Fig. 2.1, the user position is on the x-axis, which is a one-dimensional case. If the satellite position S_1, and the distance to the satellite x_1 are both known, the user position can be at two places, either to the left or the right of S_1. In order to determine the user position, the distance to another satellite with a known position must be measured. In this figure, the positions of S_2 and x_2 uniquely determine the user position U.

Fig. 2.2 shows a two-dimensional case. In order to determine the user position, three satellites and three distances are required. The trace of a point with constant distance to a fixed point is a circle in the two-dimensional case. Two satellites and two distances give two possible solutions because two circles intersect at two points. A third circle is needed to uniquely determine the user position.

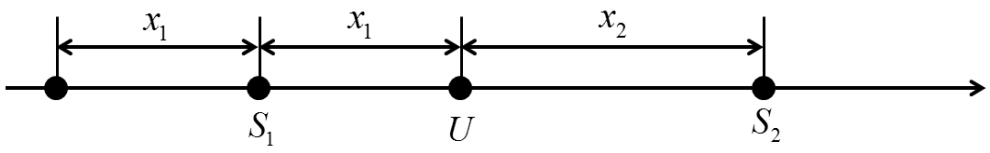

Figure 2.1 One-dimensional user position

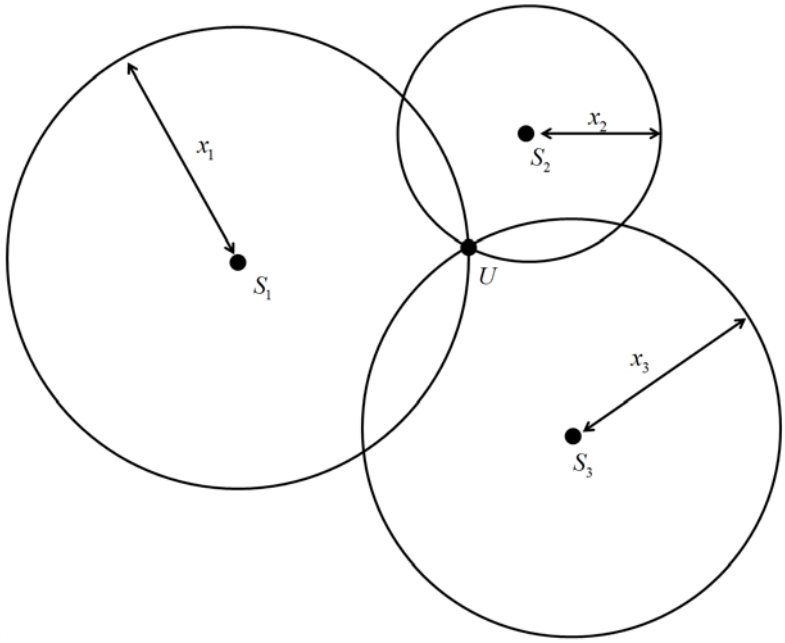

Figure 2.2 Two-dimensional user positions

For similar reasons, one might decide that in a three-dimensional case, four satellites and four distances are needed. The equal-distance trace to a fixed point is a sphere in a three-dimensional case. Two spheres intersect to make a circle. This circle intersects another sphere to produce two points. In order to determine which point is the user position, a further satellite is needed. In GPS, the position of the satellite is known from the ephemeris data transmitted by the satellite. One can measure the distance from the receiver to the satellite. Therefore, the position of the receiver can be determined (Kaplan 2006).

In the above discussion, the distance measured from the user to the satellite is

assumed to be very accurate and there is no bias error. However, the distance measured between the receiver and the satellite has a constant unknown bias, because the user clock usually differs from the GPS clock. In order to resolve this bias error, a further satellite is required. Therefore, in order to find the user position, five satellites are needed.

If four satellites and the measured distance with bias error are used to measure a user position, two possible solutions can be obtained. Theoretically, one cannot determine the user position. However, one of the solutions is close to the earth's surface and the other one is in space. Since the user position is usually close to the surface of the earth, it can be uniquely determined. Therefore, the general statement is that four satellites can be used to determine a user position, even though the distance measured has a bias error.

2.3 Determining Satellite to User

GPS satellite transmissions utilize direct sequence spread spectrum (DSSS) modulation (Frrell 1999 & Kaplan 2006). DSSS provides the structure for the transmission of ranging signals and essential navigation data, such as satellite ephemerides and satellite health. The ranging signals are PRN codes, whereby the binary phase shift key (BPSK) modulates the satellite carrier frequencies. These codes have a similar appearance and have similar spectral properties to those of random binary sequences, but are actually deterministic. These codes have a predictable pattern, which is periodic and can be replicated by a suitably equipped receiver. At the time of writing, each GPS satellite is broadcasting two types of PRN ranging codes.

Earlier, we examined the theoretical aspects of using satellite ranging signals and multiple spheres to solve user portioning in three dimensions. While that earlier example was predicted on the assumption that the receiver clock was perfectly synchronized to system time, in reality this is generally not the case. Prior to solving issues of three-dimensional user positioning, we will examine the fundamental concepts involving satellite to user range determination with no non-synchronized clocks and PRN codes. However, a number of error sources affect range measurement accuracy; these can generally be considered negligible when compared to from non-synchronized clocks.

In Fig. 2.3, we attempt to determine vector $\mathbf{u}$, which represents a user receiver's

position with respect to the ECEF coordinate system. The user's position coordinates x_u, y_u, and z_u are considered to be unknown. Vector $\mathbf{r}$ represents the vector offset from the user to the satellite. The satellite is located at coordinates x_s, y_s, and z_s within the ECEF coordinate system. Vector $\mathbf{s}$ represents the position of the satellite relative to the coordinate. Vector $\mathbf{s}$ is computed using ephemeris data broadcast by the satellite.

The satellite-to-user vector $\mathbf{r}$ is

$$\mathbf{r} = \mathbf{s} - \mathbf{u} \tag{2.1}$$

$$\|\mathbf{r}\| = \|\mathbf{s} - \mathbf{u}\| \tag{2.2}$$

$$r = \|\mathbf{s} - \mathbf{u}\| \tag{2.3}$$

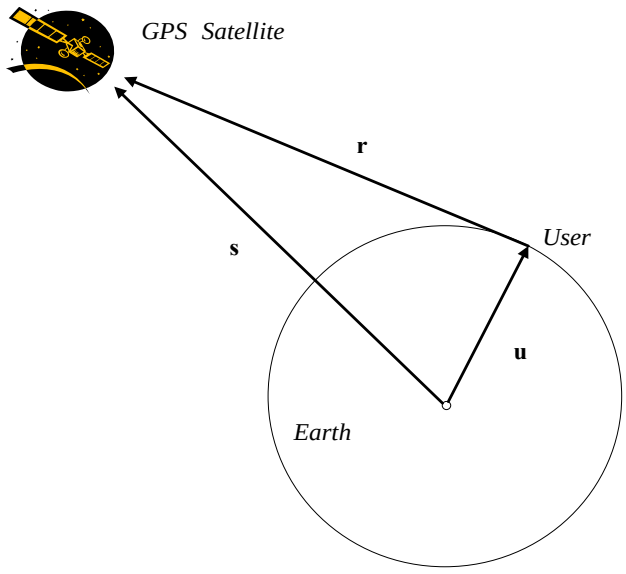

Figure 2.3 User position vector representations

The distance r is computed by measuring the propagation time required for a satellite-generated ranging code to transit from the satellite to the user receiver antenna. The propagation time measurement process is illustrated in Fig. 2.4. A specific code phase generated by the satellite at t_1 arrives at the receiver at t_2. The propagation time is represented by Δt. Within the receiver, an identical coded ranging signal is generated at t, with respect to the receiver clock. This replica code is shifted in time until it achieves correlation with the received satellite-generated ranging code. If the satellite clock and the receiver clock were perfectly synchronized, the correlation process would yield the true propagation time. By multiplying this propagation time Δt by the speed of light, the true satellite to user distance can be computed.

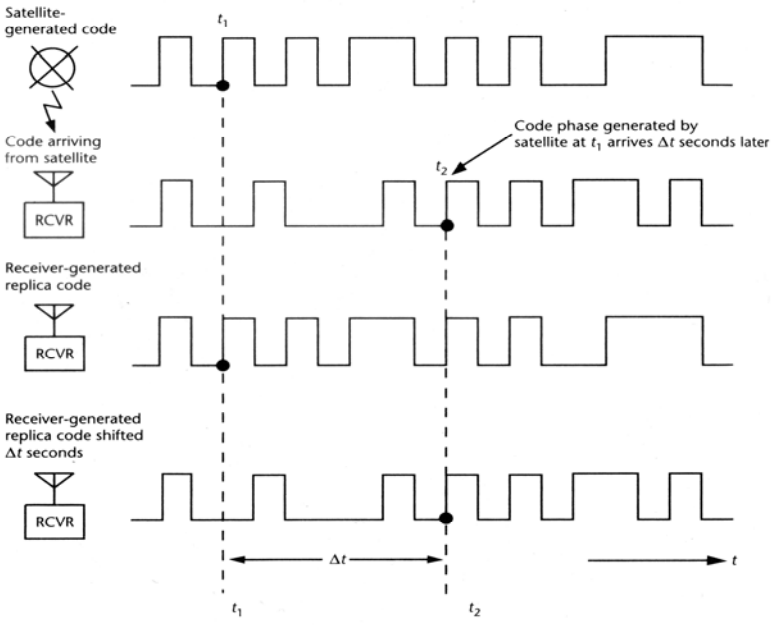

Figure 2.4 Determine satellite code transmission time

The receiver clock will generally have a bias error from the system time. Further satellite frequency generation and timing is based on a highly accurate free running cesium atomic clock which is typically offset from the system time. Thus the rang determined by the correlation process is denoted as the pseudorange ρ. The measurement is called pseudorange because it is the range determined by multiplying the signal propagation velocity c by the time difference between the satellite clock and the receiver clock. The timing relationships are shown in Fig. 2.5.

where ,

T_s	=	System time at which the signal left the satellite
T_u	=	System time at which the signal reached the user receiver
δt	=	Offset of the satellite clock from the system time
t_u	=	Offset of the receiver clock from the system time
$T_s + \delta t$	=	Satellite clock reading at the time when the signal left the satellite
$T_u + t_u$	=	User receiver clock reading at the time when the signal reached the user receiver
c	=	Speed of light

$$r = c\left(T_u - T_s\right) = c\,\Delta t \tag{2.4}$$

$$\begin{aligned} \rho &= c\left[\left(T_u + t_u\right) - \left(T_s + \delta t\right)\right] \\ &= c\left(T_u - T_s\right) + c\left(t_u - \delta t\right) \\ &= r + c\left(t_u - \delta t\right) \end{aligned} \tag{2.5}$$

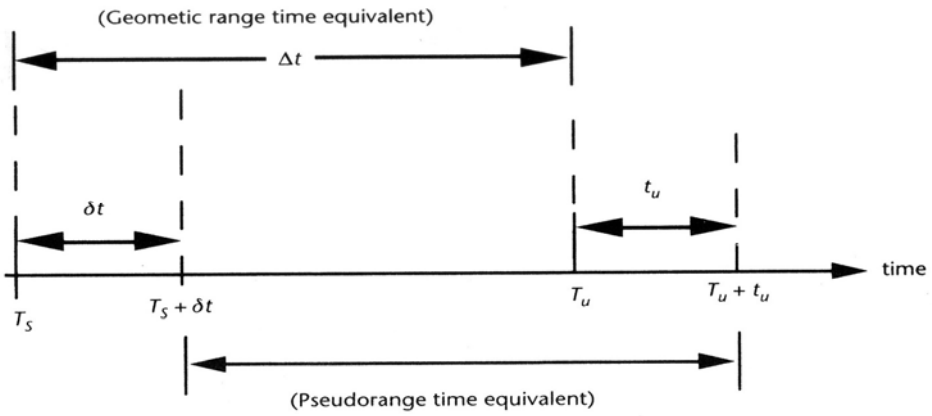

Figure 2.5 Range measurement timing relationships

Therefore Ep. (2.1) can be rewritten as

$$\rho - c\left(t_u - \delta t\right) = \left\|\mathbf{s}-\mathbf{u}\right\| \tag{2.6}$$

where, t_u represents the advance of the receiver clock with respect to system time, δt represents the advance of the satellite clock with respect to sys time, and c is the speed of light.

The satellite clock offset from system time, δt is composed of bias and drift contributions. The GPS ground-monitoring network determines corrections for these offset contributions and transmits the corrections to the satellites for rebroadcasting to the user in the navigation message. These corrections are applied within the user

receiver to synchronize the transmission of each ranging signal to system time. Therefore, we assume that this offset is compensated for and no longer consider δt as an unknown. Hence, the preceding equation can be expressed as

$$\rho - ct_u = \|\mathbf{s} - \mathbf{u}\| \tag{2.7}$$

2.4 Calculation of User Position

In order to determine the user position in three dimensions $(x_{u,}y_u, z_u)$ and the offset t_u, pseudorange measurements are made to four satellites, resulting in the system of equations.

$$\rho_j = \|\mathbf{s}_j - \mathbf{u}_j\| + ct_u \tag{2.8}$$

where j ranges from 1 to 4 and refer to the satellites. Eq. (2.8) can be expanded into the following set of equations in the unknowns of $x_{u,}y_u, z_u$, and t_u

$$\rho_1 = \sqrt{(x_1 - x_u)^2 + (y_1 - y_u)^2 + (z_1 - z_u)^2} + ct_u \tag{2.9}$$

$$\rho_2 = \sqrt{(x_2 - x_u)^2 + (y_2 - y_u)^2 + (z_2 - z_u)^2} + ct_u \tag{2.10}$$

$$\rho_3 = \sqrt{\left(x_3 - x_u\right)^2 + \left(y_3 - y_u\right)^2 + \left(z_3 - z_u\right)^2} + ct_u \tag{2.11}$$

$$\rho_4 = \sqrt{\left(x_4 - x_u\right)^2 + \left(y_4 - y_u\right)^2 + \left(z_4 - z_u\right)^2} + ct_u \tag{2.12}$$

where, $x_j y_j$, and z_j denote the j-th satellite's position in three dimensions.

These nonlinear equations can be solved for the unknowns by employing either closed-form solutions, iterative techniques based on linearization, or Kalman filtering. If we know the approximate location of the receiver, then we can denote the offset of the true position $\left(x_{u,} y_u, z_u\right)$ from the approximate position $\left(\hat{x}_{u,} \hat{y}_u, \hat{z}_u\right)$ by displacement $\left(\Delta x_{u,} \Delta y_u, \Delta z_u\right)$. By expanding Eq. (2.9) to (2.11) in a Taylor series for the approximate position, we can obtain the position offset $\left(\Delta x_{u,} \Delta y_u, \Delta z_u\right)$ as linear functions of the known coordinate and pseudorange measurements. Let a single pseudorange be represented by

$$\begin{aligned} \rho_j &= \sqrt{\left(x_j - x_u\right)^2 + \left(y_j - y_u\right)^2 + \left(z_j - z_u\right)^2} + ct_u \\ &= f\left(x_u, y_u, z_u, t_u\right) \end{aligned} \tag{2.13}$$

Using the approximate position location $\left(\hat{x}_{u,} \hat{y}_u, \hat{z}_u\right)$ and time bias estimate $\hat{t}_u$, an approximate pseudorange can be calculated:

$$\begin{aligned}\hat{\rho}_j &= \sqrt{\left(\hat{x}_j - x_u\right)^2 + \left(\hat{y}_j - y_u\right)^2 + \left(\hat{z}_j - z_u\right)^2} + c\hat{t}_u \\ &= f\left(\hat{x}_u, \hat{y}_u, \hat{z}_u, \hat{t}_u\right)\end{aligned} \tag{2.14}$$

As stated earlier, the unknown user position and receiver clock offset is considered to consist of an approximate component and an incremental component

$$\begin{aligned}x_u &= \hat{x}_u + \Delta x_u \\ y_u &= \hat{y}_u + \Delta y_u \\ z_u &= \hat{z}_u + \Delta z_u \\ t_u &= t_u + \Delta t_u\end{aligned} \tag{2.15}$$

Therefore, we can write

$$f\left(x_{u,} y_u, z_u, t_u\right) = f\left(\hat{x}_u + \Delta x_u, \hat{y}_u + \Delta y_u, \hat{z}_u + \Delta z_u, t_u + \Delta t_u\right) \tag{2.16}$$

This latter function can be expanded about the approximate point and associated predicted receiver clock offset $\left(\hat{x}_u, \hat{y}_u, \hat{z}_u, \hat{t}_u\right)$ using a Taylor series:

$$
\begin{aligned}
& f\left(\hat{x}_u+\Delta x_u, \hat{y}_u+\Delta y_u, \hat{z}_u+\Delta z_u, t_u+\Delta t_u\right)=f\left(\hat{x}_u, \hat{y}_u, \hat{z}_u, \hat{t}_u\right) \\
& +\frac{\partial f\left(\hat{x}_u, \hat{y}_u, \hat{z}_u, \hat{t}_u\right)}{\partial \hat{x}_u} \Delta x_u+\frac{\partial f\left(\hat{x}_u, \hat{y}_u, \hat{z}_u, \hat{t}_u\right)}{\partial \hat{y}_u} \Delta y_u \\
& +\frac{\partial f\left(\hat{x}_u, \hat{y}_u, \hat{z}_u, \hat{t}_u\right)}{\partial \hat{z}_u} \Delta z_u+\frac{\partial f\left(\hat{x}_u, \hat{y}_u, \hat{z}_u, \hat{t}_u\right)}{\partial \hat{t}_u} \Delta t_u+\ H.O.T
\end{aligned}
\tag{2.17}
$$

The expansion has been truncated after the first order partial derivatives to eliminate nonlinear terms. The partial derivatives are evaluated as follows

$$
\begin{aligned}
\frac{\partial f\left(\hat{x}_u, \hat{y}_u, \hat{z}_u, \hat{t}_u\right)}{\partial \hat{x}_u} &= -\frac{x_j-x_u}{\hat{r}_j} \\
\frac{\partial f\left(\hat{x}_u, \hat{y}_u, \hat{z}_u, \hat{t}_u\right)}{\partial \hat{y}_u} &= -\frac{y_j-y_u}{\hat{r}_j} \\
\frac{\partial f\left(\hat{x}_u, \hat{y}_u, \hat{z}_u, \hat{t}_u\right)}{\partial \hat{z}_u} &= -\frac{z_j-\hat{z}_u}{\hat{r}_j} \\
\frac{\partial f\left(\hat{x}_u, \hat{y}_u, \hat{z}_u, \hat{t}_u\right)}{\partial \hat{t}_u} &= c
\end{aligned}
\tag{2.18}
$$

where,

$$
\hat{r}_j=\sqrt{\left(x_j-\hat{x}_u\right)^2+\left(y_j-\hat{y}_u\right)^2+\left(z_j-\hat{z}_u\right)^2}
$$

Substituting (2.14) and (2.18) into (2.17) yields

$$\rho_j = \hat{\rho}_j - \frac{x_j - \hat{x}_u}{\hat{r}_j}\Delta x_u - \frac{y_j - \hat{y}_u}{\hat{r}_j}\Delta y_u - \frac{z_j - \hat{z}_u}{\hat{r}_j}\Delta z_u + ct_u \tag{2.19}$$

We have now completed the linearization of (2.13) with respect to the unknowns Δx_u, Δy_u, Δz_u, and Δt_u. Rearranging this expression with the known quantities on the left and unknowns quantities on the right yields

$$\hat{\rho}_j - \rho_j = \frac{x_j - \hat{x}_u}{\hat{r}_j}\Delta x_u + \frac{y_j - \hat{y}_u}{\hat{r}_j}\Delta y_u + \frac{z_j - \hat{z}_u}{\hat{r}_j}\Delta z_u - ct_u \tag{2.20}$$

For convenience, we will simplify the previous equation by introducing new variables where

$$\begin{aligned} \Delta\rho &= \hat{\rho}_j - \rho_j \\ a_{xj} &= \frac{x_j - \hat{x}_u}{\hat{r}_j} \\ a_{yj} &= \frac{y_j - \hat{y}_u}{\hat{r}_j} \\ a_{zj} &= \frac{z_j - \hat{z}_u}{\hat{r}_j} \end{aligned} \tag{2.21}$$

The a_{xj}, a_{yj}, and a_{zj} terms in (2.21) denote the direct cosine of the unit vector

pointing from the approximate user position to the j-th satellite. For the j-th satellite, this unit vector is defined as

$$\mathbf{a}_j = \left(a_{xj}, a_{yx}, a_{zj} \right) \tag{2.22}$$

Eq. (2.20) can be rewritten more simply as

$$\Delta\rho_j = a_{xj}\Delta x_u + a_{yj}\Delta y_u + a_{zj}\Delta z_u - c\Delta t_u \tag{2.23}$$

We now have four unknown quantities Δx_u, Δy_u, Δz_u, and Δt_u, which can be solved by making ranging measurements to four satellites. The unknown quantities can be determined by solving the following set of linear equations:

$$\begin{aligned}
\Delta\rho_1 &= a_{x1}\Delta x_u + a_{y1}\Delta y_u + a_{z1}\Delta z_u - c\Delta t_u \\
\Delta\rho_2 &= a_{x2}\Delta x_u + a_{y2}\Delta y_u + a_{z2}\Delta z_u - c\Delta t_u \\
\Delta\rho_3 &= a_{x3}\Delta x_u + a_{y3}\Delta y_u + a_{z3}\Delta z_u - c\Delta t_u \\
\Delta\rho_4 &= a_{x4}\Delta x_u + a_{y4}\Delta y_u + a_{z4}\Delta z_u - c\Delta t_u
\end{aligned} \tag{2.24}$$

These equations can be placed in matrix form by deriving the following definitions

$$\Delta\boldsymbol{\rho} = \begin{bmatrix} \Delta\rho_1 \\ \Delta\rho_2 \\ \Delta\rho_3 \\ \Delta\rho_4 \end{bmatrix} \qquad \mathbf{H} = \begin{bmatrix} a_{x1} & a_{y1} & a_{z1} & 1 \\ a_{x2} & a_{y2} & a_{z2} & 1 \\ a_{x3} & a_{y3} & a_{z3} & 1 \\ a_{x4} & a_{y4} & a_{z4} & 1 \end{bmatrix} \qquad \Delta\mathbf{x} = \begin{bmatrix} \Delta x_u \\ \Delta y_u \\ \Delta z_u \\ -c\Delta t_u \end{bmatrix} \tag{2.25}$$

The following is finally obtained,

$$\Delta\boldsymbol{\rho} = \mathbf{H}\Delta\mathbf{x} \tag{2.26}$$

which has the solution,

$$\Delta\mathbf{x} = \mathbf{H}^{-1}\Delta\boldsymbol{\rho}. \tag{2.27}$$

Once the unknowns are computed, the user's coordinate, $x_{u,}y_u, z_u$, and the receiver clock offset t_u are then calculated. This linearization scheme will work well, provided the displacement $\left(\Delta x_{u,}\Delta y_u, \Delta z_u\right)$ is within close proximity of the linearization point.

2.5 GPS Error Sources

Table 2.2 lists typical standard deviations for the various sources of noise that corrupts the GPS observables. Common-mode error refers to those error sources that would be common to every receiver operating in a limited geographic region. Non-common-mode errors refer to those errors that could be distinct to receivers operating even within close proximity. The actual amount of non-common-mode noise will be dependent on the receiver type and techniques used to mitigate multipath effects. Based on the estimates of the standard deviation of the various noise sources shown in Table 2.2, the standard GPS with active SA produces a range standard deviation error in the order of 25.27 m from common-mode errors.

Table 2.2 Error due to Noise Source

Errors	Standard deviation (m)
Common mode	
SA	24.0
Ionosphere	7.0
Clock and Ephemeris	3.6
Troposphere	0.7
Noncommon mode	
Receiver noise	0.1 – 0.7
Multipath	0.1 – 3.0

2.5.1 Receiver Clock Bias

Receiver clock bias is a time-varying error that affects all simultaneous range measurements in a similar way. Therefore, if four simultaneous satellite range measurements are available, both the clock bias and position can be estimated. For this reason, the clock bias error is not included in the position error budget discussed.

Fig. 2.6 shows the least-square estimate of the receiver clock bias corresponding to the position-estimation experiment. This figure is included to illustrate a few features of the clock bias. First, the clock bias is, shaped like a ramp with a reasonably stable slope. Second, the figure clearly shows that the clock bias resembles a sawtooth signal with large, fixed-magnitude discontinuities.

The discontinuity in the clock bias has a magnitude approximately equal to 0.001 c = 297,000 m. The pseudorange measurement is based on the delay between the satellite generated and the receiver generated copies of the C/A code sequences. Since each code sequence has period equal to 0.001 s, the estimated clock bias cannot exceed 1 ms. The receiver clock bias can be managed by at least three methods:

1. Differencing two simultaneous range measurements from the same receiver.
2. Estimating the clock bias independently at each time step.
3. Developing a dynamic model for the change in the clock bias and estimating the clock model state by means of Kalman filtering.

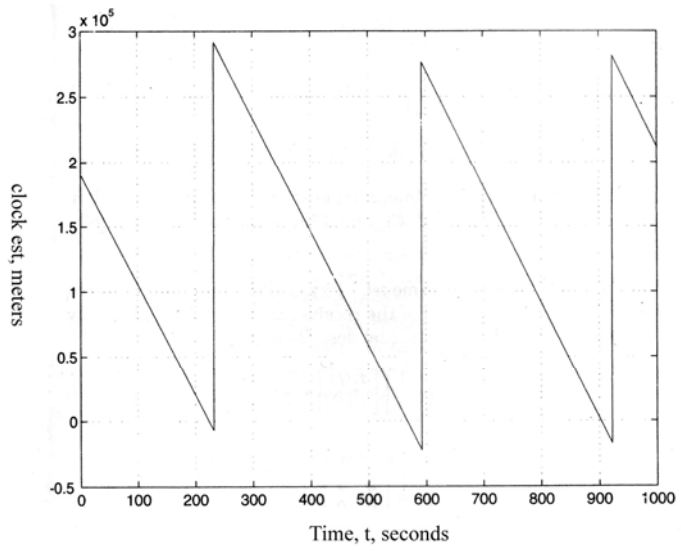

Figure 2.6 Estimated clock bias during L1 C/A code position estimation

2.5.2 Satellite Clock Bias

Each satellite clock is free running and, over time, will drift away from the GPS system time. The control segment is responsible for estimating and monitoring the satellite clock bias. The ground stations do not actually correct the satellite clock, but monitor the errors and send the correction formula parameters to the user. The user reads these parameters and corrects the predicted portion of the satellite clock error.

The satellite clock correction should be used to correct the transit time before calculating the time of transmission, satellite position, or corrected pseudorange. In addition to the actual satellite clock drift, one implementation of the policy of SA is the

addition of an apparent clock error. The SA portion of the satellite clock error is not accounted for in the broadcast clock corrections. The satellite clock error affects all users (i.e., those using C/A code, P code, or double frequency receivers) in the same way. The error is independent of the location of the user relative to the satellite. Therefore, the satellite clock component of the differential correction is accurate for all users, regardless of position.

2.5.3 Atmospheric Delay

Atmospheric delay can be classified into one of two types: non-dispersive and dispersive. Although the following terminology hides some portions of the atmosphere, the non-dispersive portion is usually associated with the troposphere, while the dispersive portion is associated with the ionosphere. The troposphere is the lower part of the atmosphere, expending nominally from 8 to 40 km above the earth's surface. The troposphere undergoes changes in temperature pressure, and humidity associated with weather. Since these same variables affect the speed of light, changes in tropospheric conditions will result in errors in the measured range. The ionosphere is the layer of the atmosphere above 50 km that consists of ionized air. Changes in the level of ionization affect the refractive indices of the various layers of the ionosphere and therefore affect the travel time of GPS signals through the ionosphere. With these associations, the atmospheric delay can be decomposed into two components,

$$\Delta t_a = \Delta t_{trop} \pm \Delta t_{ion}(f) \tag{2.28}$$

where, f denotes the frequency of the carrier signal, the $+$ sign refers to the code pseudorange, and the $-$ sign refers to the phase range. The user combining code and phase based ranging technique must be known to properly account for the sign differences.

Tropospheric delays can be quite considerable for satellites at low elevations. Tropospheric delay errors are consistent between the L1 and the L2 signals and carrier and code signals. Tropospheric delay is normally represented as having a wet component and a dry component. The wet component is difficult to model due to local variations in the water vapor content of the troposphere and accounts for approximately 10% of the tropospheric delay. The dry component is relatively well modeled and accounts for approximately 90% of the tropospheric delay. Several models exist for the tropospheric wet and dry components. For example, the Chao model is

$$\Delta\rho_{dry} = 2.276\times10^{-5}P \tag{2.29}$$

$$F_{dry} = \frac{1}{\sin(E) + \frac{0.00143}{\tan(E)+0.045}} \tag{2.30}$$

$$\Delta\rho_{wet} = 4.70\times10^{2}\frac{e^{1.23}}{T^{2}} + 1.705\times10^{6}\alpha\frac{e^{1.46}}{T^{3}} \tag{2.31}$$

$$F_{wet} = \frac{1}{\sin(E) + \frac{0.00035}{\tan(E)+0.017}} \tag{2.32}$$

$$\Delta\rho_{trop} = \Delta\rho_{dry}F_{dry} + \Delta\rho_{wet}F_{wet} \tag{2.33}$$

where, $\Delta\rho$ is the tropospheric delay in meters, P is the atmospheric pressure, T is the temperature in degrees Kelvin, e is the partial pressure of water vapor in milliards, α is the temperature lapse rate in degrees Kelvin per meter, and E is the satellite elevation angle in degrees.

Tropospheric delay is dependent on local variables, receiver altitude, and the user-satellite line of sight; the ability of differential techniques to compensate for tropospheric effects will depend on the position of the user relative to the base station. The user of differential corrections needs to know whether the differential station is compensating for tropospheric delay in the broadcast corrections. If the broadcast corrections include tropospheric error and the user is at an altitude different from that of the reference station, the user can correct the broadcast corrections for tropospheric delay at the reference station and correct the measured range for tropospheric delay at the user location.

Ionospheric group delay can be approximated to the first order as

$$\Delta t_{ion}(f) = \frac{40.3}{f^2} TEC \tag{2.34}$$

where, f is the carrier frequency and TEC is the time and spatially varying total electron count. In discussing ionospheric compensation by two frequency receivers, it is convenient to define

$$I_a = \frac{40.3}{f_1 f_2} TEC \tag{2.35}$$

With this definition, the L1 and the L2 ionospheric delays are $(f_2 / f_1)I_a$, and $(f_1 / f_2)I_a$, respectively. The two frequency receivers can take advantage of the frequency dependence of delay. Single frequency receivers must rely on either the differential operation or an ionospheric delay model.

2.5.4 Ephemeris Delay

The three components of ephemeris error can be represented as radial, tangential, and cross track. In general, the radial errors are smallest and most important. The tangential and the cross track errors do not affect the ranging accuracy.

The control segment monitors the satellite orbits and calculates the ephemeris parameters broadcast to the user by the satellite. Since the ephemeris model is a curve fit to the measured orbit, it will contain a time varying residual error relative to the

actual orbit. In general, the radial component of the ephemeris error will slowly increase as a function of the time since the last control segment update.

2.5.5 Multipath Error

Multipath propagation of the GPS signal is a dominant error source of the GPS positioning system. Objects in the vicinity of a receiver antenna can easily reflect the GPS signal, resulting in one or more secondary propagation paths. These secondary path signals, which are superimposed on the desired direct-path signal, always have a longer propagation time and can significantly distort the amplitude and phase of the direct-path signal.

Error due to multipath cannot be reduced by the use of differential GPS, since they depend on local reflection geometry near each receiver antenna. In a receiver without multipath protection, a C/A code ranging error of 10m or more can occur. A multipath can cause large code ranging errors and can severely degrade the ambiguity resolution process required for carrier phase ranging such as that used in a precision surveying application.

Multipath propagation can be divided into two classes: static and dynamic. For a stationary receiver, the propagation geometry changes slowly as the satellites move across the sky, making the multipath parameters essentially constant for perhaps several minutes. However, in mobile applications, rapid fluctuations can occur within

fractions of a second. Therefore, different multipath mitigation techniques are generally employed for these two types of multipath environments. Most current research has focused on static applications such as surveying, where greater demand for high accuracy exists.

2.5.5.1 Multipath Ranging Error

To facilitate an understanding of how a multipath causes ranging errors, several simplifications can be made that do not obscure the fundamentals involved. We will assume that the receiver processes only the C/A-code and that the received signal has been converted to a complex signal from at baseband (nominally zero frequency), where all Doppler shifts have been removed by a carrier tracking phase-lock loop. It is also assumed that the 50-bps (bits per second) GPS data modulation has been removed from the signal, which can be achieved by standard techniques. When no multipath is present, the received waveform is represented by

$$r(t) = ae^{j\phi}c(t-\tau) + n(t) \tag{2.36}$$

where, $c(t)$ is the normalized, undelayed C/A-code waveform as transmitted, τ is the signal propagation delay, a is the signal amplitude, ϕ is the carrier phase, and $n(t)$ is Gaussian receiver thermal noise having flat power spectral density.

Pseudoranging involves estimating the delay parameter τ. An optimal estimate of τ can be obtained by forming the cross-correlation function of $r(t)$ with a replica $c_r(t)$ of the transmitted C/A-code and choosing the delay estimate to be the value of τ that maximizes this function.

$$R(t) = \int_{T_1}^{T_2} r(t)\, c_r(t-\tau)dt \tag{2.37}$$

Except for an error due to receiver thermal noise, this occurs when the received and replica waveforms are in time alignment. A typical cross-correlation function without multipath for C/A-code receivers having a 2-MHz precorrelation bandwidth is as solid lines in Fig. 2.7. These plots ignore the effect of noise, which would add small random variations to the curves.

If a multipath is present with a single secondary path, the waveform of Eq. (2.36) changes to

$$r(t) = ae^{j\phi_1}c(t-\tau_1) + be^{j\phi_2}c(t-\tau_2) + n(t) \tag{2.38}$$

where, the direct and secondary paths have respective propagation delays τ_1 and τ_2, amplitudes a and b, and carrier phases ϕ_1 and ϕ_2. In a receiver not designed expressly to handle a multipath, the resulting cross-correlation function will now need

two superimposed components, one from the direct path and one from the secondary path. The result is a function with a distortion depending on the relative amplitude, delay, and phase of the secondary-path signal, as illustrated at the Fig. 2.7 for an in-phase secondary path and the Fig. 2.8 for an out-of-phase secondary path. Most importantly, the location of the peak of the function has been displaced from its correct position, resulting in a pseudorange error. In vintage receivers employing standard code tracking techniques (early and late codes separated by one C/A-code chip), the magnitude of pseudorange error caused by a multipath can be quite large, reaching 70–80 m for a secondary-path signal half as large as the direct-path signal and having a relative delay of approximately 250 m.

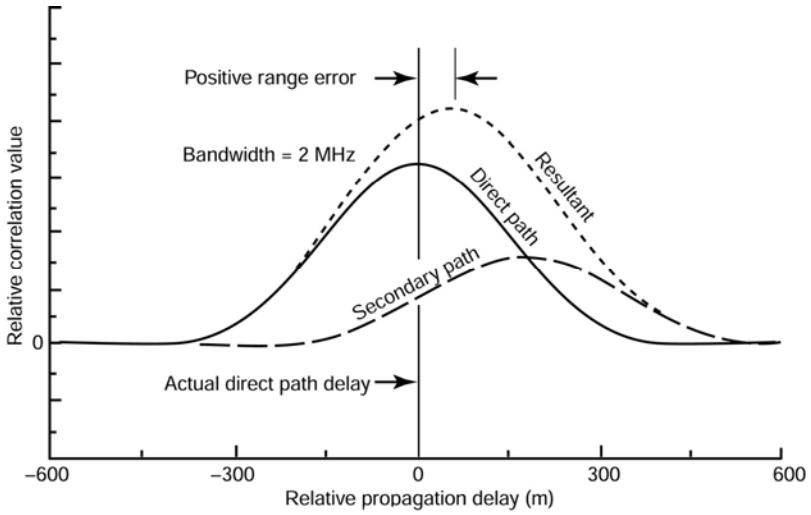

Figure 2.7 Effect of multipath on C/A-code correlation function (In-phase)

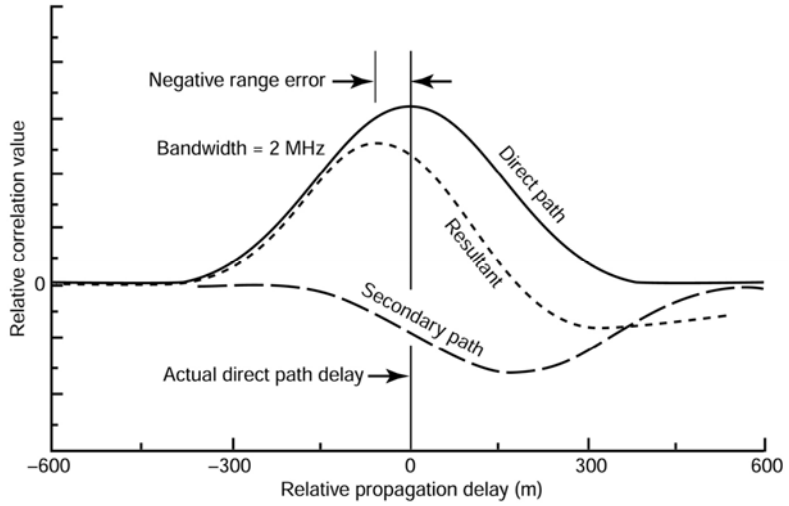

Figure 2.8 Effect of multipath on C/A-code correlation function (Out-phase)

2.5.5.2 Multipath Ranging Error Simulation

The simplest way to represent a multipath problem is the two-ray model as depicted in Fig. 2.9, where a transmitted signal reaches a receiver in two paths, one through a line-of-sight and the other through a reflected path that is τ seconds longer. The transfer function representing the path characteristics may be expressed in impulse response as follows

$$h(t) = \delta(t) + \alpha \exp(j\theta\pi / 180)\delta(t - \tau) \tag{2.39}$$

where, α and θ represent the relative magnitude and phase of the second path. τ is the time delay of the second path relative to the line-of-sight path.

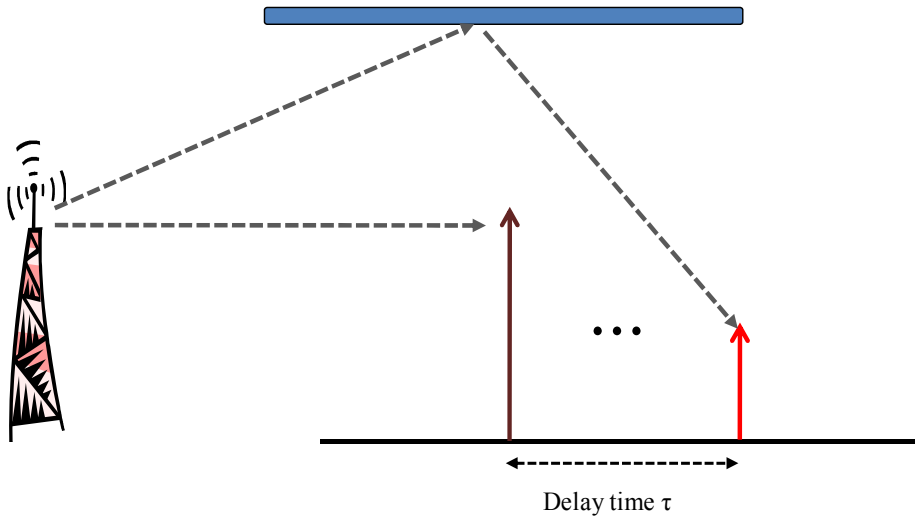

Figure 2.9 Two-ray multipath model

Without the multipath, the autocorrelations of GPS systems are symmetric as shown in Figs. 2.10 However, the symmetry does not hold if a code is delivered with a multipath such as the two-ray model. Fig. 2.11 shows the autocorrelation and its asymmetry when α=0.5, θ=0 deg, and τ=0.5 chip in Eq. (2.39). An asymmetric autocorrelation is plotted on the left-hand side, while following functional value is plotted on the right-hand side,

$$s(t') = c(t' - 0.5) - c(t' + 0.5) \tag{2.40}$$

where, $c(t')$ is an autocorrelation value at t' plotted on the left-hand side figure. Therefore, $s(t')$ represents a difference in the autocorrelation value of one chip length between (t'-0.5) and (t'+0.5). t' varies from –1 to +1.

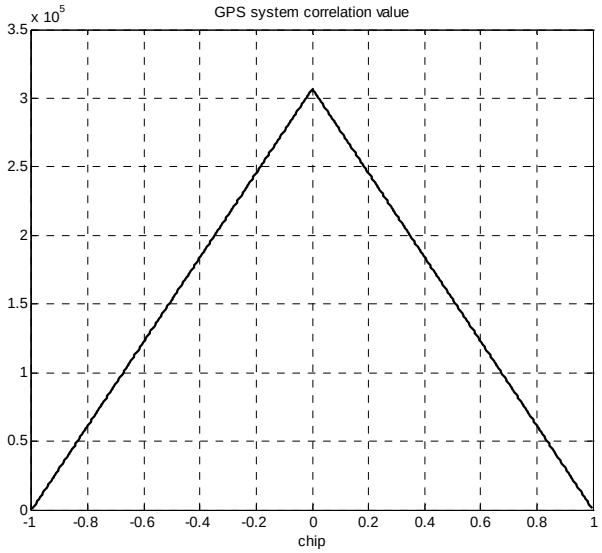

Figure 2.10 Autocorrelation function of GPS

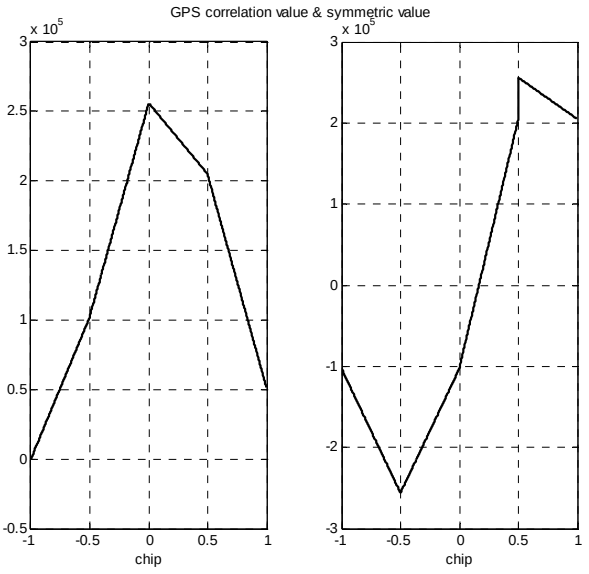

Figure 2.11 Autocorrelation value and its asymmetry of GPS

For example, if t' =−0.5, then, $c(-1)=0$ and, $c(0)=2.51\times10^5$; therefore, $s(t')=-2.51\times10^5$. We can find a correlation error due to a multipath by solving $s(t')=0$ for t'. In Fig. 2.11, which represents a case of τ =0.5 chip, $s(t')=0$ if t'=0.171 chip. That is, the correlation error is 0.171 chip if there is a multipath delay of 0.5 chip. The correlation error of 0.171 chip is equivalent to 50 m in position error. Correlation errors by varying multipath delay τ as defined in Fig. 2.9 are plotted in Fig. 2.12. The upper part of the figure represents a case of α=0.5 and θ=0 deg and the lower part represents a case of α=0.5 and θ=180 deg. The ranging error has maximum values of ±75 m at τ =-0.25 and τ =0.75 chips. The figure also show that the ranging error becomes zero if τ is larger than the 1.5 chip.

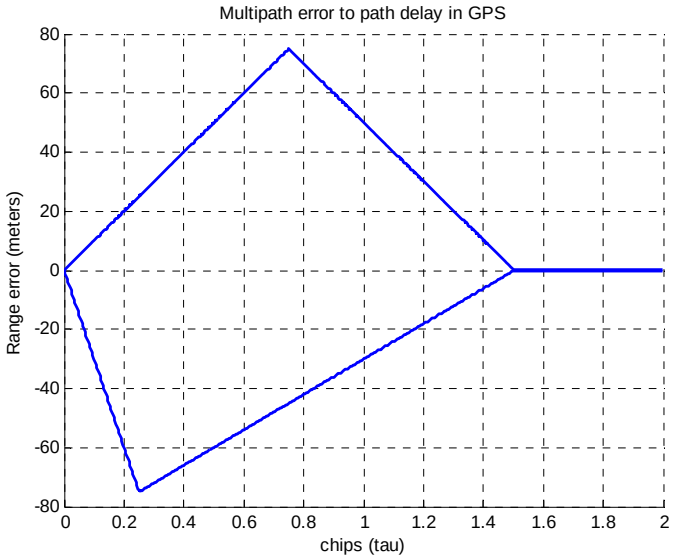

Figure 2.12 Multipath correlation error of GPS system

2.5.6 Receiver Noise

This is the error the receiver makes in measuring the transit time. The error is due to such factors as component nonlinearity and thermal noise. The magnitude of this error is dependent on the technology incorporated in a particular receiver. The noise is usually modeled as white noise and is independent between both the satellite and receivers.

2.6 Summary

In this chapter, the overview of the GPS system was briefly introduced. A basic concept of the GPS system, determining the satellite to user distance, calculation of user positioning, and GPS system error sources are described. One of these errors, multipath, is a major error source of the GPS system. Multipath error depends on local reflection geometry near each receiver antenna; the multipath cannot be reduced by using the differential method. The multipath error mitigation in the GPS system will be discussed in more detail in the next chapter.

Chapter 3
Antenna Array Processing and Beamforming

3.1 Background on Antenna Arrays and Beamformers

Although nowadays, employing antenna array processing in GPS applications is becoming a breakthrough technique, especially for interference suppression (e. g. Lorenzo 2007, Kappen et al 2012, Basta et al 2012, Cuntz et al 2011, Daneshmand 2013), beamforming and antenna array processing have been studied for several decades in other areas (Van Trees 2002, Van Veen & Buckley 1998, Krim & Viberg 1996). There are numerous applications for array processing, in radar, sonar, navigation, wireless communications, direction finding, acoustics, radio astronomy, seismology and biomedicine, to name some. Beamforming is referred to as a spatial domain signal processing method employing an array of sensors or antennas (Van Veen & Buckley 1998). The received signals of antenna elements are gained or delayed, differently to provide the desired spatial characteristics. Usually, the received signals from different antennas are combined to attenuate the undesired signals (null steering), and to amplify the desired signals. One of the earliest beamforming methods was derived by Capon (1969), which has been referred to as the Capon beamformer, or the minimum variance distortionless response (MVDR) beamformer (Van Trees 2002). This beamformer has

been considered a popular method for a variety of signal processing applications, such as radar, wireless communications, and speech enhancement. The MVDR beamformer has a distortionless response for the desired signal while suppressing all signals arriving from other directions. Over the years, many other beamformers have been introduced in the literature. Some important beamformers are addressed in Section 2.2.

Fig. 3.1 provides an example to demonstrate the antenna array processing concept. Two signals from two different directions are impinging on an antenna array consisting of N antenna elements. It is assumed that the transmitters are located in a far-field region of the array, and that therefore the received signals are plane waves. Consider that one of them is a desired signal (e.g. a GPS signal), and the other one is an unwanted signal (e.g. a CW interfering, multipath signal). Since they have different incident angles, they are received with different delays and phases at each antenna. The antenna array processor aims to assign extra delays or phases (array gains) to the received signal of each antenna, so that the desired signal is passed through the beamformer whereas the undesired one is suppressed, or significantly attenuated. Optimal phases and delays can be obtained, in terms of different criteria. Generally, they are obtained from a constraint optimization problem, which depends on the model chosen to describe the system and the required objectives. By employing array processing techniques, spatial discrimination among signals coming from different directions is possible. This feature of antenna array processing cannot be realized by

any spectral processing techniques.

The combination of antennas' outputs results in a new gain pattern, called the antenna array beam pattern. In fact, it is possible to shape this beam pattern, by changing the array gain vector, such that the beam pattern with desired features is achieved. Therefore, there is no need to physically change the orientation of antennas. Moreover, the main lobe, side lobe, nulls and directivity of the array can be controlled by array gains. This is especially useful suppressing interfering signal in particular directions by nullifying them and to steer the main lobe in the direction of the desired signal. Fig. 3.2 illustrates an antenna array beam pattern for a scenario in which one interfering signal and one LOS GPS signal impinge on an antenna array. The beam pattern has been shaped to put a null in the direction of interference, and to steer the main lobe toward the GPS signal direction.

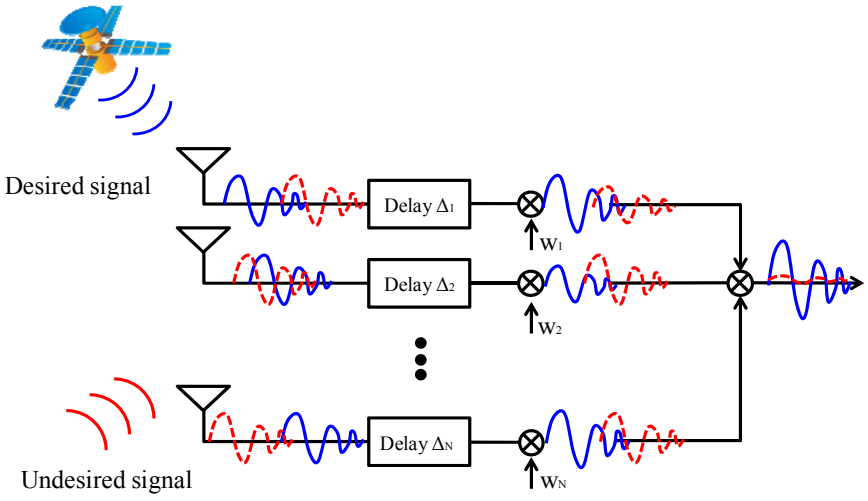

Figure 3.1 General block diagram of a beamformer

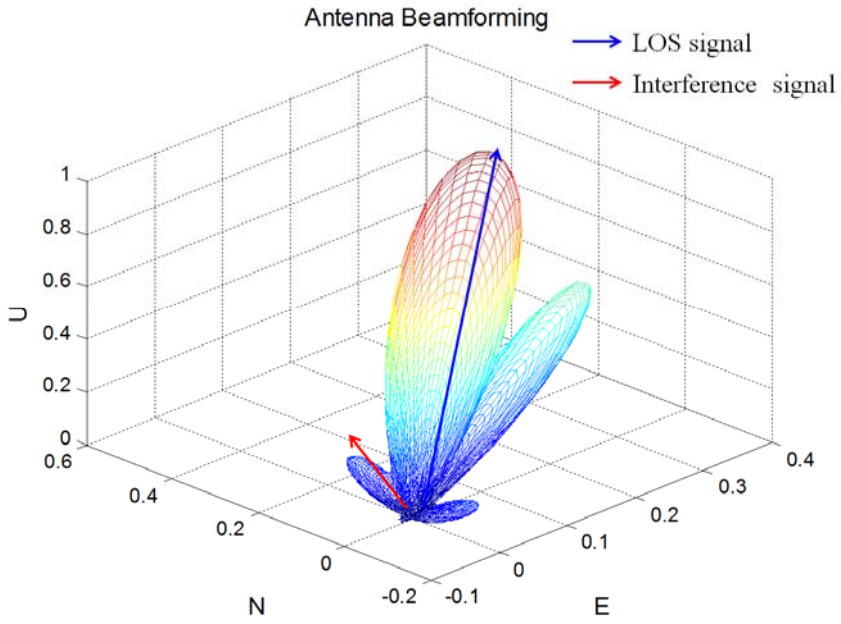

Figure 3.2 Three-dimensional antenna array beam pattern

3.1.1 Signal Model

In this section, a general signal model of an array and some basic principles are presented. Assume a GPS signal impinges on antenna array with N isotropic antennas. The arbitrary positions of these elements are shown with vectors $\mathbf{d}_1^{ant}, \mathbf{d}_2^{ant}, \ldots \mathbf{d}_N^{ant}$, which are pointing from the origin of the coordinate system to the antenna elements, as shown in Fig. 3.3. Without loss of generality, it can be assumed that the origin of the coordinate system is located at the position of the first antenna.

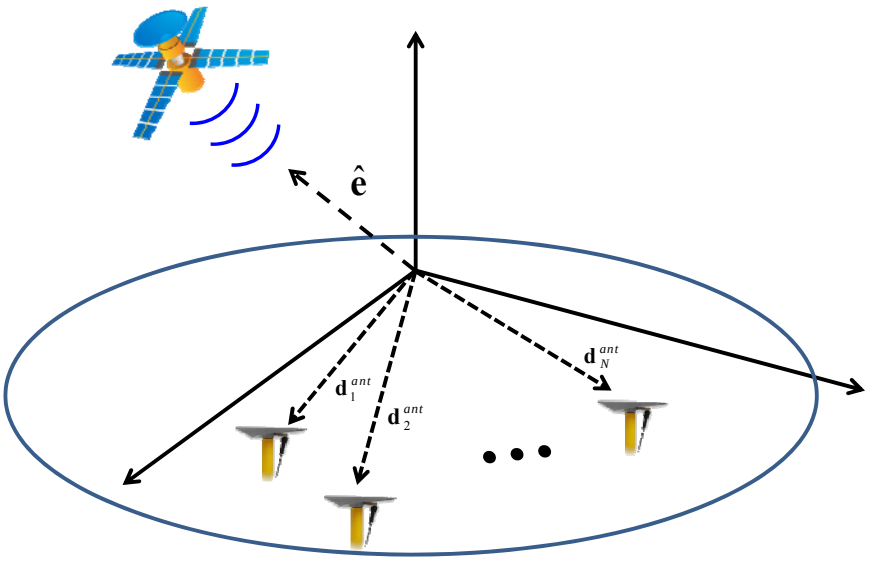

Figure 3.3 Plane wave impinging on an antenna array with *N* elements

Assume that the received signal is a band pass signal (e.g. GSP L1 C/A). The signal received by the first antenna can be modeled as

$$x_{ant}(t) = \mathrm{Re}\left\{ s_{ant}(t) e^{j2\pi f_c t} \right\} \tag{3.1}$$

where, f_c is the carrier frequency, and $s_{ant}(t)$ is the complex envelope signal, which is band limited as

$$|f - f_c| \le \frac{B_s}{2} \tag{3.2}$$

where, B_s is a bandwidth of the complex envelope signal (for GPS L1 C/A, f_c =1575.42 MHz and B_s =2.046 MHz). The set of received signals of all antennas can be expressed in vector form as

$$\mathbf{x}_{ant}(t) = \begin{bmatrix} \mathrm{Re}\left\{ s_{ant}(t-t_1) e^{j2\pi f_c (t-t_1)} \right\} \\ \mathrm{Re}\left\{ s_{ant}(t-t_2) e^{j2\pi f_c (t-t_2)} \right\} \\ \vdots \\ \mathrm{Re}\left\{ s_{ant}(t-t_N) e^{j2\pi f_c (t-t_N)} \right\} \end{bmatrix} \tag{3.3}$$

where, $t_1, t_2 \cdots t_N$ are the received signal delays with respect to the first antenna, where $t_1 = 0$. The generic structure of the beamformer is shown in Fig. 3.4. Assume that the maximum travel time across the antenna elements is max $\Delta t_{\max}$. It can be easily verified that if

$$B_s \Delta t_{\max} << 1 \tag{3.4}$$

then the following approximation is valid (Van Trees 2002):

$$s_{ant}(t) \approx s_{ant}(t - t_i) \qquad i = 1, 2, \cdots N. \tag{3.5}$$

(For GPS L1 C/A and for an antenna array with maximum antenna elements separation

equal to 1m, $B_s \Delta t_{\max}$ is approximately equal to 0.007). Hence, by substituting Eq. (3.5) in Eq. (3.3), one obtains

$$\mathbf{x}_{ant}(t) \approx \begin{bmatrix} \mathrm{Re}\left\{ s_{ant}(t) e^{j2\pi f_c (t-t_1)} \right\} \\ \mathrm{Re}\left\{ s_{ant}(t) e^{j2\pi f_c (t-t_2)} \right\} \\ \vdots \\ \mathrm{Re}\left\{ s_{ant}(t) e^{j2\pi f_c (t-t_N)} \right\} \end{bmatrix} \tag{3.6}$$

These signals are then down converted (see Figure 3.4). It can be easily verified that the received signal vector after down conversion becomes

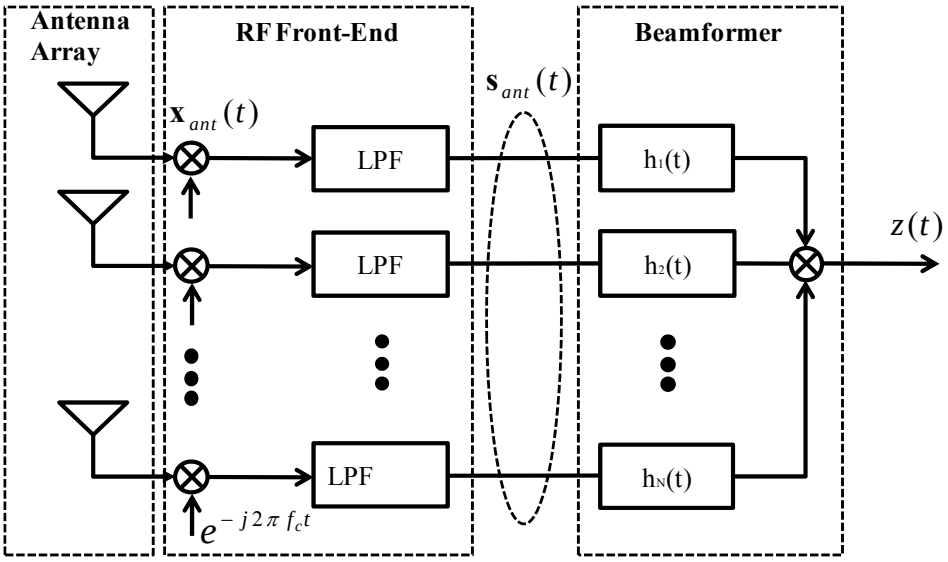

Figure 3.4 General structure of a beamformer

$$\mathbf{s}_{ant}(t) \approx \begin{bmatrix} s_{ant}(t)e^{-j2\pi f_c t_1} \\ s_{ant}(t)e^{-j2\pi f_c t_2} \\ \vdots \\ s_{ant}(t)e^{-j2\pi f_c t_N} \end{bmatrix} \tag{3.7}$$

For beamforming, the down-converted signal of each antenna element passes through a time-invariant filter. The way of designing these filters will be discussed in Section 3.2 and 3.4. The beamformer output is obtained as

$$z(t) = \sum_{i=1}^{N} \int_{-\infty}^{\infty} h_i(t-\tau) s_{ant}(\tau) e^{-j2\pi f_c t_i} d\tau \tag{3.8}$$

which can be expressed in a compact form as

$$z(t) = \sum_{i=1}^{N} \int_{-\infty}^{\infty} \mathbf{h}^T(t-\tau) \mathbf{s}_{ant}(\tau) d\tau \tag{3.9}$$

where, $\mathbf{s}_{ant}$ is defined in Eq. (3.7), and $\mathbf{h}$ is defined as

$$\mathbf{h}(t) \cong \begin{bmatrix} h_1(t) \\ h_2(t) \\ \vdots \\ h_N(t) \end{bmatrix} \tag{3.10}$$

It is also convenient to express Eq. (3.9) in the frequency domain as

$$Z(f) = H^T(f) S_{ant}(f) \tag{3.11}$$

where,

$$\begin{aligned} S_{ant}(f) &\cong F\{\mathbf{s}_{ant}(t)\} \\ H(f) &\cong F\{\mathbf{h}(t)\} \\ Z(f) &\cong F\{z(t)\} \end{aligned} \tag{3.12}$$

It can be readily verified that delays $t_1, t_2 \cdots t_N$ in Eq. (3.7) are related to the relative positions of the antenna elements, and the direction of the incident signal (shown with unit vector $\mathbf{e}$ in Figure 3.3) by the relation

$$t_i = \frac{\mathbf{e}^T \mathbf{d}_i^{ant}}{c} \qquad i = 1, 2, \cdots, N \tag{3.13}$$

where, c is the propagation speed in the medium. In Eq. (3.11), $S_{ant}(f)$ can be written as

$$S_{ant}(f) = \begin{bmatrix} F\{s_{ant}(t)\} e^{-j2\pi f_c t_1} \\ F\{s_{ant}(t)\} e^{-j2\pi f_c t_2} \\ \vdots \\ F\{s_{ant}(t)\} e^{-j2\pi f_c t_N} \end{bmatrix} \tag{3.14}$$

By substituting Eq. (3.13) in Eq. (3.14), $S_{ant}(f)$ can be expressed as

$$S_{ant}(f) = \mathbf{a}_e F\{s_{ant}(t)\} \tag{3.15}$$

and in the time domain as

$$\mathbf{s}_{ant}(t) = \mathbf{a}_e s_{ant}(t) \tag{3.16}$$

where, $\mathbf{a}_e$ is defined as

$$\mathbf{a}_e \approx \begin{bmatrix} e^{-j2\pi f_c \frac{\mathbf{e}^T \mathbf{d}_1^{ant}}{c}} \\ e^{-j2\pi f_c \frac{\mathbf{e}^T \mathbf{d}_2^{ant}}{c}} \\ \vdots \\ e^{-j2\pi f_c \frac{\mathbf{e}^T \mathbf{d}_N^{ant}}{c}} \end{bmatrix} \tag{3.17}$$

The vector $\mathbf{a}_e$ includes all spatial information of the incident signal, which is a function of the carrier frequency, the direction of the incident signal and the array configuration. In the literature, this vector is referred to as the array manifold vector or the steering vector. By substituting Eq. (3.15) in Eq. (3.11),

$$Z(f) = \Upsilon(f, \hat{\mathbf{e}}) F\{s_{ant}(t)\} \tag{3.18}$$

where, $\Upsilon(f, \hat{\mathbf{e}})$ is defined as

$$\Upsilon(f,\mathbf{e}) \cong H^T(f)\mathbf{a}_{\hat{\mathbf{e}}} \tag{3.19}$$

$\Upsilon(f,\hat{\mathbf{e}})$ is the beamformer response to the impinging signal with incident direction of $\hat{\mathbf{e}}$. For an antenna array, the array beam pattern (in dB) is defined as

$$BP \cong 10\log\left(\left|\Upsilon(f,\hat{\mathbf{e}})\right|^2\right) \tag{3.20}$$

In fact, the array beam pattern determines the beamformer gain in a specific frequency and direction.

As long as Eq. (3.10) and, consequently, Eq. (3.11) hold, vector $\mathbf{h}(t)$ can be modeled by a set of phase shifts (complex values) to weight the received signals. In this case, the response of the beamformer $\mathbf{h}(t)$ in Eq. (3.19) can be simplified to

$$\Upsilon(\mathbf{e}) \cong \mathbf{w}^H\mathbf{a}_{\hat{\mathbf{e}}} \tag{3.21}$$

in which $\mathbf{w}$ is a complex-value vector referred to as the weighting vector or gain vector. This implementation is referred to as a phased array beamformer and is widely employed in practice. In this case, the beamformer response only depends on the direction of the incident signal.

On the other hand, by carrying out spatial-temporal processing, the general model

shown in Fig. 3.4 utilizes some properties of the incident signals received by the antenna array. For example, this model can be employed when the approximation in Eq. (3.11) does not hold or for enhancing interference mitigation methods. Generally, filters in a beamformer are implemented by finite impulse response (FIR) filters. Section 3.4 discusses this in more detail.

After introducing the basic concepts, Eq. (3.16) is now generalized to the case of N desired signals (e.g. GPS signals) and I undesired ones (e.g. interfering signals), as

$$\mathbf{r}(t) = \sum_{m=1}^{N_{desired}} \mathbf{a}_m s_m(t) + \sum_{i=1}^{I} \mathbf{b}_i v_i(t) + \boldsymbol{\eta} \tag{3.22}$$

where, $\mathbf{a}_m$ and $\mathbf{b}_i$ are the steering vector of the *m*th desired signal and *i*th undesired signal, respectively. Correspondingly, $s_m(t)$ and $v_i(t)$ are the complex envelopes of the *m*th and *i*th desired and undesired signals, and $\boldsymbol{\eta}$ is the noise vector. $\mathbf{r}(t)$ in Eq. (3.22) can be expressed in matrix form as

$$\mathbf{r}(t) = \mathbf{A}\mathbf{s} + \mathbf{B}\mathbf{v} + \boldsymbol{\eta} \tag{3.23}$$

where, the steering matrices $\mathbf{A}$ and $\mathbf{B}$ consider all spatial characteristics of the signals received by an array, and are defined as

$$\begin{aligned}\mathbf{A} &= [\mathbf{a}_1 \;\; \mathbf{a}_2 \;\; \cdots \mathbf{a}_{N_{de}}] \\ \mathbf{B} &= [\mathbf{b}_1 \;\; \mathbf{b}_2 \;\; \cdots \mathbf{b}_I]\end{aligned} \tag{3.24}$$

$\mathbf{A}$ and $\mathbf{B}$ are assumed to be full column rank matrices. This assumption implies that the incident signals are not coming from the same direction. In Eq. (3.23), $\mathbf{s}$ and $\mathbf{v}$ are the desired and interfering waveform vectors, respectively, and are defined as

$$\begin{aligned}\mathbf{s} &= [s_1(t) \;\; s_2(t) \;\; \cdots s_{N_{de}}(t)] \\ \mathbf{v} &= [v_1(t) \;\; v_2(t) \;\; \cdots v_I(t)]\end{aligned} \tag{3.25}$$

The following assumptions are used in the rest of this thesis:

Assumption 1: the noise term in Eq. (3.22) is a spatially-temporally white zero-mean complex vector with covariance matrix $\sigma^2\mathbf{I}$.

Assumption 2: both the desired signals (GPS signals) and undesired signals (interfering signals) are considered as unknown deterministic signals.

Based on these assumptions, a number of well-known beamformers are described in the following section,.

3.2 Conventional Optimum Beamformers

An *N*-antenna phase array implementation is considered in this section. For the sake of simplicity, assume that only one desired signal exists.

3.2.1 Minimum Variance Distortionless Response Beamformer

By assuming one desired signal, Eq. (3.23) becomes

$$\mathbf{r}(t) = \mathbf{a}s(t) + \mathbf{B}\mathbf{v} + \boldsymbol{\eta} \tag{3.26}$$

The spatial correlation matrix of the received signal vector is obtained as

$$\mathbf{R}_{\mathbf{r}} = E\left\{\mathbf{r}(t)\mathbf{r}(t)^H\right\} \tag{3.27}$$

Considering Eq. (2.26), $\mathbf{R}_{\mathbf{r}}$ can be expressed as

$$\mathbf{R}_{\mathbf{r}} = \mathbf{a}\sigma_s^2\mathbf{a}^H + \mathbf{B}\tilde{\mathbf{R}}_V\mathbf{B}^H + \sigma^2\mathbf{I} \tag{3.28}$$

where, σ_s^2 are $\tilde{\mathbf{R}}_V$ the desired signal variance (power) and temporal correlation

matrix, respectively, of the interference (for simplicity, interfering and desired signals are assumed to have zero mean), and are defined as

$$\begin{aligned} \sigma_s^2 &= E\left\{s(t)s(t)^H\right\} \\ \tilde{\mathbf{R}}_V &= E\left\{v(t)v(t)^H\right\} \end{aligned} \tag{3.29}$$

Assume that $\mathbf{R}_{\mathbf{v},\boldsymbol{\eta}}$ is defined as

$$\mathbf{R}_{\mathbf{v},\boldsymbol{\eta}} = \mathbf{B}\tilde{\mathbf{R}}_V\mathbf{B}^H + \sigma^2\mathbf{I} \tag{3.30}$$

which is the spatial correlation matrix of the undesired signals. The distortionless criterion is considered for the MVDR beamformer, which implies

$$z(t) = s(t) \tag{3.31}$$

where, $z(t)$ is the beamformer output. Considering Eq. (3.21), the constraint of no distortion can be also expressed as

$$\mathbf{w}^H\mathbf{a} = 1 \tag{3.32}$$

The goal is to minimize $\mathbf{R}_{\mathbf{v},\boldsymbol{\eta}}$, subject to the constraint in Eq. (3.31). This minimization problem can be solved by using a Lagrange multiplier approach (see Appendix A). The optimal gain vector is obtained as

$$\mathbf{w}_{MVDR} = \mathbf{R}_{\mathbf{v},\boldsymbol{\eta}}^{-1}\mathbf{a}\left(\mathbf{a}^H\mathbf{R}_{\mathbf{v},\boldsymbol{\eta}}^{-1}\mathbf{a}\right)^{-1} \tag{3.33}$$

This beamformer is called a minimum variance distortionless response (MVDR) beamformer, and it was first derived by Capon (1969). In Van Trees (2002), this optimal gain vector is obtained in the frequency domain, and further analyses have been performed.

3.2.2 Maximum Likelihood Estimator

It can be easily verified that the MVDR beamformer is the maximum likelihood (ML) estimator, under the assumption that the noise distribution is a circular complex Gaussian random vector (Van Trees 2002). Under this assumption, the conditional probability density function of the received signal, given $s(t)$, would be

$$p_{\mathbf{r}|s}\left(\mathbf{r}(t)\,|\,s(t)\right) = \frac{e^{-(\mathbf{r}^H(t)-\mathbf{a}^H s^*(t))\mathbf{R}_{\mathbf{v},\boldsymbol{\eta}}^{-1}(\mathbf{r}^H(t)-\mathbf{a}s(t))}}{\det\left(\pi\mathbf{R}_{\mathbf{v},\boldsymbol{\eta}}\right)} \tag{3.34}$$

Then, maximizing the log-likelihood function requires minimizing the following term

$$\underset{s(t)}{Min}\,(\mathbf{r}^H(t)-\mathbf{a}^H s^*(t))\mathbf{R}_{\mathbf{v},\boldsymbol{\eta}}^{-1}(\mathbf{r}^H(t)-\mathbf{a}s(t)) \tag{3.35}$$

By taking the complex gradient with respect to $s(t)$, and setting the result equal to zero, the maximum likelihood estimate of $s(t)$ is obtained as

$$s(t)_{ML}=\left(\mathbf{a}^H\mathbf{R}_{\mathbf{v},\boldsymbol{\eta}}^{-1}\mathbf{a}\right)^{-1}\mathbf{a}^H\mathbf{R}_{\mathbf{v},\boldsymbol{\eta}}^{-1}\mathbf{r}(t) \tag{3.36}$$

which indicates that the optimal gain vector applied to the received signal is

$$\mathbf{w}_{ML}=\mathbf{R}_{\mathbf{v},\boldsymbol{\eta}}^{-1}\mathbf{a}\left(\mathbf{a}^H\mathbf{R}_{\mathbf{v},\boldsymbol{\eta}}^{-1}\mathbf{a}\right)^{-1} \tag{3.37}$$

It can be observed that this result is the same as Eq. (3.33).

3.2.3 Maximum Signal to Noise Interference Ratio Beamformer

In this beamformer, the optimization criterion is maximizing the signal-to-noise-plus interference ratio (SINR) of the beamformer signal output. The SINR of the

beamformer output is

$$\underset{\mathbf{w}}{Max} = \frac{\left|z(t)\right|^2}{Noise + Interference} = \underset{\mathbf{w}}{Max} \frac{\mathbf{w}^H \mathbf{R}_{\mathbf{r}} \mathbf{w}}{\mathbf{w}^H \mathbf{R}_{\mathbf{v},\eta} \mathbf{w}} \tag{3.38}$$

This is a generalized Eigen decomposition problem (GED). In order to estimate $\mathbf{w}$, the following problem should be solved:

$$\mathbf{R}_{\mathbf{r}} \mathbf{w} = \lambda_{GE} \mathbf{R}_{\mathbf{v},\eta} \mathbf{w} \tag{3.39}$$

where, λ_{GE} is the largest generalized eigenvalue, and $\mathbf{w}$ is its corresponding eigenvector. It is also possible to come up with the closed form solution for $\mathbf{w}$. To this end, considering that $\mathbf{R}_{\mathbf{v},\eta}$ is a full rank matrix and it is invertible, $\bar{\mathbf{w}}$ can be defined as

$$\bar{\mathbf{w}}^H = \mathbf{w}^H \mathbf{R}_{\mathbf{v},\eta}^{1/2} \tag{3.40}$$

By substituting Eq. (3.40) in Eq. (3.38), the maximization problem is transformed into

$$\underset{\bar{\mathbf{w}}}{Max}\frac{\bar{\mathbf{w}}^H\mathbf{R}_{v,\eta}^{-1/2}\mathbf{R}_r\bar{\mathbf{w}}^H\mathbf{R}_{v,\eta}^{-1/2}\bar{\mathbf{w}}}{\bar{\mathbf{w}}^H\mathbf{R}_{v,\eta}^{-1/2}\mathbf{R}_{v,\eta}\mathbf{R}_{v,\eta}^{-1/2}\bar{\mathbf{w}}}=\underset{\bar{\mathbf{w}}}{Max}\frac{\bar{\mathbf{w}}^H\mathbf{R}_{v,\eta}^{-1/2}\mathbf{R}_r\mathbf{R}_{v,\eta}^{-1/2}\bar{\mathbf{w}}}{\bar{\mathbf{w}}^H\bar{\mathbf{w}}} \tag{3.41}$$

Substituting Eq. (3.28) and Eq. (3.30) in Eq. (3.41) results in

$$\underset{\bar{\mathbf{w}}}{Max}\frac{\bar{\mathbf{w}}^H\mathbf{R}_{v,\eta}^{-1/2}\left(\mathbf{a}\sigma_s^2\mathbf{a}^H+\mathbf{R}_{v,\eta}\right)\bar{\mathbf{w}}^H\mathbf{R}_{v,\eta}^{-1/2}\bar{\mathbf{w}}}{\bar{\mathbf{w}}^H\bar{\mathbf{w}}}=\underset{\bar{\mathbf{w}}}{Max}\frac{\bar{\mathbf{w}}^H\mathbf{R}_{v,\eta}^{-1/2}\mathbf{a}\sigma_s^2\mathbf{a}^H\mathbf{R}_{v,\eta}^{-1/2}\bar{\mathbf{w}}}{\bar{\mathbf{w}}^H\bar{\mathbf{w}}} \tag{3.42}$$

Assuming $\|\bar{\mathbf{w}}\|=1$, this maximization becomes

$$\underset{\|\bar{\mathbf{w}}\|=1}{Max}\,\bar{\mathbf{w}}^H\mathbf{R}_{v,\eta}^{-1/2}\mathbf{a}\sigma_s^2\mathbf{a}^H\mathbf{R}_{v,\eta}^{-1/2}\bar{\mathbf{w}} \tag{3.43}$$

It can be readily verified that

$$\bar{\mathbf{w}}=\frac{\mathbf{R}_{v,\eta}^{-1/2}\mathbf{a}}{\left(\mathbf{a}^H\mathbf{R}_{v,\eta}^{-1}\mathbf{a}\right)} \tag{3.44}$$

and by substituting in Eq. (3.40), $\mathbf{w}_{MSINR}$ is obtained as

$$\mathbf{w}_{MSINR}=\mathbf{R}_{v,\eta}^{-1}\mathbf{a}\left(\mathbf{a}^H\mathbf{R}_{v,\eta}^{-1}\mathbf{a}\right)^{-1} \tag{3.45}$$

The same result was also derived in the frequency domain (Van Trees 2002). It can

be seen that the obtained gain vector is the same as the previously introduced beamformers. In fact, for a wide class of criteria, the optimal gain vector is obtained from Eq. (3.33), followed by a scalar that depends on the criterion (Van Trees 1966)

3.2.4 Minimum Power Distortionless Response Beamformer

The main problem with the MVDR beamformer is that the interference-plus-noise spatial correlation matrix is assumed to be known, which is difficult or impossible to estimate in some applications. To deal with this problem, the minimum power distortionless response (MPDR) beamformer was developed. In this beamformer, instead of using $\mathbf{R}_{v,\eta}$, $\mathbf{R}_{r}$ is employed in the beamforming process. Hence, the gain vector for a MPDR beamformer is obtained as

$$\mathbf{w}_{MPDR} = \mathbf{R}_{r}\mathbf{a}\left(\mathbf{a}^{H}\mathbf{R}_{v,\eta}^{-1}\mathbf{a}\right)^{-1} \tag{3.46}$$

MVDR and MPDR are equivalent, as long as there is no mismatch between the estimated steering vector of the desired signal and the actual value. However, in the case of a steering vector mismatch, the MVDR beamformer outperforms the MPDR beamformer (Van Trees 2002). The MPDR beamformer was first pointed for GPS by Zoltowski & Gecan (1995), who also extended the concept for the case when the

steering vectors of the GPS signals are unknown.

3.2.5 Linear Constrained Minimum Variance and Linear Constrained Minimum Power Beamformers

In the MVDR and MPDR beamformers, only one constraint is considered. These beamformers can be generalized to the cases in which several constraints are imposed in the optimization problem. This can be advantageous for multi-constraint optimization problems, or for beam shaping (Van Trees 2002, Buckley & Griffits 1986, Er & Cantoni 1983). The extended versions of MVDR and MPDR beamformers are referred to as linear constrained minimum variance (LCMV), and linear constrained minimum power (LCMP), respectively. Assume that there are several linear constraints put in matrix . $\mathbf{C}_{const}$, of which columns are linearly independent. These constraints can be expressed as

$$\mathbf{w}^H \mathbf{C}_{const} = \mathbf{f}^H. \tag{3.47}$$

The value of $\mathbf{f}$ depends on the problem at hand. Therefore, the optimization problem in LCMV is

$$\begin{aligned} &\underset{\mathbf{w}}{Min}\, \mathbf{w}^H \mathbf{R}_{\mathbf{v},\eta} \mathbf{w} \\ &subject\ to\ \mathbf{w}^H \mathbf{C}_{const} = \mathbf{f}^H. \end{aligned} \tag{3.48}$$

and similarly for LCMP is

$$\begin{aligned} &\underset{\mathbf{w}}{Min}\, \mathbf{w}^H \mathbf{R}_{\mathbf{r}} \mathbf{w} \\ &subject\ to\ \mathbf{w}^H \mathbf{C}_{const} = \mathbf{f}^H. \end{aligned} \tag{3.49}$$

The Lagrange multiplier method can be also employed to solve the optimization problem in Eq. (3.48) and Eq. (3.49) (Van Trees 2002, Frost 1972). The results are given as follows (see Appendix A):

$$\begin{aligned} \mathbf{w}_{LCMV} &= \mathbf{R}_{\mathbf{v},\eta}^{-1} \mathbf{C}_{const} \left(\mathbf{C}_{const}^H \mathbf{R}_{\mathbf{v},\eta}^{-1} \mathbf{C}_{const} \right)^{-1} \mathbf{f} \\ \mathbf{w}_{LCMP} &= \mathbf{R}_{\mathbf{r}}^{-1} \mathbf{C}_{const} \left(\mathbf{C}_{const}^H \mathbf{R}_{\mathbf{r}}^{-1} \mathbf{C}_{const} \right)^{-1} \mathbf{f} \end{aligned} \tag{3.50}$$

3.2.6 Eigenvector Beamformer

In order to reduce the computational complexity of beamforming, eigenvector beamformers were introduced. In addition, they can also be useful for applications in which the environment is stationary over only a short period, and the number of samples is limited, in order to form the spatial correlation matrix (Van trees 2002).

Generally, these beamformers project the received signals into the reduced rank subspace, including the desired signal and interference. Then, the beamforming methods are applied to this subspace. Therefore, there is no need to completely calculate the spatial correlation matrix $\mathbf{R}_r$ or $\mathbf{R}_{v,\eta}$. This approach was studied under different names, although they are essentially the same. Under the eigenvector name, there are algorithms introduced by Hung & Tunder (1983), Citron & Kailath (1984), Friedlander (1988), Haimovich & Bar-Ness (1988), Haimovich & Bar-Ness (1991), Van Veen & Buckley (1988), Chang & Yeh (1992), Youn & Un (1994) and Yu & Yeh (1995). Under the name of reduced covariance matrix, this beamformer was studied by Kirstein & Tufts (1985), and under the projection name, this approach was studied by Feldman & Griffiths (1991, 1994), and there are so many other papers in this context. Eigenvector beamformers have been extensively studied in Van Tees (2002), where more references are provided.

In GPS applications, beamforming can be performed in two different ways: before despreading, and after despreading. If a beamformer is applied after despreading, the conventional eigenvector can be applied (for example for multipath mitigation). On the other hand, for mitigating high power interfering signals, since the desired signal is below the noise floor, the eigenvector beamforming should be modified and applied, before despreading. In this case, the desired signal belongs to the noise subspace. Therefore, instead of projecting the received signal into the interference-plus-signal

subspace, the received signal should be projected to the noise-plus-signal subspace (e.g. Sun & Amin 2005b). Herein, the eigenvector beamformer is reformulated for this case.

The spatial correlation matrix $\mathbf{R}_{\mathrm{r}}$ is first decomposed in terms of its eigenvalues and eigenvectors, as

$$\begin{aligned}\mathbf{R}_{\mathrm{r}} &= \begin{bmatrix} \underset{N\times 1}{\mathbf{U}_{Int}} & \underset{N\times(N-1)}{\mathbf{U}_{S+N}} \end{bmatrix} \begin{bmatrix} \underset{I\times I}{\mathbf{\Lambda}_{Int}} & \underset{I\times(N-I)}{\mathbf{0}} \\ \underset{(N-I)\times I}{\mathbf{0}} & \underset{(N-I)\times(N-I)}{\mathbf{\Lambda}_{S+N}} \end{bmatrix} \begin{bmatrix} \mathbf{U}_{Int}^{H} \\ \mathbf{U}_{S+N}^{H} \end{bmatrix} \\ &= \mathbf{U}_{Int}\mathbf{\Lambda}_{Int}\mathbf{U}_{Int}^{H} + \mathbf{U}_{S+N}\mathbf{\Lambda}_{S+N}\mathbf{U}_{S+N}^{H}\end{aligned} \tag{3.51}$$

where, $\mathbf{U}_{Int}$ and $\mathbf{U}_{S+N}$ are the eigenvector matrices of the interference and noise-plus-signal subspaces, respectively, and $\mathbf{\Lambda}_{Int}$ and $\mathbf{\Lambda}_{S+N}$ are the corresponding eigenvalue matrices. It can be easily verified that

$$\mathbf{R}_{\mathrm{r}}^{-1} = \mathbf{U}_{Int}\mathbf{\Lambda}_{Int}^{-1}\mathbf{U}_{Int}^{H} + \mathbf{U}_{S+N}\mathbf{\Lambda}_{S+N}^{-1}\mathbf{U}_{S+N}^{H} \tag{3.52}$$

In order to be effective, an interfering signal should have stronger power than that of the noise and GNSS signals. Consequently, the eigenvalues of the interference subspace are much larger than those of the noise-plus-GPS subspace. Hence, $\mathbf{R}_{\mathrm{r}}^{-1}$ in Eq. (3.52) can be approximated as

$$\mathbf{R}_{\mathbf{r}}^{-1} \cong \mathbf{U}_{S+N}\mathbf{\Lambda}_{S+N}^{-1}\mathbf{U}_{S+N}^{H} \tag{3.53}$$

By substituting Eq. (3.53) in Eq. (3.46), the optimal gain vector for the eigenvector beamformer becomes

$$\mathbf{w}_{EG} = \beta\mathbf{U}_{S+N}\mathbf{\Lambda}_{S+N}^{-1}\mathbf{U}_{S+N}^{H}\mathbf{a} \tag{3.54}$$

in which β is a scale factor, equal to

$$\beta = \left(\mathbf{a}^{H}\mathbf{U}_{S+N}\mathbf{\Lambda}_{S+N}^{-1}\mathbf{U}_{S+N}^{H}\mathbf{a}\right)^{-1} \tag{3.55}$$

To study this from the projection concept point of view, assume that $\bar{\mathbf{a}}$ is the projected steering vector of the desired signal into the noise-plus-GNSS subspace, and is defined as

$$\bar{\mathbf{a}} \cong \mathbf{P}_{N+S}\mathbf{a} \tag{3.56}$$

where, $\mathbf{P}_{N+S}$ is the projection matrix into the noise-plus-GNSS subspace, defined as

$$\mathbf{P}_{N+S} \cong \mathbf{U}_{S+N}^{H} \tag{3.57}$$

The optimal gain vector in Eq. (3.54) can be simplified as

$$\begin{aligned} \mathbf{w}_{\mathrm{Pr}oj}^{H} &= \beta \mathbf{P}_{S+N}^{H} \boldsymbol{\Lambda}_{S+N}^{-1} \mathbf{P}_{S+N} \\ \beta &= \left(\overline{\mathbf{a}}^{H} \boldsymbol{\Lambda}_{S+N}^{-1} \overline{\mathbf{a}} \right)^{-1} \end{aligned} \tag{3.58}$$

If the obtained gain vector is applied to the received signal vector, the beamformer output is equal to

$$y(t) = \beta \mathbf{P}_{S+N}^{H} \boldsymbol{\Lambda}_{S+N}^{-1} \overline{\mathbf{r}}(t) \tag{3.59}$$

where, $\overline{\mathbf{r}}(t)$ is the projected received signal into the noise-plus-GNSS subspace, defined as

$$\overline{\mathbf{r}}(t) \cong \mathbf{P}_{S+N} \mathbf{r}(t) \tag{3.60}$$

3.3 Space-Time Processing

Space-time processing techniques take advantage of both spatial and temporal processing domains. This is a mature field of study that has been in existence for several decades, and originates from radar applications for increasing SINR (Melvin

2004, Klemm 2004, Applebaum 1976, Brennan & Reed 1974, Frost 1972). It was later employed for channel equalization and multiuser code division multiple access (CDMA), in order to decrease the bit error rate of the transmitted data, and to increase the capacity of the system (Paulraj & Papadias 1997). These techniques are generally referred to as space-time adaptive processing (STAP), or space-frequency adaptive processing (SFAP), which is its corresponding use in the frequency domain. STAP and SFAP approaches have been employed and implemented in many applications. Utilizing these techniques in GPS applications, however, requires a number of considerations, in order to prevent induced biases in pseudorange and carrier phase measurements (Fante et al 2004). Considering STAP for GPS dates back to the early 1990s (Moelker et al 1996, Ramos et al 1996, Agamata 1991). In particular, the distortion and bias caused on the cross correlation function due to space-time filtering, and the related countermeasure techniques, have been of great interest in the literature (O'Brien & Gupta 2011, Lorenzo 2007, McGraw et al 2006, Lorenzo et al 2006, Falcone et al 2000, Fante et al 2004, McGraw et al 2004, Fante & Vaccaro 1998a, Fante & Vaccaro 1998b, Hatke 1998, Myrick et al 2001).

Generally, the term "Adaptive array" means that the array follows the changes in environment (e.g. alteration in the characteristics of interference signals), and constantly adapts its own pattern, by means of a feedback control. This term is employed, as opposed to the deterministic beamformer introduced in the previous

sections. Adaptivity is not the only benefit of STAP techniques. In addition to this feature, increasing the degree of freedom of the antenna array is also an important advantage, which is the topic of interest in this thesis. In the remainder of this section, space-time processing from the viewpoint of increasing the degree of freedom of the array is introduced.

The standard implementation of the STAP methods consists of an antenna array in which each antenna element is followed by a temporal filter or a tapped delay line (TDL), with the tap delay time typically equal to the sampling duration (see Figure 3.5).

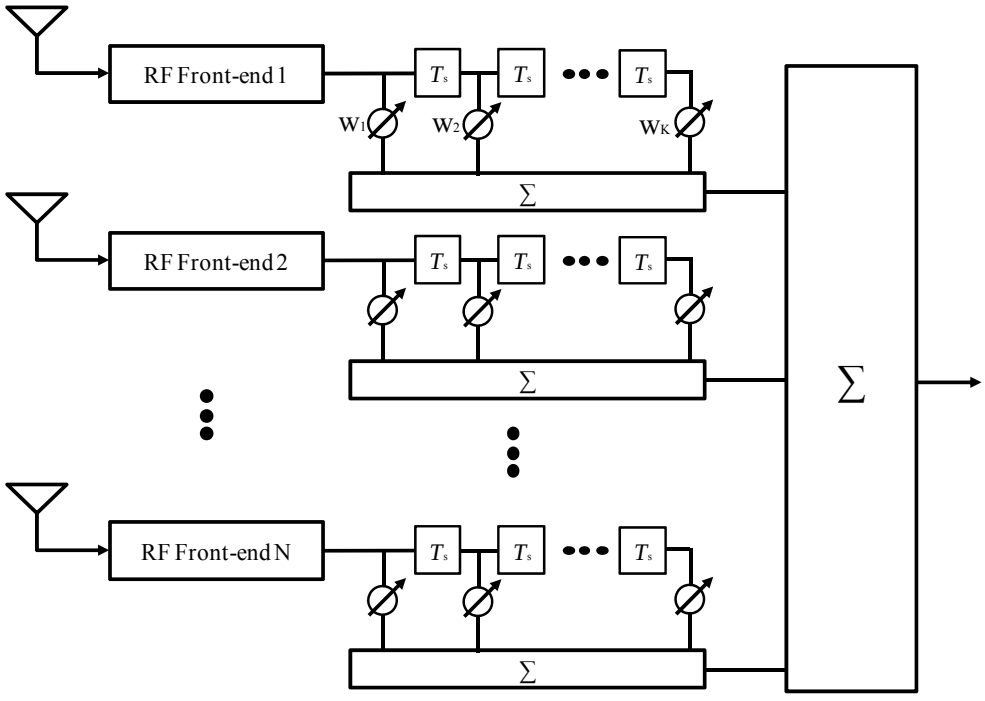

Figure 3.5 General structure of a space-time processor

A space-time antenna array with *N* antenna elements and TDLs with *K* taps leaves *KN* unknown gains, which should be determined. For each time snapshot, *KN* samples of all TDL taps form a $KN \times 1$ received signal vector, as

$$\vec{\mathbf{r}} = \left[r_{1,1}\, r_{2,1} \cdots r_{1,N} \quad r_{2,1}\, r_{2,2} \cdots r_{2,N} \cdots r_{K,1}\, r_{K,1} \cdots r_{K,N} \right]^T \tag{3.61}$$

in which, $r_{k,n}$ is the time sample of the *k*th tap, $k = 1, 2, \cdots, K$, for the *n*th antenna element, $n = 1, 2, \cdots, N$. Then the augmented spatial correlation matrix can be formed as

$$\mathbf{R}_{\vec{\mathbf{r}}} = E\left\{ \vec{\mathbf{r}}(t) \vec{\mathbf{r}}^H(t) \right\} \tag{3.62}$$

Considering the dimension of $\mathbf{R}_{\vec{\mathbf{r}}}$, the array degree of freedom becomes at most $KN - 1$, which is increased by the factor of K, compared to only-space processing. The augmented correlation matrix can be utilized in the beamforming methods introduced in Section 3.2. Nevertheless, more constraints should be put on optimization problems, in order to avoid the bias and distortion in the cross correlation function (e. g. Myrick et al 2001).

3.4 Array Calibration

Array calibration is one of the main challenges in employing antenna arrays. (Gupta et al 2003). Due to mutual coupling between antennas, antenna gain/phase mismatches, antenna phase center variations and RF front-end distortions and etc., there are additional unknown phase offsets that should be taken into account, during most antenna array-based applications. Array calibration becomes a critical stage of the antenna array processing, if in the beamformer structure, the array manifold vector of one or more incident signals is assumed to be known, or to be estimated. Much research on array calibration has been pursued, since the antenna array and beamforming techniques were introduced. In GNSS applications, there are also several publications that have studied different array calibration methods (e. g. Church & Gupta 2009, Backen et al. 2008, Gupta et al. 2003, Ng & See 1996). Studying calibration methods is out of the scope of this research. In this dissertation, if the steering vectors of the incident signals are explicitly employed in optimization problems, it is assumed that array calibration is already performed; otherwise there is no need for array calibration. Herein, the beamformer that does need require any array calibration is referred to as a blind beamformer. In other words, the array manifold vectors of the incident signals are not employed in the beamforming process.

3.5 Summary

This chapter concisely brings together the fundamentals of antenna array processing focused on the topics related to GPS applications. Section 3.1 provides a brief background on antenna array processing and beamforming, a general signal model, and basic principles. Section 3.2 presents a number of important optimum beamformers, which are referred to, or employed, in the succeeding chapters. Finally, space-time array processing and array calibration are briefly introduced in Section 3.3 and Section 3.4, respectively.

Chapter 4
Multipath Mitigation using Code-Carrier Information

4.1 Introduction

The Global Positioning System (GPS) has been widely used around the world. It provides the information required to obtain a precise time reference and position in many applications, such as navigation, land surveying, and synchronization for telecommunication networks. The GPS receiver measures the travelling time of the signal from the satellite to the receiver. In order to measure the precise signal travelling time, the synchronization of the receiver is a key factor. However, strong interference (including jamming signals) and multipath effects make GPS vulnerable to receiver synchronization problems. Therefore, GPS receivers must be designed to mitigate these interference and multipath effects. In the literature, various algorithms have been proposed for interference cancellation, such as power minimization, the MVDR algorithm, beam forming and nulling etc (Van Trees 2002, Van Veen & Buckley 1998, Krim & Viberg 1996 & Amin 2006). In this thesis, a subspace projection scheme was proposed to remove interference signals. It was shown that the interference signals can

be effectively cancelled out by projecting the received GPS signal into an interference free subspace. The projection matrix was obtained by the singular value decomposition of the correlation matrix of the received signals. In practice, however, multipath signals as well as interference signals should be suppressed to achieve good receiver synchronization.

4.2 **Interference Suppression and Multipath Mitigation**

4.2.1 **Signal Model**

A GPS receiver with a spatial array is considered. The signal received by the array consists of the GPS signal and its multipath, interference, and noise. As a discrete time baseband signal model, the received signal vector from the antenna array can be presented as follows (Amin 2006)

$$\mathbf{x}_k = \sum_{k=0}^{K} s_k(n)\, c_k\left(nT_s - \tau_k(n)\right)\mathbf{a_k} + \sum_{l=1}^{L} u_l(n)\,\mathbf{d_l} + \mathbf{v}(n) \tag{4.1}$$

where,

T_s = Nyquist sampling interval

K = Number of multipath components

$s_k(n)$	=	k-th signal component
c_k	=	k-th C/A code sample
$\tau_k(n)$	=	Time delay of the k-th component
$\mathbf{a_k}$	=	Spatial signature of the k-th satellite multipath
L	=	Number of interference components
$u_l(n)$	=	Waveform of the l-th interference
$\mathbf{d}_l$	=	Spatial signature of the l-th interference
$\mathbf{v(n)}$	=	Additive white Gaussian noise samplevector
n	=	Time index

where only one satellite is considered due to the very low cross-correlation of the C/A-codes between different satellites. Eq.(4.1) can be rewritten as

$$\mathbf{x}(n) = \mathbf{s}(n) + \mathbf{s_m}(n) + \mathbf{u}(n) + \mathbf{v}(n) \tag{4.2}$$

where, $\mathbf{s}(n)$ denotes the direct-path signal, $\mathbf{s_m}(n)$ denotes the contributions from K multipath superposition and $\mathbf{u}(n)$ is the L superposed interference vector.

$$\begin{aligned}\mathbf{s}(n) &\cong s_0(n)c_0\left(nT_s-\tau_0(n)\right)\mathbf{a_0}\\ \mathbf{s_m}(n) &\cong \sum_{k=1}^{K} s_k(n)c_k\left(nT_s-\tau_k(n)\right)\mathbf{a_k}\\ \mathbf{u}(n) &\cong \sum_{l=1}^{L} u_l(n)\mathbf{d_l}\end{aligned} \tag{4.3}$$

4.2.2 **Interference Suppression by Subspace Projection**

Under the assumption that the GPS signals, interference, and noise are independent, the covariance matrix of the received signal becomes

$$\mathbf{R}_{xx} = E\left\{\mathbf{x}(n)\,\mathbf{x}^{\mathbf{H}}(n)\right\} = \mathbf{R_s} + \mathbf{R_u} + \mathbf{R_v} \tag{4.4}$$

where, $E\{\bullet\}$ represents the statistical expectation, $(\bullet)^H$ denotes the conjugate transpose, and $\mathbf{R_s}$, $\mathbf{R_u}$, and $\mathbf{R_v}$ are the covariance matrices of the GPS signals, the interference, and the noise, respectively, which are defined respectively as:

$$\mathbf{R_s} \cong E\left\{\left[\mathbf{s}(n)+\mathbf{s_m}(n)\right]\left[\mathbf{s}(n)+\mathbf{s_m}(n)\right]^H\right\} \tag{4.5}$$

$$\mathbf{R_u} \cong E\left\{\mathbf{u}(n)\mathbf{u}^{\mathbf{H}}(n)\right\} \tag{4.6}$$

$$\mathbf{R}_{\mathbf{v}} \cong E\left\{\mathbf{v}(n)\mathbf{v}^{\mathbf{H}}(n)\right\} = \sigma_v^2 \mathbf{I}_{\mathbf{M}} \tag{4.7}$$

where, $\mathbf{I}_{\mathbf{M}}$ is an $M \times M$ identity marix.

The subspace tracking based GPS anti-jam receiver is motivated by the fact that in GPS, the desired GPS signals are sufficiently below the noise floor (usually 20 to 30 dB below the noise floor). As such, the total received signal power is dominated by the jamming signals. In this case, the covariance matrix $\mathbf{R}_{xx}$ is approximated as follows

$$\mathbf{R}_{xx} \cong \mathbf{R}_{\mathbf{v}} + \mathbf{R}_{\mathbf{u}} \tag{4.8}$$

The received signal space can be decomposed into two subspaces (i.e., the interference subspace and noise subspace) by the singular value decomposition (SVD) of $\mathbf{R}_{xx}$.

$$\begin{aligned} \mathbf{R}_{xx} &= \sum_{i=1}^{M} \lambda_i \mathbf{e}_{\mathbf{i}} \mathbf{e}_{\mathbf{i}}^{\mathbf{H}} \\ &\cong \sum_{i=1}^{L} \lambda_i \mathbf{e}_{\mathbf{i}} \mathbf{e}_{\mathbf{i}}^{\mathbf{H}} + \sigma_v^2 \sum_{i=L+1}^{M} \mathbf{e}_{\mathbf{i}} \mathbf{e}_{\mathbf{i}}^{\mathbf{H}} \\ &\cong \mathbf{U}_{\mathbf{I}} \sum_{\mathbf{I}} \mathbf{U}_{\mathbf{I}}^{\mathbf{H}} + \mathbf{U}_{\mathbf{V}} \sum_{\mathbf{V}} \mathbf{U}_{\mathbf{V}}^{\mathbf{H}} \end{aligned} \tag{4.9}$$

where $\sum_{\mathbf{I}}$ is an $L \times L$ diagonal matrix of which the elements are the L largest eigenvalues, $\lambda_1, \lambda_2, \cdots \lambda_L$. $\mathbf{U}_{\mathbf{I}}$ is an $M \times L$ matrix of which the columns are the

eigenvectors, $\mathbf{e}_1, \mathbf{e}_2, \cdots \mathbf{e}_L$, associated with the L largest eigenvalues. These eigenvectors, $\mathbf{e}_1, \mathbf{e}_2, \cdots \mathbf{e}_L$, span the interference subspace. $\sum_{\mathbf{V}} = \sigma_v^2 \mathbf{I}_{M-L}$ is an $(M-L)\times(M-L)$ diagonal matrix of which the elements are the $M-L$ constant eigenvalues. The columns of the $M \times (M-L)$ matrix, $\mathbf{U}_{\mathbf{V}}$, are the associated $M-L$ eigenvectors of the constant eigenvalues, which span the noise subspace. The interference-free signal can be obtained from the orthogonal projection of the received signal into the interference-free subspace. In this case, the projection matrix, $\mathbf{U}_{\mathbf{I}}^{\perp}$, is represented as

$$\mathbf{U}_{\mathbf{I}}^{\perp} = \mathbf{I}_{\mathbf{M}} - \mathbf{U}_{\mathbf{I}} \left(\mathbf{U}_{\mathbf{I}}^{\mathbf{H}} \mathbf{U}_{\mathbf{I}} \right)^{-1} \mathbf{U}_{\mathbf{I}}^{\mathbf{H}} \tag{4.10}$$

where, $(\bullet)^{-1}$ denotes the matrix inverse. In other words, the interference-free signal, $y(n)$, is obtained by the projection of $x(n)$ onto $\mathbf{U}_{\mathbf{I}}^{\perp}$, as follows

$$\begin{aligned} y(n) &= \mathbf{U}_{\mathbf{I}}^{\perp} x(n) \\ &= \mathbf{U}_{\mathbf{I}}^{\perp} \left[\mathbf{s}(n) + \mathbf{s}_{\mathbf{m}}(n) \right] + \mathbf{U}_{\mathbf{I}}^{\perp} \mathbf{u}(n) + \mathbf{U}_{\mathbf{I}}^{\perp} \mathbf{v}(n) \\ &= \mathbf{U}_{\mathbf{I}}^{\perp} \left[\mathbf{s}(n) + \mathbf{s}_{\mathbf{m}}(n) \right] + \mathbf{U}_{\mathbf{I}}^{\perp} \mathbf{v}(n) \end{aligned} \tag{4.11}$$

$\mathbf{U}_{\mathbf{I}}^{\perp}$ is orthogonal to $\mathbf{u}(n)$.

4.2.3 **Multipath Mitigation by Subspace Projection**

Multipath signals are known to be often generated from local scatters near the horizon. Therefore, without knowing the exact directions of the multipath signals, in many of the previous studies it is assumed that most of the multipath signals are derived from properly spaced directions of r_d, $d = 1, 2, \cdots, D$, covering a particular angle, Ω, near the horizon(Amin 2005), as shown in Fig. 4.1. This is a theoretical limitation of the conventional method to estimate the spatial signature vectors of the multipath signals. Let $\mathbf{A} \equiv \left[\mathbf{b}(r_1) \cdots \mathbf{b}(r_D)\right]$ be the $M \times D$ matrix consisting of the spatial signature vectors of the multipath signals. We assume that the number of multipath signals is less than the number of antennas (i.e. $D < M$) and that each spatial signature is linearly independent. At first, the multipath signal spatial signature vectors, $\mathbf{A}$, should be projected into $\mathbf{U}_\mathbf{I}^\perp$, which means that we need to obtain the interference-free multipath signal spatial signature vectors, $\mathbf{B}$, as follows

$$\mathbf{B} = \mathbf{U}_\mathbf{I}^\perp \mathbf{A} \tag{4.12}$$

Performing the singular value decomposition (SVD) of B yields

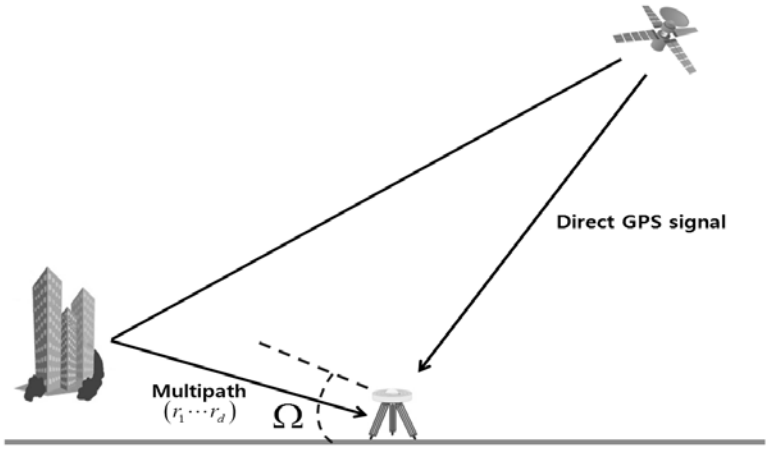

Figure 4.1 Ranging of GPS multipath angles

$$\mathbf{U}_{\Omega}^{H}\mathbf{B}^{H}\mathbf{V}_{\Omega}^{H} = \begin{bmatrix} \Lambda & 0 \\ 0 & 0 \end{bmatrix} \tag{4.13}$$

where, $\mathbf{U}_{\Omega}$ and $\mathbf{V}_{\Omega}$ are two unitary matrices with dimensions $M \times M$ and $D \times D$, respectively, and

$$\lambda_1, \lambda_2, \cdots, \lambda_r \ \lambda = diag\{\lambda_1, \lambda_2, \cdots, \lambda_r\} \tag{4.14}$$

where, $\lambda_1 \geq \lambda_2 \geq \cdots \geq \lambda_r$ are the eigenvalues of $\mathbf{B}$ arranged in decreasing order. Let $\mathbf{U}_{\mathbf{B}}$ be formed from the first D columns of $\mathbf{U}_{\Omega}$. Then, $\mathbf{U}_{\mathbf{B}}$ spans the multipath subspace inside the interference-free space. The multipath-free subspace can be

obtained from the orthogonal projection of the multipath subspace, which is given by

$$\mathbf{U}_{\mathbf{B}}^{\perp} = \mathbf{I}_{\mathbf{M}} - \mathbf{U}_{\mathbf{B}} \left(\mathbf{U}_{\mathbf{B}}^{\mathbf{H}} \mathbf{U}_{\mathbf{B}} \right)^{-1} \mathbf{U}_{\mathbf{B}}^{\mathbf{H}} \tag{4.15}$$

4.3 Determination of Multipath Satellites using Code-Carrier Information

In the previous chapter, it was shown that the conventional multipath subspace projection techniques may not completely estimate the spatial signature vectors of the multipath signals. Therefore, to mitigate multipath error, prior knowledge about the steering vector of the LOS signal is required in this method. In this thesis, in order to estimate the spatial signature vectors of the multipath signals, code carrier information was used. The determination of a multipath satellite is the main problem when applying a beamforming algorithm using a multiple array antenna system. A multiple array antenna system is plotted in Fig. 4.2. As shown in Fig. 4. 2, if the elevation angel (θ), azimuth angle (ϕ_n), and distance to the antenna (a) are available, the positioning vector is obtained as follows

$$\hat{\rho}_n = \cos\phi_n \hat{x} + \sin\phi_n \hat{y} \tag{4.16}$$

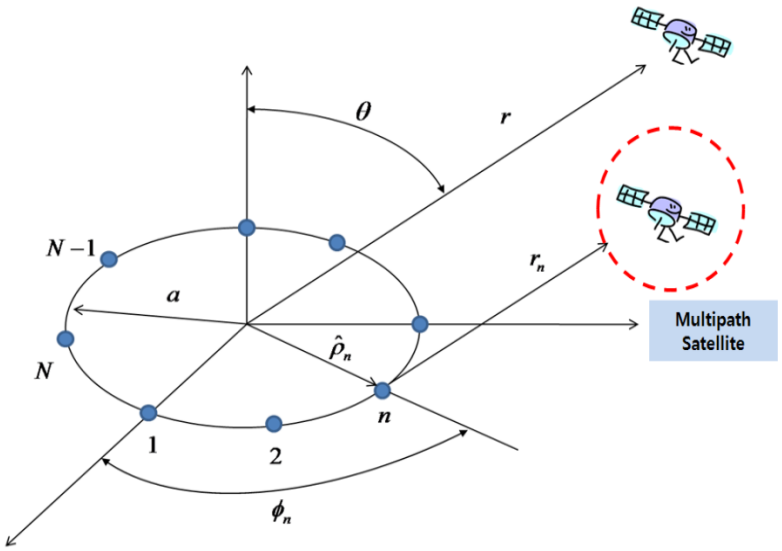

Figure 4.2 Multiple array antenna system

$$\hat{r} = \sin\theta\cos\phi_n\hat{x} + \sin\theta d\cos\phi_n\hat{y} + \cos\theta\hat{z} \tag{4.17}$$

$$r_n = r - a\hat{\rho}_n \cdot \hat{r} \tag{4.18}$$

where, $\hat{x}, \hat{y}, \hat{z}$ the represent unit vectors of x, y, z, respectively. $\hat{\rho}_n$ is the position vector of n-th antenna on the surface. $\hat{r}$ is a unit vector of r and a is the distance from the center of the antenna.

From the ephemeris information in the GPS system, the information of the satellite azimuth and elevation can be easily obtained. Therefore, if it is possible to distinguish between the line of sight satellite and the non-line of sight satellite, beamforming toward a multipath satellite is possible. To calculate the spatial signature vectors, a

code carrier measurement is used to distinguish them when including a multipath satellite. A code and carrier measurements are represented as follows

$$r_k = \rho_k + \Delta\delta_k + I_k + T_k + U_k^1 \tag{4.19}$$

$$\lambda\Phi_k = \rho_k + \lambda N - I_k + T_k + U_k^2 \tag{4.20}$$

where,

ρ_k	=	Distance between receiver and satellite
δ_k	=	Clock bias between receiver and satellite
I_k	=	Ionospheric error
T_k	=	Tropospheric error
λ	=	Wavelength of phase
U_k	=	Uncommon error (Multipath)
L	=	Number of interference components
N	=	Ambiguity integer
R	=	Pseudo range

The difference of code and phase measurement is defined by z_k, z_k is represented as

$$r_k - \lambda\Phi_k = 2I_k - \lambda N + U_k \tag{4.21}$$

$$z_k = r_k - \lambda\Phi_k \tag{4.22}$$

The carrier phase and pseudorange (code) double differences (DDs) is defined as follows

$$\begin{aligned} d_{k+1} &= z_{k+1} - z_k \\ &= 2I_{k+1} - \lambda N + U_{k+1} - 2I_k + \lambda N - U_k \\ &= 2\left(I_{k+1} - I_k\right) + \left(U_{k+1} - U_k\right) \end{aligned} \tag{4.23}$$

Inospheric propagation delay can be ignored for a short period of time (1 hour). Therefore, Eq. (4.23) consists of only the uncommon error source (Multipath). The double difference of code and carrier phase information can be used to estimate the spatial signature vectors of the multipath. The formation of the double difference of the code and carrier phase offers considerable advantage because of the ultimate cancellation of the receiver and satellite clock biases, and most of the inospheric propagation delay. If the two antennas are located at the same elevation, the tropospheric propagation delay will also be largely cancelled.

The spatial signature vectors of the multipath signal using code carrier information can be expressed as

$$\mathbf{A}_{code-carrier} \equiv \left[\mathbf{b}\left(r_1\right) \cdots \mathbf{b}\left(r_D\right)\right] \tag{4.24}$$

The interference-free multipath signal spatial signature vectors based on code carrier information, $\mathbf{B}_{code-carrier}$, are as follows

$$\mathbf{B}_{code-carrier} = \mathbf{U}_{\mathbf{I}}^{\perp}\mathbf{A}_{code-carrier} \tag{4.25}$$

The multipath-free subspace can be obtained from the orthogonal projection of the multipath subspace, which is given by

$$\mathbf{U}_{\mathbf{B}_{code-carrier}}^{\perp} = \mathbf{I}_{\mathbf{M}} - \mathbf{U}_{\mathbf{B}_{code-carrier}}\left(\mathbf{U}_{\mathbf{B}_{code-carrier}}^{\mathbf{H}}\mathbf{U}_{\mathbf{B}_{code-carrier}}\right)^{-1}\mathbf{U}_{\mathbf{B}_{code-carrier}}^{\mathbf{H}} \tag{4.26}$$

The interference and multipath free signal using code carrier information, $\mathbf{f}\left(n\right)$, is obtained by the projection of $\mathbf{y}\left(n\right)$ onto $\mathbf{U}_{\mathbf{B}_{code-carrier}}^{\perp}$, as follows

$$\begin{aligned}\mathbf{f}\left(n\right) &= \mathbf{U}_{\mathbf{B}_{c-c}}^{\perp}\mathbf{y}\left(n\right) \\ &= \mathbf{U}_{\mathbf{B}_{c-c}}^{\perp}\mathbf{U}_{\mathbf{I}}^{\perp}\mathbf{s}\left(n\right) + \mathbf{U}_{\mathbf{B}_{c-c}}^{\perp}\mathbf{U}_{\mathbf{I}}^{\perp}\mathbf{v}\left(n\right)\end{aligned} \tag{4.27}$$

4.4 **MSNR Beamformer**

After the interference cancellation and multipath mitigation, the GPS signal is still very weak compared to the noise level. The synchronization is performed by identifying the maximum point of cross-correlation between the received signal and a locally generated C/Acode (Amin 2006 & Shin 2007). The weakness of the GPS signal means it is difficult to synchronize the receiver with the satellite. In order to enhance the GPS signal level, we use a maximum signal-to-noise ratio (MSNR) filter following the previous series of subspace projection processes. The MSNR filter coefficients are denoted by the $M \times 1$ weight vector, $\boldsymbol{\omega}$. Then, the output of the filter is given by

$$\begin{aligned} z(n) &= \boldsymbol{\omega}^H \mathbf{f}(n) \\ &= \boldsymbol{\omega}^H \mathbf{U}_{\mathbf{B}_{c-c}}^{\perp} \mathbf{U}_{\mathbf{I}}^{\perp} \mathbf{s}(n) + \boldsymbol{\omega}^H \mathbf{U}_{\mathbf{B}_{c-c}}^{\perp} \mathbf{U}_{\mathbf{I}}^{\perp} \mathbf{v}(n) \end{aligned} \tag{4.28}$$

and the filter coefficient vector, $\boldsymbol{\omega}$, is determined to maximize the signal-to-noise ratio as follows

$$
\begin{aligned}
\boldsymbol{\omega}_{MSNR} &= \underset{\omega}{\operatorname{argmax}} \frac{E\left\{\left|\boldsymbol{\omega}^H \mathbf{U}_{\mathbf{B}_{c-c}}^{\perp} \mathbf{U}_{\mathbf{I}}^{\perp} \mathbf{s}(n)\right|^2\right\}}{E\left\{\left|\boldsymbol{\omega}^H \mathbf{U}_{\mathbf{B}_{c-c}}^{\perp} \mathbf{U}_{\mathbf{I}}^{\perp} \mathbf{v}(n)\right|^2\right\}} \\
&= \underset{\omega}{\operatorname{argmax}} \frac{\boldsymbol{\omega}^H \mathbf{U}_{\mathbf{B}_{c-c}}^{\perp} \mathbf{U}_{\mathbf{I}}^{\perp} \mathbf{R}_{\mathbf{s}} \mathbf{U}_{\mathbf{I}}^{H} \mathbf{U}_{\mathbf{B}_{c-c}}^{H} \boldsymbol{\omega}}{\boldsymbol{\omega}^H \mathbf{U}_{\mathbf{B}_{c-c}}^{\perp} \mathbf{U}_{\mathbf{I}}^{\perp} \mathbf{R}_{\mathbf{v}} \mathbf{U}_{\mathbf{I}}^{H} \mathbf{U}_{\mathbf{B}_{c-c}}^{H} \boldsymbol{\omega}} \\
&= \underset{\omega}{\operatorname{argmax}} \frac{\boldsymbol{\omega}^H \mathbf{U}_{\mathbf{B}_{c-c}}^{\perp} \mathbf{U}_{\mathbf{I}}^{\perp} \mathbf{R}_{\mathbf{s}} \mathbf{U}_{\mathbf{I}}^{H} \mathbf{U}_{\mathbf{B}_{c-c}}^{H} \boldsymbol{\omega}}{\sigma_v^2 \boldsymbol{\omega}^H \mathbf{U}_{\mathbf{B}_{c-c}}^{\perp} \mathbf{U}_{\mathbf{I}}^{\perp} \mathbf{U}_{\mathbf{I}}^{H} \mathbf{U}_{\mathbf{B}_{c-c}}^{H} \boldsymbol{\omega}} \\
&= \underset{\omega}{\operatorname{argmax}} \frac{\boldsymbol{\omega}^H \mathbf{U}_{\mathbf{B}_{c-c}}^{\perp} \mathbf{U}_{\mathbf{I}}^{\perp} \left(\mathbf{R}_{xx} - \mathbf{R}_u - \mathbf{R}_v\right) \mathbf{U}_{\mathbf{I}}^{H} \mathbf{U}_{\mathbf{B}_{c-c}}^{H} \boldsymbol{\omega}}{\sigma_v^2 \boldsymbol{\omega}^H \mathbf{U}_{\mathbf{B}_{c-c}}^{\perp} \mathbf{U}_{\mathbf{I}}^{\perp} \mathbf{U}_{\mathbf{I}}^{H} \mathbf{U}_{\mathbf{B}_{c-c}}^{H} \boldsymbol{\omega}} \\
&= \underset{\omega}{\operatorname{argmax}} \left(\frac{\boldsymbol{\omega}^H \mathbf{U}_{\mathbf{B}_{c-c}}^{\perp} \mathbf{U}_{\mathbf{I}}^{\perp} \mathbf{R}_{xx} \mathbf{U}_{\mathbf{I}}^{H} \mathbf{U}_{\mathbf{B}_{c-c}}^{H} \boldsymbol{\omega}}{\sigma_v^2 \boldsymbol{\omega}^H \mathbf{U}_{\mathbf{B}_{c-c}}^{\perp} \mathbf{U}_{\mathbf{I}}^{\perp} \mathbf{U}_{\mathbf{I}}^{H} \mathbf{U}_{\mathbf{B}_{c-c}}^{H} \boldsymbol{\omega}} - 1 \right)
\end{aligned}
\tag{4.29}
$$

where, we exploit the fact that $\mathbf{U}_v$ is $\sigma_v^2 \mathbf{I}_{\mathbf{M}}$ and $\mathbf{U}_{\mathbf{I}}^{\perp}$ is orthogonal to $\mathbf{u}(n)$. Equivalently, the weight vector can be obtained by

$$
\boldsymbol{\omega}_{MSNR} = \underset{\omega}{\operatorname{argmax}} \frac{\boldsymbol{\omega}^H \mathbf{U}_{\mathbf{B}_{c-c}}^{\perp} \mathbf{U}_{\mathbf{I}}^{\perp} \mathbf{R}_{xx} \mathbf{U}_{\mathbf{I}}^{H} \mathbf{U}_{\mathbf{B}_{c-c}}^{H} \boldsymbol{\omega}}{\sigma_v^2 \boldsymbol{\omega}^H \mathbf{U}_{\mathbf{B}_{c-c}}^{\perp} \mathbf{U}_{\mathbf{I}}^{\perp} \mathbf{U}_{\mathbf{I}}^{H} \mathbf{U}_{\mathbf{B}_{c-c}}^{H} \boldsymbol{\omega}} \tag{4.30}
$$

The above maximization can be the generalized eigenvalue problem, as follows

$$
\mathbf{U}_{\mathbf{B}_{c-c}}^{\perp} \mathbf{U}_{\mathbf{I}}^{\perp} \mathbf{R}_{xx} \mathbf{U}_{\mathbf{I}}^{H} \mathbf{U}_{\mathbf{B}_{c-c}}^{H} \boldsymbol{\omega} = \mu \mathbf{U}_{\mathbf{B}_{c-c}}^{\perp} \mathbf{U}_{\mathbf{I}}^{\perp} \mathbf{U}_{\mathbf{I}}^{H} \mathbf{U}_{\mathbf{B}_{c-c}}^{H} \boldsymbol{\omega} \tag{4.31}
$$

where, μ denotes the dominant eigenvalue, and the optimum $\boldsymbol{\omega}$ is the eigenvector corresponding to the dominant eigenvalue.

4.5 **Simulation Results**

4.5.1 **Subspace Projection and Beamforming**

A linear uniform array consisting of seven sensors with half wavelength spaced antennas is used in the simulation. We first consider the case where there are two jammers located at 30 and 60 degrees and the satellite is at 10 degree. We also consider two incoming multipath signals at angles of 75 degrees and 80 degrees. The wideband jamming (interference) signals are considered, which are generated by another random C/A code. We set the signal to noise ratio (SNR) to -20dB and the signal to interference ratio (SIR) to -40dB. Simulation environmental conditions are summarized in Table 4.1. For the performance analysis, the synchronization is performed by identifying the maximum point of cross-correlation between the received signal and a locally generated C/A-code.

Table 4.1 Simulation Environmental Conditions

Element	Values
Type of GPS antenna	7-element uniform array antenna
GPS signal	Random C/A code
Direction of Line of sight signal	10 degree
Direction of jamming signal	30 degree and 60 degree
Direction of multipath signal	75 degree and 80 degree
SNR of GPS signal	-20dB
SIR of GPS signal	-40dB

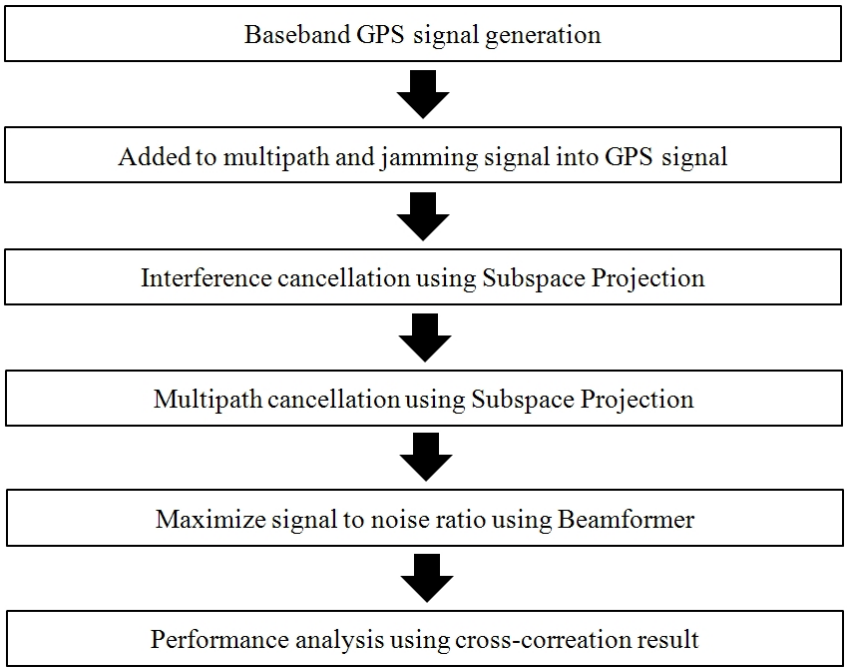

Figure 4.3 Performance evaluation procedures

Fig. 4.3 shows the performance evaluation procedures used in this simulation. In the first simulation, an ideal baseband GPS signal is generated by GPS toolbox and multipath and jamming signals are added to the ideal baseband GPS signal to create a real GPS measurement signal. We then examine the interference and multipath suppression performance of the proposed GPS receiver. First, the jamming signal is suppressed using the sub-space projection method. The multipath is also then suppressed using the sub-space projection method. After removing the interference and multipath signal using code-carrier information, a beamforming algorithm is applied to

maximize signal to noise ratio (MSNR). Finally, we investigate the proposed receiver's synchronization capability. The synchronization can be achieved by cross-correlating the received signal with the locally generated C/A code. When the receiver synchronizes with the satellite, maximum correlation occurs. We present the cross-correlation result at each signal processing step. A block diagram of the proposed method is plotted in Fig 4.4.

Fig.4.5 shows the cross correlation of the received signal without the interference, multipath suppression, and beamforming processes. The cross-correaltion results without any processes show that the synchronization failed due to the GPS error sources. The signal to interference and noise ratio (SINR) without any interference suppression was calculated as 1.93dB. Fig. 4.6 shows the cross correlation of the interference cancelled signal with the first subspace projection. It is shown that the receiver can effectively cancel the interference, but the noise and multipath signal contribution remains significant.

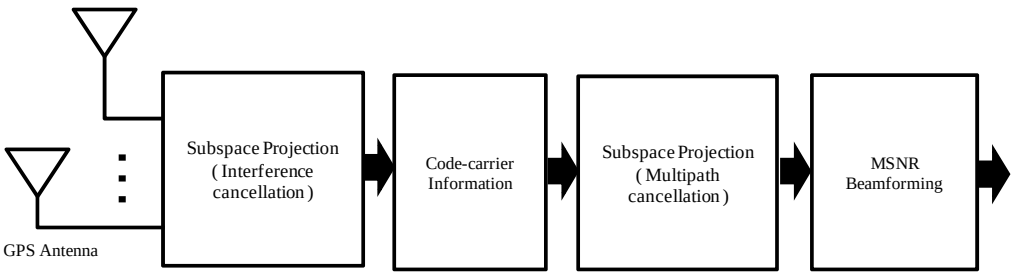

Figure 4.4 Block diagram of the proposed method

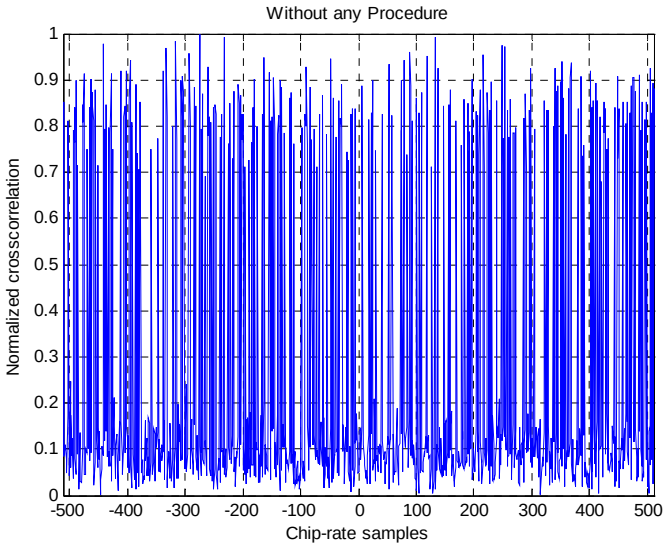

Figure 4.5 Normalized cross-correaltion

(without interference and multipath suppression and beamforming)

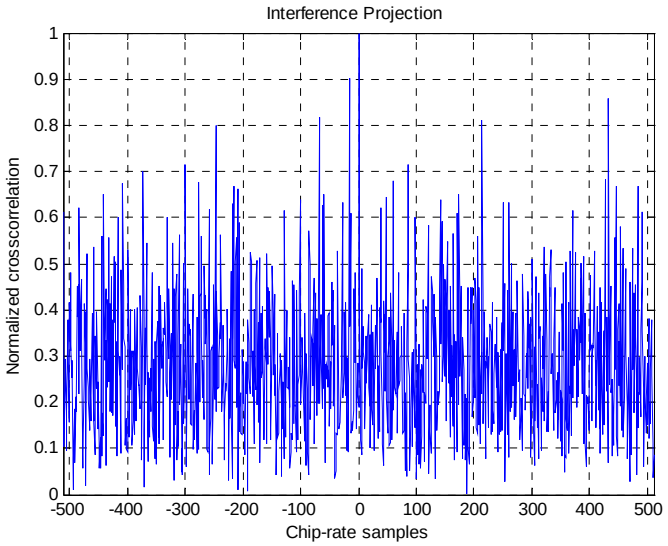

Figure 4.6 Normalized cross-correaltion

(with interference suppression but without multipath suppression and beamforming)

The SINR after the interference subspace projection was increased to 11.40dB. After the multipath subspace projection, the multipath signals and noise are reduced as shown in Fig. 4.7. After multipath suppressing, the SNR of the correlation result was enhanced to 13.50dB, but the noise contribution remains significant. Nevertheless, it is difficult to determine the GPS signal acquisition.

After the multipath subspace projection using code carrier information and MSNR beamforming, the noise can be drastically reduced. This result is depicted in Fig. 4.8. The SINR after the second subspace projection and beamforming was enhanced to 16.50dB. The proposed algorithm definitely works well and it was able to determine the GPS signal aqusition.

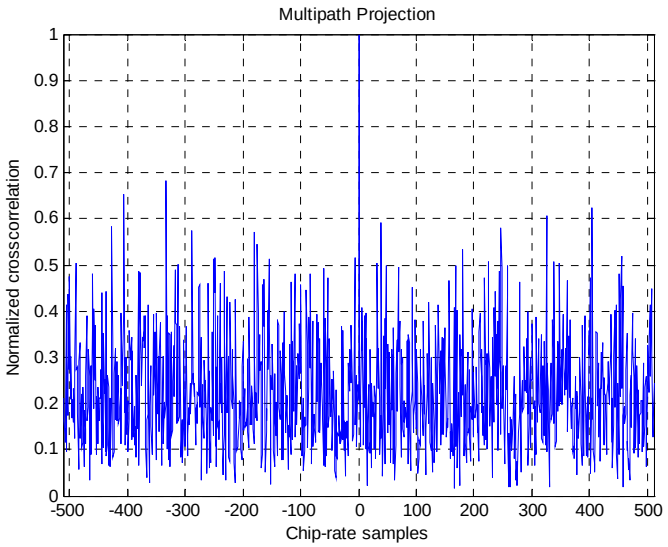

Figure 4.7 Normalized cross-correaltion

(with interference and multipath suppression but without beamforming)

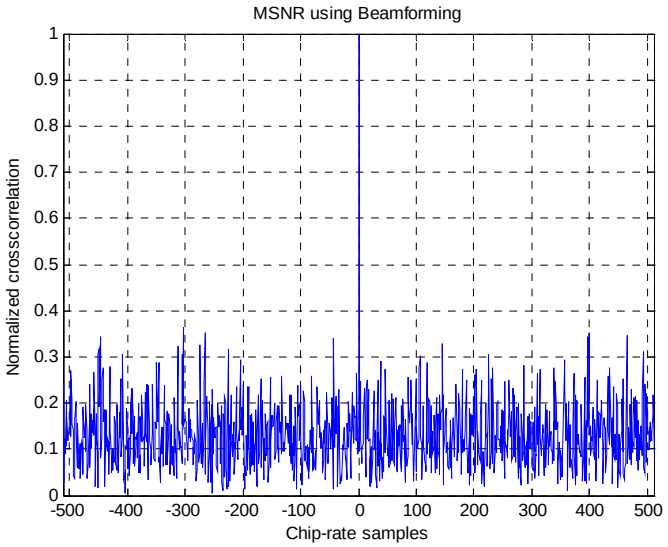

Figure 4.8 Normalized cross-correaltion

(with interference and multipath suppression with beamforming)

Figs 4.9 and 4.10 show the results of beam pattern with proposed method and without proposed method. In the previous section, we assume the direct path signal is arrived at the array with an angle of 10 degrees, and the multipath signal is arrived at 75 degrees and 80 degrees. If the interference and multipath signals are not removed effectively, the beam is formed in the direction of the GPS and multipath signals as shown in the figures. However, after subspace projection and beamforming, the dominant beam is formed in the direction of the GPS signal (10 degrees). Furthermore, the directions of the multipath signal beams are effectively removed. A beamformer is used to maximize the SNR of the received GPS signal.

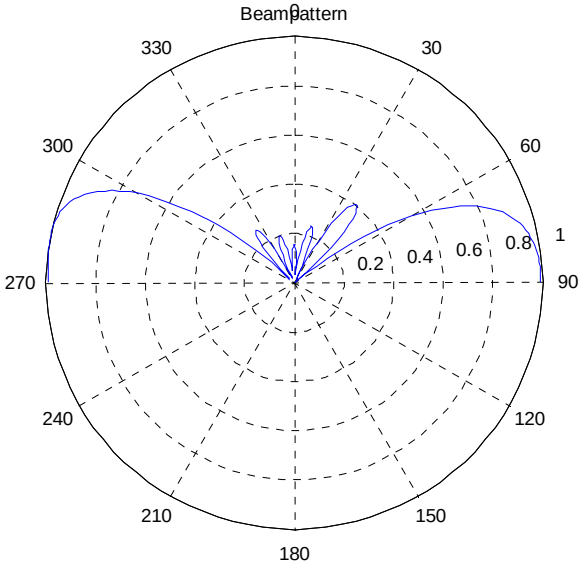

Figure 4.9 Beam pattern without proposed method

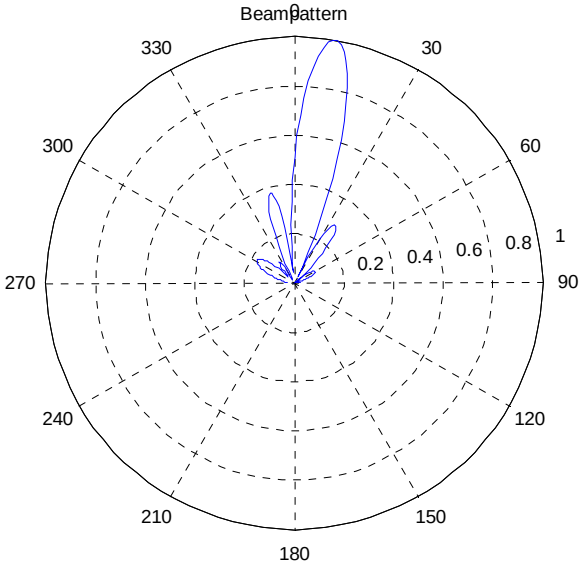

Figure 4.10 Beam pattern with proposed method

4.5.2 **Performance Comparison**

To verify the effectiveness of the proposed beamformer, a simulation test was performed. This simulation compares the interference and multipath error performance of four different methods that have employed the Early-Minus-Late (EML) discriminator. GPS pseudorange measurements are obtained by tracking the correlation peak. Multipath signals distort the correlation peak and cause a bias in the pseudorange measurements. In the absence of the multipath and the filtering effect of the RF front-end, the correlation function should be an isosceles triangle due to the square pulse shape. In Fig 4.11, the normalized cross correlation functions for both the proposed beamformer and the conventional beamformers. It is observed that the proposed method beamformer has an outstanding performance of correlation ambiguity function (CAF) and almost distortionless correlation peaks are obtained compared with the conventional methods. Furthermore, it is observed that increasing the degree of freedom increases the SNR values; therefore, a stronger correlation peak is obtained. This also means that the proposed method performs a role similar to that of a narrow-correlator.

Fig. 4.12 presents the result of RMS error using a two-ray model for each method. From the results, the black line shows that the maximum RMS error of the proposed beamformer is 2.31 meters. The green, blue, and red dotted lines represent the results

of a sigle antenna, The MVDR beamformer and the eigen-vector beamformer, respectively. Their maximum RMS errors are 12.08, 6.23, and 3.79 meters, respectively. It can be seen that the proposed beamformer sucessfully mitigated interference and multipath error.

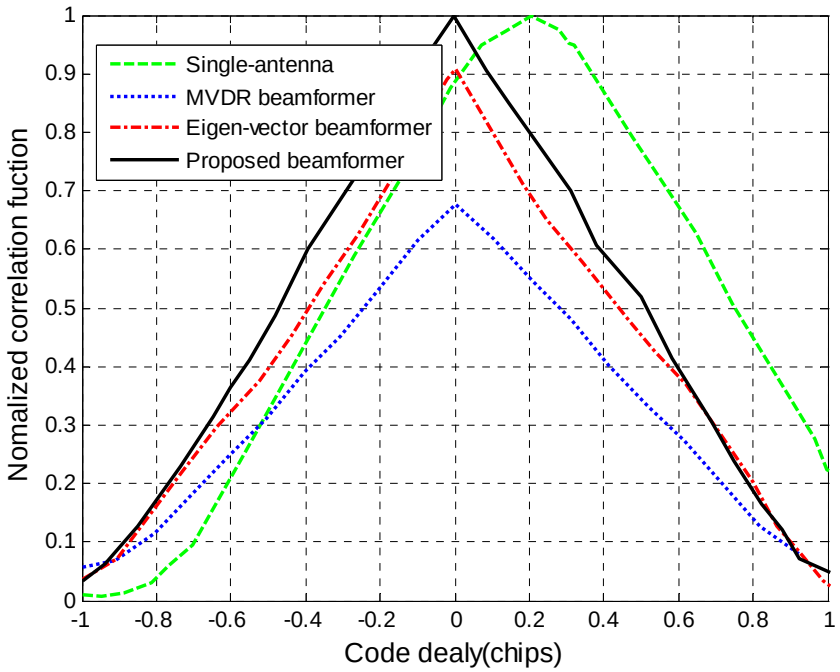

Figure 4.11 Comparison of CAF, beamformer

with the MVDR, the eigen-vector, and the proposed method

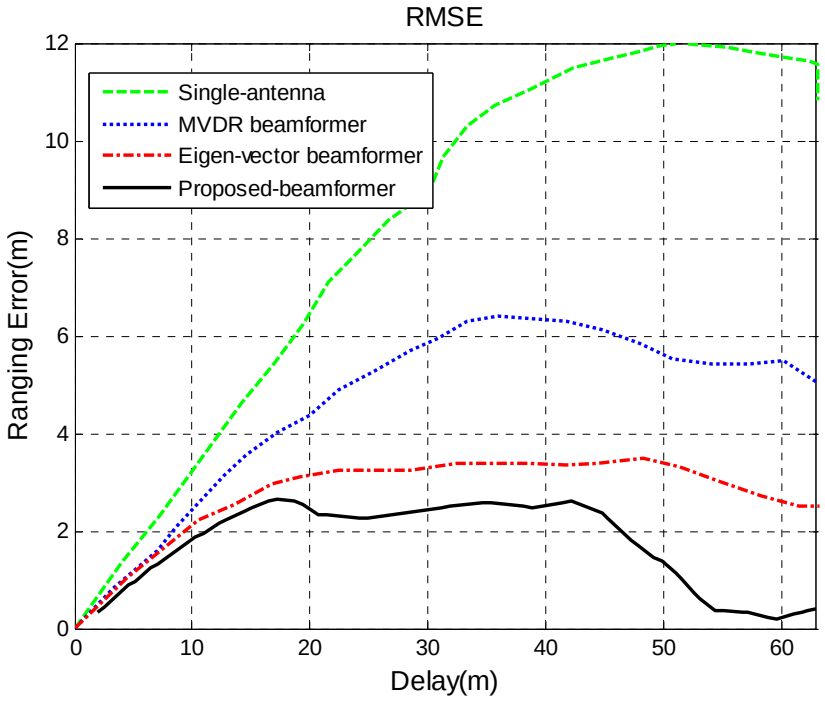

Figure 4.12 Comparison of RMS errors, beamformer

with the MVDR, the eigen-vector, and the proposed method

4.6 **Summary**

In this chapter, we propose a serial subspace projection scheme for both interference suppression and multipath mitigation, followed by maximum signal to noise ratio beamforming. Specifically, without any prior knowledge of the directional information of either the interference or multipath signals, the received signal is first projected into its interference-free subspace, and the interference-free signal is then projected into the

multipath-free subspace. The first projection matrix is obtained from the auto correlation matrix of the received signal with the assumption that the power of the interference signals is much stronger than that of the GPS signal. The second projection matrix is obtained by code carrier information. The code carrier information is used to estimate spatial the signature vectors of the multipath. The resulting interference-free and multipath-free signal is maximized by a maximum signal-to-noise ratio (MSNR) beamformer. The performance verification is expressed by synchronization capability, correlation ambiguity function (CAF) and RMS error. From the simulation results, It can be seen that the proposed beamformer is effective for both interference suppression and multipath mitigation. Thus, it is an excellent candidate for the multipath mitigation method in a GPS navigation system.

Chapter 5
Performance Verification using Software-Defined GPS Receiver

5.1 Introduction

Global Positioning System (GPS) signals are vulnerable to interfering signals such as jamming and multipath signals, due to low signal power. Adaptive beam and null steering of the gain pattern of a GPS antenna array can significantly increase the resistance of GPS sensors to signal interference. Since adaptive array processing requires intensive computational power, beam steering GPS receivers have usually been implemented using hardware, such as field-programmable gate arrays (FPGAs). However, software implementation using general-purpose processors is much more desirable for flexibility and cost-effectiveness. A software-defined GPS receiver with adaptive beam steering capability is presented for interference suppression and multipath mitigation. The software-defined GPS receiver design is based on an optimized desktop parallel processing architecture using a quad-core central processing unit (CPU). This software-defined GPS receiver demonstrates sufficient computational capability to support four-element antenna array processing.

The interference suppression and multipath mitigation technique described in Chapter 4 was first tested on simulated data. After having successfully demonstrated the mitigation of a interference and multipath on simulated data, the same approach was applied to software-defined GPS receiver simulated IF data. In this chapter, the performance of the proposed interference and multipath mitigation method is verified by a software-defined GPS receiver. The multipath and interference are successfully suppressed by the proposed method, which can be easily adopted in civil GPS applications requiring anti-interference capabilities.

5.2 Software-Defined GPS Receiver Methodology

The final goal of any GPS receiver is to generate a navigation solution. To achieve this goal, it is necessary for the received signals from the antenna be acquired and tracked. When tracking is complete, useful information is extracted that can be used to generate measurements, which in turn are used to compute a position. Fig. 5.1 shows an overview of a general GPS receiver. The received signals from the antenna are passed to the RF front-end, where they are down-converted to the desired intermediate frequency, and are sampled at the desired sampling rate. This process generally differs for each frequency band of interest. Samples are then sent to each tracking channel in parallel. Each tracking channel consists of tracking loops, navigation message

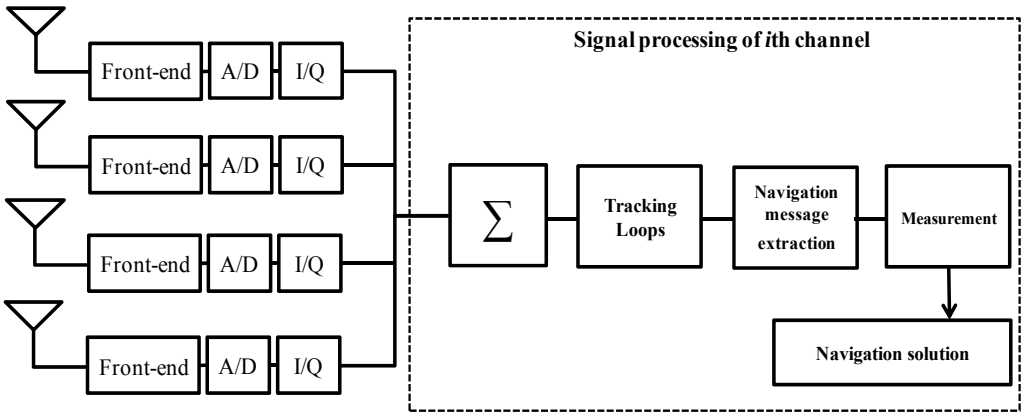

Figure 5.1 GPS software receiver overview

extraction, and a measurement generation block. Finally, measurements from all channels whose satellites are above a minimum elevation angle are used to compute the navigation solution.

5.2.1 Software-Defined GPS Receiver Signals

The GPS signal consists of pseudo random noise (PRN) code with a frequency of 1.023 MHz and a period of 1023 b (1 μs per code chip). The PRN code spreads the navigation message, which has a frequency of 50 Hz. The resultant signal denoted as the coarse acquisition (C/A) signal is then modulated with a carrier frequency of 1575.42 MHz (L1), and is then sent through the communication channel. The PRN

code is generated using linear feedback shift registers, and belongs to the gold code class of maximum length sequences. The multiplication of the 50-Hz navigation signal with the PRN will spread its power spectral density over a wider range of frequencies, as a type of spread spectrum communication. Because of the long traveling path from the satellite to the receiver on earth, the power levels of the signal will be lower than the noise floor, making the signal invisible. Several amplification stages in the receiver, as well as utilization of the correlation property of the PRN code, will bring back the signal and make it detectable by the receiver, and the navigation data is processed.

5.2.2 Software-Defined GPS Receiver Modules

Radio Frequency Front-End

After the RF signal has been collected by the antenna, it is amplified using a low-noise amplifier (LNA) (preamplifier) that has a low noise figure. The signal is then filtered with a bandpass filter (BPF) to reduce band noise. Such filters should possess sharp transitions. Surface acoustic wave (SAW) filters are widely used in current receivers. The signal is then down-converted to an IF via an RF-IF mixer. This process is needed to reduce the frequency of the signal for the ADC process. The RF L1 signal needs to be reduced to some 100s of MHz to enable to use of commercial ADC converter chips. This is the task of the down-conversion section. Some receivers utilize

single or multiple IF stages based on the frequency plan of the receiver architecture (Borre. Kai 2007).

ADC

The ADC will transform the analog IF signal into a digital IF signal for baseband processing. In low-end receivers, single-bit (hard limiters) ADCs are used in narrow bandwidths (2 MHz). High-end receivers use up to 3 b (eight levels) of sampling in bandwidths of 2–20 MHz. If a multibit ADC is used, automatic gain control (AGC) is utilized on the incoming signal before entering the ADC to adjust the signal amplitudes based on the ADC dynamic range.

Signal Acquisition

The purpose of acquisition is to find the visible satellites and coarse values of carrier frequency and code phase of their signals. The satellites are differentiated by 32 PRN sequences. The code phase is the time alignment of the incoming PRN code in the current block of data with that of the locally generated one. The code phase is necessary to generate a local PRN code that is perfectly aligned with the incoming code. Only when this is the case can the incoming code be removed from the signal. Another parameter that is important to estimate is the Doppler shift. The line-of-sight velocity of the satellite causes a Doppler effect that result in a higher or lower

frequency value for the incoming signal. In the worst case, the frequency can deviate by up to ±10 kHz. It is important to know the frequency of the signal to be able to generate a local carrier signal. This signal is used to remove the incoming carrier from the signal. In most cases, it is sufficient to search the frequencies in steps of 500 Hz. Two types of signal acquisition are usually adopted in GPS receiver implementations:

The first type, serial search acquisition, is performed by stepping the code phase of the locally generated PRN to cover the length of the sequence (i.e., 1023) to find the correlation peak and find the code phase offset between the locally generated and incoming GPS signal.

The second type, parallel search acquisition, is performed by eliminating the full stepping of a whole PRN sequence by utilizing the circular correlation between the incoming signal and the locally generated one. This will require fewer steps (and correlation time), since circular correlation can be performed in the frequency domain utilizing the fast Fourier transform (FFT). Then, an inverse FFT is performed to bring the signal back into the time domain, but now the correlation peak has been identified. This method is much faster than the serial search method, but the serial search method can operate on weaker signals.

Tracking

After the acquisition, the frequency and code offset parameters of a satellite signal

are roughly known. The main purpose of tracking is to refine these values, and to keep track of and demodulate the navigation data for the specific satellite. First, the input signal is multiplied with a carrier replica. This is done to remove the carrier wave from the signal. Next, the signal is multiplied with a code replica, and the output of this multiplication gives the navigation message. So, the tracking module has to generate two replicas, one for the carrier and one for the code, to perfectly track and demodulate the signal of one satellite.

The goal for a code-tracking loop is to keep track of the code phase of a specific code in the signal. The output of such a code tracking loop is a perfectly aligned replica of the code. The code tracking loop in the GPS receiver is a delay lock loop (DLL) called an early-late tracking loop. The idea behind the DLL is to correlate the input signal with three replicas of the code, the early, prompt, and late. The three replicas are often generated with a chip spacing of ±0.5. The three outputs are then integrated over a whole C/A code period and stored. The output of these integrations is a term indicating how much the specific code replica correlates with the code in the incoming signal.

To demodulate the navigation data successfully, an exact carrier wave replica has to be generated. To track a carrier wave signal, phase lock loops (PLL) or frequency lock loops (FLL) are often used. A loop discriminator block is used to find the phase error on the local carrier wave replica. The output of the discriminator, which is the phase

error, is then filtered and used as a feedback to the numerically controlled oscillator (NCO), which adjusts the frequency of the local carrier wave. Using this approach, the local carrier wave can be almost an exact replica of the input signal carrier wave.

5.3 Architecture of Software-Defined GPS Receiver

In order to verify the proposed multipath mitigation method described in Chapter 4, a software receiver was developed to evaluate its performance. A software-defined GPS receiver consists of three modules: a signal generator module, an anti-jamming, multipath suppression process module, and a software receiver module. The architecture of the software-defined receiver is illustrated in Fig. 5.2. A signal generator module is designed to generate simulated IF data, which can be directly used for performance verification of the proposed method. The signal processing module is operated to mitigate interference, and employs the multipath algorithm presented in previous chapters. Finally, the software receiver module shows the performance of the proposed method in the navigation domain.

5.3.1 GPS Signal Generation

When implementing the signal processing parts of the GPS receiver, data is

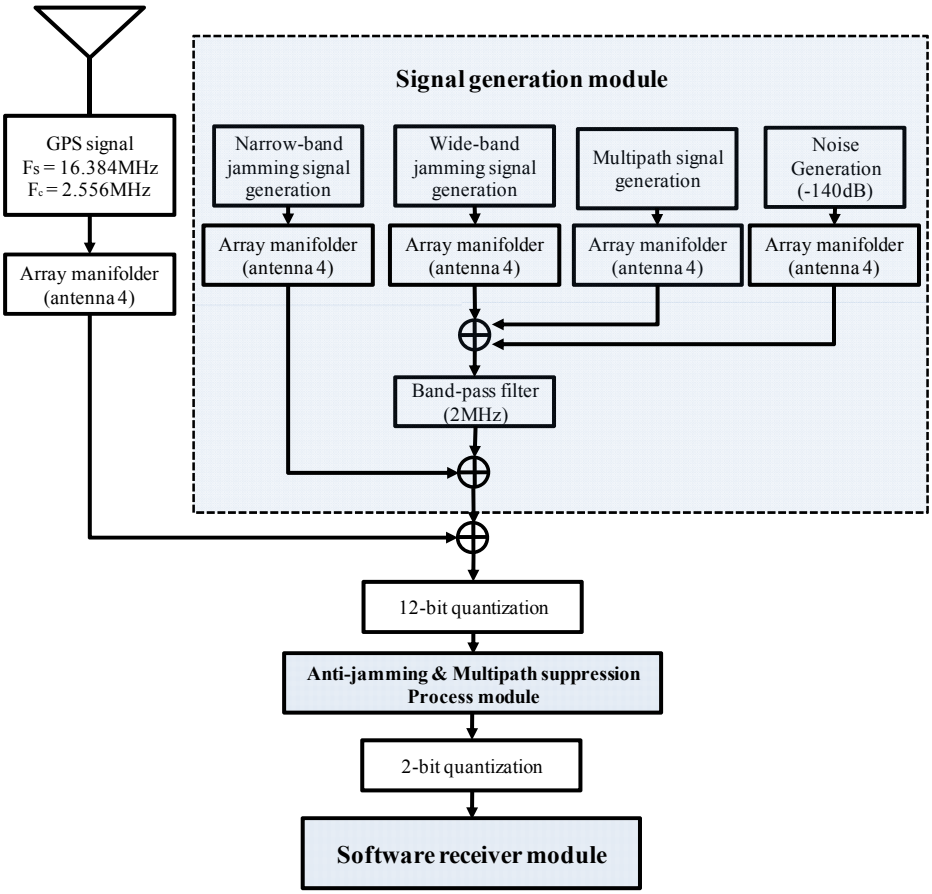

Figure 5.2 Architecture of software-defined receiver

necessary for testing functionality. The final goal is to have a GPS receiver working in real time on data obtained from a GPS antenna through an RF front-end and an ADC. However, in the phase of developing the signal processing algorithms it is not optimal to use real sampled data. The main reason for this is that it is impossible to control the properties of the received and sampled GPS signals. Additionally, it is also impossible

to know all the properties of the received signals. The solution to this problem is to use simulated IF data. A useful L1 GPS signal simulator should include the following global parameters associated with the down-conversion and sampling of the signal:

Intermediate Frequency: It should be possible to input the value of the IF. The IF will then be the reference frequency to which the Doppler shift of the satellite signals should be compared.

Sampling Frequency: It should be possible to input the value of the sampling frequency used to sample the GPS signals.

With the possibility of setting these parameters, it would be possible to test the algorithms with simulated IF data with the same properties as the data sampled from a GPS antenna through an RF front-end. Below is list of the properties of a GPS signal from a satellite.

PRN: The pseudorandom noise number corresponding to the satellite. This number indicates which of the C/A codes should be used.

Doppler: The Doppler count is the frequency deviation from the IF. The Doppler count is directly associated with line-of-sight dynamics between the satellite and the receiver.

Code Phase: The code phase is the time alignment of the PRN code in the received data.

P(Y) Code: In addition to the C/A code, the L1 signal contains the P(Y) code. This code is modulated onto the carrier wave as a quadrature component, while the C/A

code is present in the in-phase component.

Data Bits: The navigation data bits are phase-modulated onto the carrier wave with a frequency of 50 Hz.

Signal Strength: Due to the long signal path from the satellite to the receiver in combination with a low power transmitter at the satellite, the received signal is very weak. An additional property of the GPS signal is the signal-to-noise ratio (SNR), the ratio between the signal and the noise originating from the signal path.

The signal simulator should meet the above description of the global parameters and the GPS signal properties. A GPS satellite signal uses L1 and L2 frequencies. The L1 signal carrier frequency is 1575.42 MHz, and the signal includes a C/A Code and a P(Y) code. The L2 signal carrier frequency is 1227.660 MHz, and the signal includes only the P(Y) code. The designed GPS signal generation module generates the L1 C/A signal, which is mainly used by civil GPS receivers, including GBAS receivers. The GPS signal generation module outputs a 12-channel GPS signal by combining 12 individual signal generation module's outputs. In this simulator, the IF center frequency is 2.556 MHz and the sampling frequency is 16.384 MHz (see Figure 5.2) but these values can be changed by specifications in the user software of a GPS receiver. An individual GPS signal includes a PRN, Doppler frequency, sampling time, signal power, C/A code phase, navigation bit, Doppler rate, and Doppler rate change.

5.3.2 Interference Signal Generation

The interference signal generation is designed to generate a jamming signal, multipath signal, and band-limited white Gaussian noise that depends on user (Lorenzo 2007 & Yang 2013). In order to design a GPS interference signal generation, it is necessary to know the characteristics of the signal and data transmitted from GPS satellites and received by the GPS receiver antenna. GPS signals are modeled differently depending on the signal modulation scheme. However, the current GBAS is based on GPS a L1 C/A signal, so the simulator is designed to primarily generate a GPS L1 C/A signal. The received GPS L1 C/A signal is modeled as:

$$r(t) = \sqrt{2P_{L1}} \times D(t-\tau)c(t-\tau)\cos\left[2\pi(f_{L1} + f_d)t + \varphi\right] + i(t) + m(t) + n(t) \quad (5.1)$$

where, P_{L1} is the L1 signal power, $D(t)$ is the navigation data, $c(t)$ is the C/A code, τ the is code phase, f_d is the doppler frequency shift, φ is the carrier phase, $i(t)$ is the interference, $m(t)$ is the multipath signal, and $n(t)$ is additive white Gaussian noise. The additive white Gaussian noise (AWGN) is modeled with a variance of $\sigma_n^2 = \frac{N_0 f_s}{2}$, where $\frac{N_0}{2}$ is the power spectral density of the noise and f_s is the sampling frequency. The interference signal is modeled as:

$$i(t) = \sqrt{2P_i} \times \cos\left[2\pi f_i t + \varphi_i\right] \tag{5.2}$$

where, P_i is the signal power of the interference, f_i is the interference frequency, and φ_i is the interference phase offset. The multipath signal is expressed as:

$$m(t) = \alpha \cdot \sqrt{2P_{L1}} \times D(t-\tau_m)c(t-\tau_m)\cos\left[2(f_{L1} + f_d)(t-\tau_m) + \varphi_m\right] \tag{5.3}$$

where, α is the attenuation factor of the multipath signal, τ_m is the time delay of the multipath, and φ_m is the phase offset of the multipath signal.

5.3.3 Front-End Signal Processing

The front-end signal processing module is described in Fig. 5.3. This module obtains a GPS signal, interference signal, and multipath signal as input, and integrates them with noise. Then, the module processes the integrated signal according to the front-end module's signal processing, which includes pre-amplifying, down-conversion, filtering, sampling, and digitization. The 'dB Gain', 'Bandpass Filter', 'AGC', and '12-bit ADC' blocks simulate the front-end module's signal processing, and the simulated data saves the generated IF data in a binary format. The generated IF data can be used for a software GPS receiver as signal data.

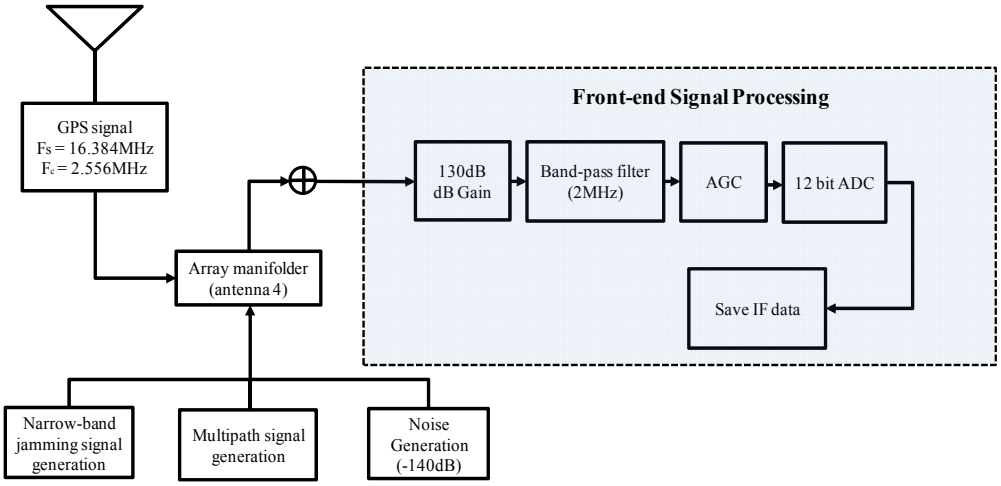

Figure 5.3 Front-end signal processing block diagram

5.4 Experimental Results

This chapter demonstrates the experimental verification using the software receiver with ths operational signal processing module. This verification involves a two-tiered approach that addresses both interference rejection and multipath mitigation. The data recording setup consists of custom-designed front-ends that perform down-conversion and sampling, and one simulated IF data bridge connected to a computer. The front-end and the A/D converter for all antenna channels are connected to a common clock. The receiver-to-receiver phase biases are calibrated and removed during post-processing by the software receiver. This designed system uses simulated IF data, which consist of GPS C/A-code signals, plus interference and multipath signals. To evaluate the

performance of the proposed method, a linear uniform array consisting of four-elements with half wavelength-spaced antennas is used. A static model and dynamic model are applied to verify the proposed method. The experimental conditions are given in Table 5.1. To assess the interference and multipath impact, the GPS signal data with realistic interference and multipath were applied under static and dynamic conditions. The generated inference types were continuous wave and swept continuous wave interference signals. The power of the interference injected by the software defined GPS receiver behavior is 35 dBm. A multipath signal is added to 0.1 chips, which is equivalent to 10 m of position error. For the generation of code and pseudorange measurement, white Gaussian noise is applied to $(1,\ 0.01^2)$ m. The velocity of the moving receiver remains constant at 10 m/sec under the dynamic condition. All errors mentioned previously are injected after a certain period of time. In order to verify the proposed method, 100 Monte-Carlo trials are carried out. All true values are assume to be known, so the esimation error of the navigation solution and trajectory error are exactly obtained.

For comparison with the proposed method, a conventional MVDR beamformer and the eigen-vector beamformer (Sturza & Brenner 1990, Amin 2006) are considered. The beamforming method is selected as the interference rejection and multipath mitigation method since it is the most representative interference suppressing method for various GPS applications.

Table 5.1 Experimental Conditions (Static and Dynamic Environments)

	Static condition	Dynamic condition
Jamming (CW,SW)	35 dBm	35 dBm
Multipath	0.1 chip	0.1 chip
AWGN	$(1, 0.01^2)$ m	$(1, 0.01^2)$ m
Velocity	0 m/sec	10 m/sec
Interference profile Injected time	1500~3000 msec	2000~5000 msec

5.4.1 Static Environments

In order to evaluate the performance of the proposed method against interference and multipath signals in real-time kinematic positioning, an experimental simulation is performed. The proposed method is applied to multiple GPS receivers with the static situation. The performance verification was expressed in the navigation domain with pseudorange bias error, SNR loss, height error and 2-dimensional positioning errors. For comparison with the proposed method, a conventional MVDR beamformer, an eigen-vector beamformer, and the proposed beamformer method are considered in simulations.

The pseudorange error results from before and after interference suppression and

multipath mitigation are shown in Fig. 5.4. The interference and multipath signals appear in the figure after 1500 msec. After interference and multipath injection, the pseudorange error suddenly increased, and conventional beamformer and the proposed beamformer were activated. From the results, blue dotted line represents the result of the MVDR beamformer, which had an RMS error is 15.08 meters. The red dotted line and the black line represent the results of the eigen-vector beamformer, and the proposed beamformer. Their RMS errors were 7.56 and 2.86 meters, respectively. The proposed beamformer is successfully mitigated the interference and multipath pseudorange bias error. Fig. 5.5 shows the height error results. Addressing the height error is associated with the DOP of the GPS system is important to reduce the positioning error. The blue dots, red dots and black lines represent results of the MVDR beamformer, the eigen-vector beamformer, and the proposed beamformer, respectively. Their RMS errors were 10.08, 4.92 and 2.01 meters, respectively. It can be observed that the proposed beamformer also effectively suppresses the interference and multipath height error. In the Fig. 5.6, the SNR loss is shown before and after the intentional injection of interference and multipath signals. The proposed beamformer has better performance regarding SNR loss than the other methods. Fig. 5.7 shows the error distributions by (a) the MVDR beamformer method's position estimates, (b) the eigen-vector beamformer method's position estimates and (c) the proposed method at specific time. By comparing the results of (a), (b) and (c) after the intentional injection

of interference and multipath, the propose method of (c) is observed to guarantee the small error distribution which changes less in response to the apparent interference and multipath than the error distribution generated by the MVDR beamformer and (b) the eigen-vector beamformer. Thus, under the static condition, the proposed method provides efficient position estimation in interference and multipath environments.

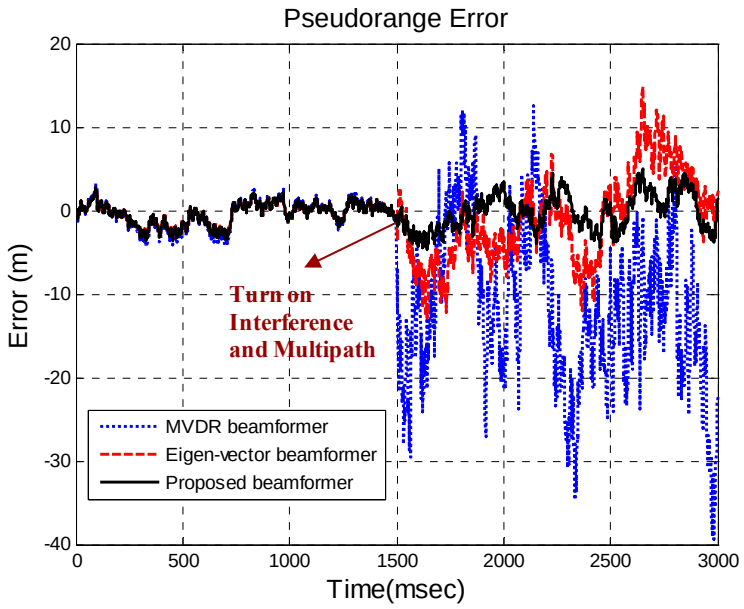

Figure 5.4 Pseudorange errors (static conditions)

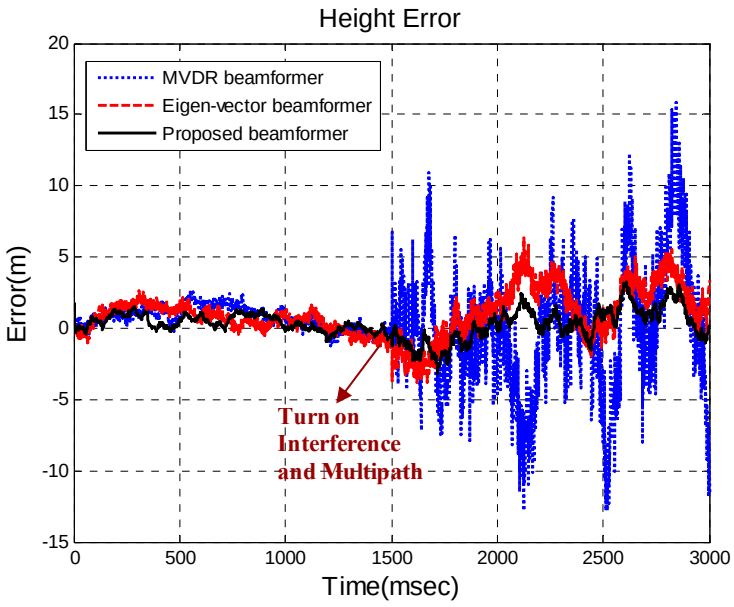

Figure 5.5 Height errors (static conditions)

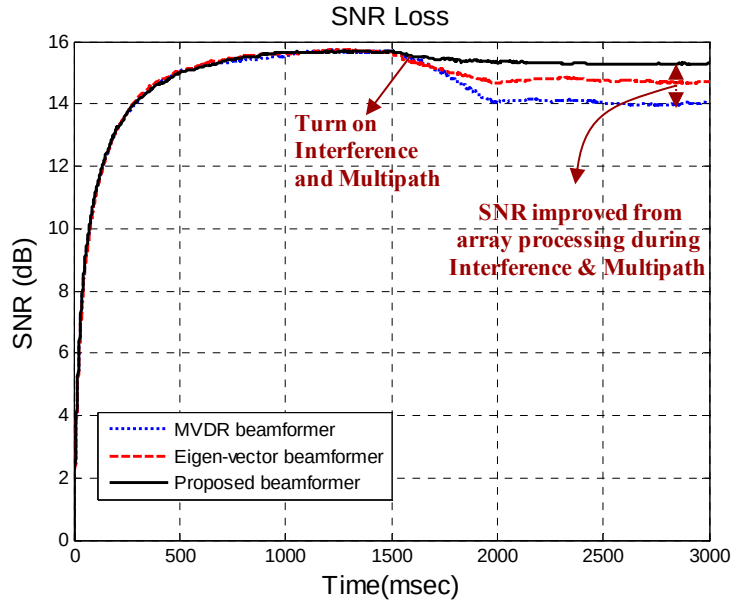

Figure 5.6 SNR loss (static conditions)

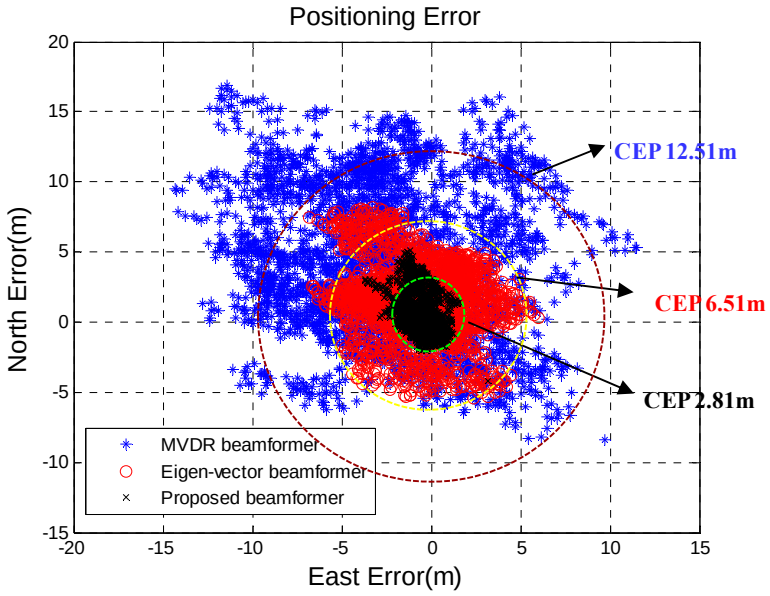

Figure 5.7 Comparison of position errors by raw GPS position (static conditions), for the MVDR, the eigen-vector and the proposed beamformers

Table 5.2 Experimental Results (Static Environments)

	Pseudorange Error [m]	Height Error [m]	SNR loss [dB]	Positioning Error [m]
MVDR beamformer	15.08	10.08	1.56	12.51
Eigen-vector beamformer	7.56	4.92	1.02	6.51
Proposed beamformer	2.86	2.01	0.27	2.81

Table 5.2 summarizes the experimental results regarding pseudorange bias error, height error, SNR loss, and positioning error. The experimental results show that the proposed algorithm has greatly superior performance for both interference suppression and multipath mitigation compared with conventional methods in static conditions.

5.4.2 Dynamic Environments

In order to verify the performance of the proposed method, dynamic conditions are considered. Similar to the previous chapter, the height error, SNR loss, and positioning error are adopted as performance criteria. For comparison with the proposed method, the MVDR beamformer, the eigen-vector beamformer and the proposed beamformer are also considered.

The height error result before and after interference suppression and multipath mitigation in the dynamic conditions are shown in Fig. 5.8. The interference and multipath signals that appear in the figure after 2000 msec. After interference and multipath injection, the height error is largely increased. Subsequently, array processing is adopted by the interference and multipath suppression. The blue dots, red dots, and black lines represent a result of the MVDR beamformer, the eigen-vector beamformer, and the proposed beamformer, respectively. Their RMS errors were 10.58, 4.56, and 2.51 meters. It can be see that the proposed beamformer is successfully

mitigated the interference and multipath height error. Fig. 5.9 presents the results of SNR loss before and after the intentional injection of interference and multipath signals. As can be seen from the results, the proposed beamformer has an outstanding performance regarding SNR loss compared with the other conventional methods. Fig. 5.10 shows the trajectory error by (a) the MVDR beamformer method's position estimates, (b) the eigen-vector beamformer method's position estimates, and (c) the proposed method, for a moving receiver following a trajectory. The proposed method is superior for mitigating the interference and multipath error. Under the dynamic conditions, the proposed method also provides effective position estimation in interference and multipath environments.

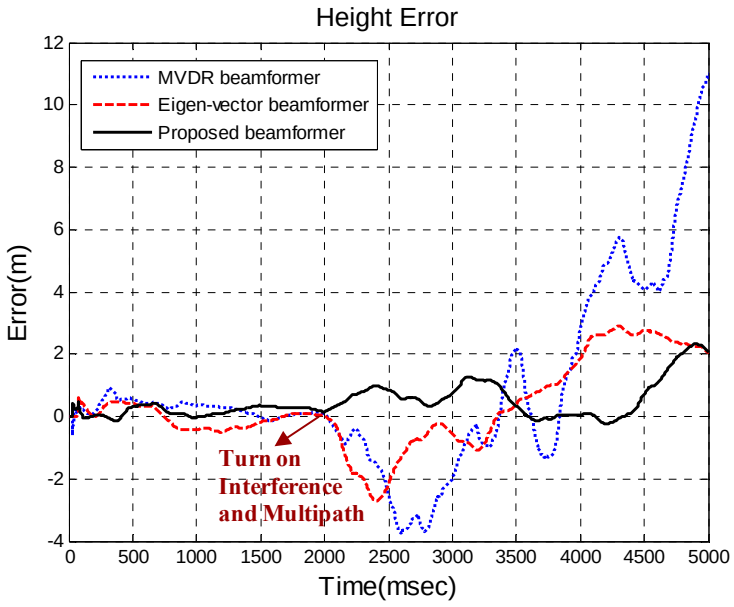

Figure 5.8 Height errors (dynamic conditions)

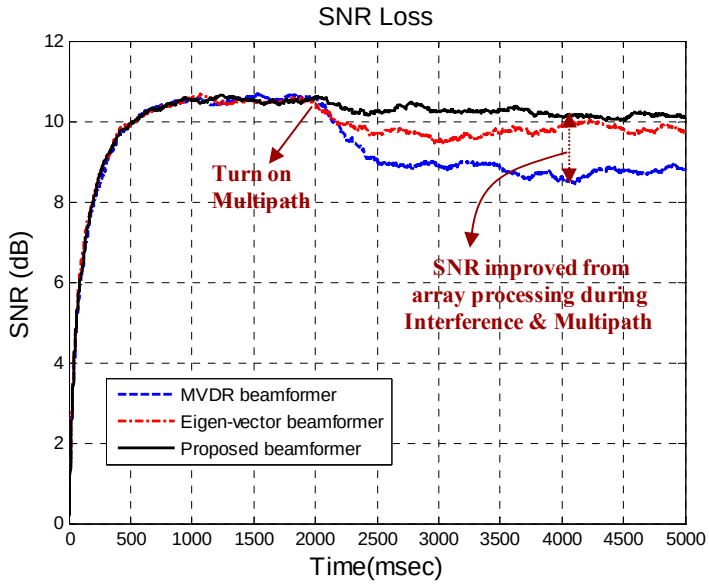

Figure 5.9 SNR loss (dynamic conditions)

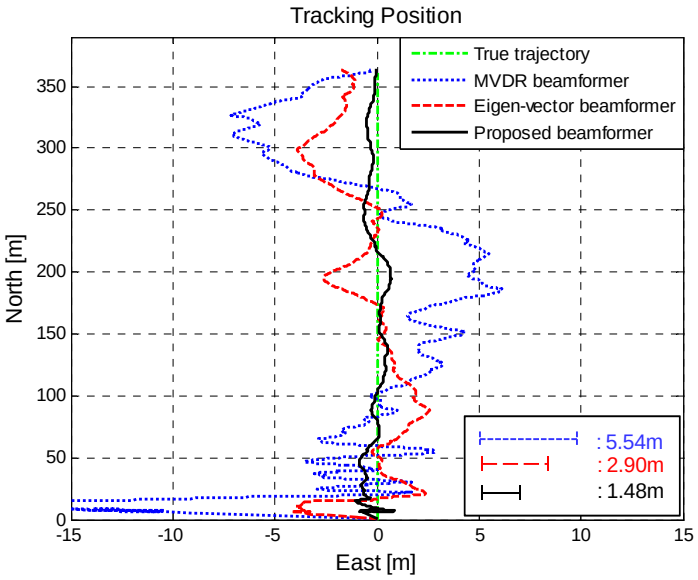

Figure 5.10 Comparison of trajectory errors (dynamic conditions), for the MVDR, the eigen-vector and the proposed beamformers

Table 5.3 Experimental Results (Dynamic Environments)

	SNR loss [dB]	Height Error [m]	Positioning Error [m]
MVDR beamformer	1.79	10.58	5.54
Eigen-vector beamformer	1.28	4.56	2.90
Proposed beamformer	0.19	2.51	1.48

Table 5.3 illustrates the experimental results in dynamic environments. The performance criteria were: the height error, SNR loss, and positioning error. The performance criteria were compared between the MVDR beamformer, the eigen-vector beamformer, and the proposed beamformer. The results show that the proposed algorithm is also effective for both interference suppression and multipath mitigation at static condition in dynamic conditions.

5.5 Summary

A new beamformer technique to suppress both interference and multipath signals with distortionless response in the direction of the LOS signal has been proposed. In the interference suppression stage, the subspace method has been used to mitigate wideband and narrowband interference signals. In the multipath mitigation stage, the proposed technique utilizes code carrier information to estimate the multipath steer

vector. Afterwards, space-time processing is applied to the synthesis array to estimate the multipath steering vectors and maximize the SNR of the LOS signal. As shown, the proposed method is robust against the signal cancellation phenomenon and interfering signals such as interference and multipath signals. This method can be implemented in vehicular or high-precision navigation applications operating in urban environments where multipath and wideband/narrowband interference signals degrade or fail the position solution. The experimental results demonstrate the effectiveness of the method for interference suppression and multipath mitigation.

Chapter 6
Conclusions and Future Work

6.1 Conclusions

In this dissertation, we proposed a modified beamformer methodology applicable for GPS positioning systems. The proposed beamformer which is based on multiple antennas using code carrier information is advantageous for applications that require both precise positioning and robustness to interfering signals such as interference and multipath.

In order to mitigate interference and multipath signals, we propose a serial subspace projection scheme based on code carrier information, followed by maximum signal to noise ratio beamforming processing. The fundamental differences between the various possible beamforming algorithms arise from the estimation of a multipath steer vector. For comparison, the conventional two-ray model was adopted. Simulation showed that the proposed beamformer possesses good estimation efficiency.

As a software receiver analysis tool, we also found that the proposed beamformer is very helpful for estimating the interference and multipath subspace and completely nullifying the interference and multipath signals. Furthermore, this method outperforms the previous approach in terms of the distortionless response in the

direction of the desired signals. The example of the GPS positioning in the specific environments showed that the proposed beamforming methodology is also useful in designing an advanced interference suppression and multipath mitigation algorithm. For comparison with the proposed method, the conventional MVDR beamformer and eigen-vector beamformer were considered under the static and dynamic conditions. Both simulation and experimental results show that the proposed beamformer efficiently mitigates multipath effects in realistic environments. These features make this method suitable for real-time applications; it can therefore either be employed as a standalone pre-processing unit connected between a GPS receiver and an antenna array or it can be easily integrated into the next generation receivers. Furthermore, this method can be used in vehicular or high precision navigation applications operating in urban environments where multipath and interference signals degrade or completely fail the position solution.

6.2 Future Work

Considering the presented theoretical, simulated and experimental results obtained herein, the following recommendations for future work are proposed:

In this dissertation, simulations and practical tests were limited to GPS L1. Although the criteria on which the proposed methods were developed are the same for other GPS

signals, different modifications and considerations may be required for each case. Applying the modified methods for other GNSS signals, simulating and performing real data tests are recommended as a further development of the research conducted herein.

In many parts of this research, the steering vectors of the LOS GPS signals are required as a priori knowledge. In order to verify the applicability and effectiveness of most methods, calibration was not needed; however, for an evaluation of these methods in the real system, a calibrated antenna array is required, which means that knowledge about the array configuration and orientation is needed. It is recommended that the GPS signals are used for calibration, along with an inertial measurement unit (IMU) to measure antenna array orientation, in order to evaluate the proposed methods in the real system.

In order to evaluate the proposed methods in the position domain, proper software and hardware implementation are required. A portable multi-channel RF front-end with synchronized channels provides the opportunity for performing more tests and evaluations on the introduced methods. This RF front-end can provide row IF samples for further processing in any GPS software receiver that support antenna array processing. Therefore, implementing the proposed methods into these software receivers provides an opportunity to further evaluate the proposed methods in many practical applications. Moreover, if in addition to the multi-channel RF front-end, the

hardware platform is also equipped with a digital processing core such as a DSP or FPGA, which does not need to be implemented inside the GNSS receiver structure, the proposed method could be tested and evaluated independently from GNSS receivers.

Bibliography

[1] Abed-Meraim, K., P. Duhamel, D. Gesbert, L. Loubaton, S. Mayrargue, E. Moulines and D. Slock (1995) “Prediction error methods for time-domain blind identification of multichannel FIR filter,” *In Proceedings of the IEEE International Conference on Acoustics, Speech, and Signal Processing (IEEE ICASSP 1995)*, 9-12 May, Detroit, MI, pp. 1968-1971.

[2] Agamata, B. N. (1991) “Time Domain Adaptive Filter Implementation of a Minimum Variance Distortionless Response (MVDR) Beamformer for a Sensor Array” *In Proceedings of the 4th International Technical Meeting of the Satellite Division of The Institute of Navigation (ION GPS 1991)*, 11-13 September, Albuquerque, NM, pp. 443- 452

[3] Amin, M. G. and W. Sun (2005) “A novel interference suppression scheme for global navigation satellite systems using antenna array,” *IEEE Journal on Selected Areas in Communications*, vol 23, no 5, May, pp. 999-1012.

[4] Amin, M. G., L. Zhao and A. R. Lindsey (2004) “Subspace array processing for the suppression of FM jamming in GPS receivers” *IEEE Transactions on Aerospace and Electronic Systems*, vol 40, no 1, January, pp. 80-92.

[5] Applebaum, S. P. (1976) “Adaptive arrays” *IEEE Transactions on Antennas and Propagation*, vol 24, no 5, September, pp. 585-598.

[6] Backen, S., D. M. Akos, and M. L. Nordenvaad (2008) “Post-Processing Dynamic GNSS Antenna Array Calibration and Deterministic Beamforming,” *in Proceedings of the 21st International Technical Meeting of the Satellite Division*, 16-19 September, Savannah, GA, pp. 2806-2814.

[7] Badke B., and A. Spanias (2002) “Partial band interference excisions for GPS using frequency-domain exponents” *In Proceedings of the IEEE International Conference on Acoustics, Speech, and Signal Processing (IEEE ICASSP 2002)*, 13-17 May, Orlando, FL, pp. 3936-3939.

[8] Basta, N., A. Dreher, S. Caizzone, M. Sgammini, F. Antreich, G. Kappen, S. Irteza, R. Stephan, M. A. Hein, E. Schafer, A. Richter, M. A. Khan, L. Kurz, and T. G. Noll (2012) “System Concept of a Compact Multi-Antenna GNSS Receiver,” *7th German Microwave Conference (GeMiC)*, 12-14 March, Ilmenau, Germany, pp. 1-4.

[9] Bai-gen, C., Wei, S., Jian, W., & Hui-chao, L. (2009) “ Design and realization of software receiver based on GPS positioning algorithm,” *In Information Science and Engineering (ICISE)*, December, vol 5, pp. 2030-2033

[10] Borio D. (2008) *A Statistical Theory for GNSS Signal Acquisition*, Doctoral Thesis, Dipartimento di Elettronica, Politecnico di Torino, Italy.

[11] Borio, D. (2010) “GNSS Acquisition in the Presence of Continuous Wave Interference”, *IEEE Transactions on Aerospace and Electronic Systems*, vol 46, no 1, January, pp. 47– 60.

[12] Borre, Kai. (2007) *A software-defined GPS and Galileo receiver: a single-frequency approach*. Springer.

[13] Brennan, L. E. and L. S. Reed (1973) “Theory of Adaptive Radar” *IEEE Transactions on Aerospace and Electronic Systems*, vol 9 no 2, March, pp. 273-252.

[14] Bresler, Y., V. U. Reddy, and T. Kailath (1988) “Optimum beamforming for coherent signal and interferences” *IEEE Transactions on Acoustic, Speech, Signal Processing*, vol 36, no 6, June, pp. 833-843.

[15] Broumandan, A., and T. Lin (2008) “Performance of GNSS Time of Arrival Estimation Techniques in Multipath Environments” *Proceedings of ION GNSS 2008*, 16-19 September Savannah, GA, USA, pp. 632–643.

[16] Broumandan, A., J. Nielsen, and G. Lachapelle (2008) “Practical results of high resolution AOA estimation by the synthetic Array,” *In IEEE Vehicular Technology Conference*, 21-24 September, Calgary AB, Canada, pp. 1-5.

[17] Broumandan, A., Nielsen, J., and G. Lachapelle (2010) “Signal detection performance in rayleigh multipath fading environments with a moving antenna”, *IET Signal Processing*, vol. 4, no. 2, April, pp. 117–129.

[18] Brown, A. (2000) “Multipath Rejection Through Spatial Processing,” *in Proceedings of ION GPS 2000*, 19-22 September, Salt Lake City, UT, pp. 2330 - 2337.

[19] Brown, A. and N. Gerein (2001) “Test Results of a Digital Beamforming GPS Receiver in a Jamming Environment,” *in Proceedings of ION GPS 2001*, 11-24 September, Salt Lake City UT, pp. 894-903.

[20] Buckley, K. M. and L. J. Griffiths (1986) “An adaptive generalized sidelobe canceller with derivative constraints,” *IEEE Transactions on Antennas Propagation*, vol AP-34, March, pp.311-319.

[21] Capon, J. (1969) “High-Resolution Frequency-Wavenumber Spectrum Analysis,” *in Proceedings of the IEEE*, vol 57, no 8, August, pp. 1408-1419.

[22] Chang, C. L., and J. C. Juang (2010) “Performance analysis of narrowband interference mitigation and near-far resistance scheme for GNSS receivers,” *Signal Processing Elseveir*, vol 90, no 9, September, pp. 2676-2685.

[23] Chang, L. and C. Yeh (1992) “Performance of DMI and eigenspace-based beamformers,” *IEEE Transactions on Antennas Propagation*, vol 40, no 11, November, pp. 1336-1347.

[24] Church, C. M. and I. J. Gupta (2009) “Calibration of GNSS Adaptive Antennas,” *in Proceedings of the 22nd International Meeting of the Satellite Division of The Institute of Navigation*, 22-25 September, Savannah, GA, pp. 344-350.

[25] Church, C., I. Gupta and A. O'Brien (2007) “Adaptive Antenna Induced Biases in GNSS Receivers,” *Proceedings of the 63rd Annual Meeting of The Institute of Navigation*, 23- 25 April, Cambridge, MA, pp. 204-212.

[26] Citron, T. K. and T. Kailath (1984) “An improved eigenvector beamformer,” *Acoustics, Speech, and Signal Processing, IEEE International Conference on ICASSP 84*, 19-21 March, San Diego CA, pp. 718-721.

[27] Closas, P., C., Fernandez-Prade, and J. A. Fernandez-Rubio(2006) “Bayesian DLL for Multipath Mitigation in Navigation Systems Using Particle Filters,” *In Proceeding of IEEE ICASSP 06*, 14-19 May, Toulouse, France, pp. 129-132.

[28] Closas, Pau, and Carles Fernández-Prades (2011) "A statistical multipath detector for antenna array based GNSS receivers," *Wireless Communications*, IEEE Transactions on vo10.3, 916-929.

[29] Cuntz, M., A. Konovaltsev, M. Sgammini, C. Hattich, G. Kappen, M. Meurer, A. Hornbostel, and A. Dreher, (2011) “Field Test: Jamming the DLR Adaptive Antenna Receiver,” *in Proceedings of the 24th International Technical Meeting of The Satellite Division of the Institute of Navigation (ION GNSS 2011)*, 20-23 September, Portland, OR, pp. 384-392.

[30] Daneshmand, Saeed.(2013) *GNSS Interference Mitigation Using Antenna Array Processing*, Doctoral Thesis, Department of Geomatics Engineering, Galgary University.

[31] Daneshmand, S., A. Broumandan and G. Lachapelle (2011a) “GNSS Interference and Multipath Suppression Using Array Antenna,” *in Proceedings of the 24th International Technical Meeting of the Satellite Division of the Institute of Navigation (ION GNSS 2011),* 20-23 September, Portland, OR, pp. 1183-1192.

[32] Daneshmand, S., A. Broumandan, J. Nielsen and G. Lachapelle (2013a) “Interference and multipath mitigation utilising a two-stage beamformer for global navigation satellite systems applications,” *IET Radar, Sonar and Navigation Journal*, vol 7, no 1, January, pp. 55-66.

[33] Daneshmand, S., A. Broumandan, N. Sokhandan and G. Lachapelle (2013b) “GNSS Multipath Mitigation with a Moving Antenna Array,” *Published in IEEE Transactions on Aerospace and Electronic Systems*, vol 49, no 1, January, pp. 693-698.

[34] Daneshmand, S., A. Jafarnia, A. Broumandan and G. Lachapelle (2011b) “A Low Complexity GNSS Spoofing Mitigation Technique Using a Double Antenna Array,” *GPS World*, vol 22, no 12, December, pp. 44-46.

[35] Daneshmand, S., A. Jafarnia, A. Broumandan and G. Lachapelle (2013c) “GNSS spoofing mitigation in multipath environments using space-time processing” *accepted to the European navigation conference (ENC) 2013*, 23-25 April, Vienna, Austria, 10 pages.

[36] Daneshmand, S., A. Jahromi, A. Broumandan and G. Lachapelle (2012) “A Low-Complexity GPS Anti-Spoofing Method Using a Multi-Antenna Array” *in Proceedings of the 25th International Technical Meeting of The Satellite Division of the Institute of Navigation (ION GNSS 2012)*, 17-21 September, Nashville TN, 11 pages.

[37] De Lorenzo, D. S. (2007), *Navigation accuracy and interference rejection for GPS adaptive antenna arrays*, Doctoral Thesis, Department of aeronautics and astronautics, Stanford University.

[38] De Lorenzo, D. S., F. Antreich, H. Denks, A. Hornbostel, C. Weber and P. Enge (2007) “Testing of Adaptive Beamsteering for Interference Rejection in GNSS Receivers,” *Proc. of ENC GNSS 2007*, 29 May-1 June Genf, Switzerland, 11 pages.

[39] De Lorenzo, D. S., J. Gautier, J. Rife, P. Enge and D. Akos (2005) “Adaptive Array Processing for GPS Interference Rejection,” *Proceedings of the 18th International Technical Meeting of the Satellite Division of The Institute of Navigation (ION GNSS 2005)*, 13-16 September 2005, Long Beach, CA, pp. 618-627.

[40] De Lorenzo, D. S., J. Rife, J., P. Enge, and D. M. Akos (2006) “Navigation Accuracy and Interference Rejection for an Adaptive GPS Antenna Array” *In Proceedings of the 19th International Technical Meeting of the Satellite Division*

of the Institute of Navigation (ION GNSS 2006), 26-29 September, Fort Worth, TX, pp. 763-773.

[41] De Lorenzo, D. S., S. C. Lo, P. K. Enge and J. Rife (2012) "Calibrating adaptive antenna arrays for high-integrity GPS," *GPS solution*, vol 16, no 2, April, pp. 221-230.

[42] Deergha Rao, K., and M. N. S. Swamy (2006) "New approach for suppression of FM jamming in GPS receivers" *IEEE Transactions on Aerospace and Electronic Systems*, vol 42, no 4, October, pp. 1464-1474.

[43] Ding, Z. (1997) "Matrix Outer-Product Decomposition Method for Blind Multiple Channel identification," *IEEE Transactions on Signal Processing*, vol 45, no 12, December, pp. 3053-3061.

[44] Ding, Z. and Y. Li (2000) *Blind equalization and identification*, Marcel Dekker, Inc., New York, Basel.

[45] Draganov, S., M. Harlacher, L. Haas, M. Wenske and C. Schneider (2011) "Synthetic aperture navigation in multipath environments," *IEEE Trans. Wireless Communications*, vol 18, no 2, April, pp. 52-58.

[46] Duvall, K. M. (1983) *Signal cancellation in adaptive antennas: The phenomenon and a remedy*, PhD Thesis, Department of electrical Engineering, Stanford University, USA.

[47] D.M. Akos, *A software radio approach to global navigation satellite system receiver design*, Ph. D. dissertation, Ohio University, 1997.

[48] Er, M. H. and A. Cantoni (1985) "An alternative formulation for an optimum beamformer with robustness capability," *In Communications, Radar and Signal Processing, IEE Proceedings*, vol 132, no 6, October, pp. 447-460.

[49] Evans, J. E., J. R. Johnson, and D. F. Sun (1982) *Application of advanced signal processing techniques to angle of arrival estimation in ATC navigation and surveillance systems*, Technical Report No. 582, M.I.T. Lincoln Laboratory, Lexington, Massachusetts, 386 pages.

[50] Falcone, K., N. B. Jarmale, F. Allen and J. Clark (2000) "GPS Anti-Jam for CAT II Landing Applications," *Proceedings of the 13th International Technical Meeting of the Satellite Division of The Institute of Navigation (ION GPS 2000)*, 19-22 September, Salt Lake City, UT, pp. 1301-1308.

[51] Falcone, K., N. B. Jarmale, F. Allen, and J. Clark (2000) "GPS Anti-Jam for CAT II Landing Applications," *In Proceedings of the 13th International Technical Meeting of the Satellite Division of The Institute of Navigation (ION GPS 2000)*, 19-22 September, Salt Lake City, UT, pp. 1301-1308.

[52] Fante, R. L., and J. J. Vaccaro (1998a) "Cancellation of jammers and jammer multipath in a GPS receiver", *IEEE Aerospace and Electronic Systems Magazine*, vol. 13, no. 13, November, pp. 25–28.

[53] Fante, R. L., and J. J. Vaccaro (1998b) “Cancellation of jammers and jammer multipath in a GPS receiver,” *Position Location and Navigation Symposium, IEEE 1998*, 20-23 April, Palm Springs, CA, pp. 622–625.

[54] Fante, R. L., and J. J. Vaccaro (2000) “Wideband Cancellation of Interference in a GPS Receive Array,” *IEEE Transactions on Aerospace and Electronic Systems*, vol 36, no 2, April, pp. 549–564.

[55] Fante, R. L., M. P. Fitzgibbons and K. F. McDonald (2004) “Effect of Adaptive Array Processing on GPS Signal Crosscorrelation,” *Proceedings of the 17th International Technical Meeting of the Satellite Division of The Institute of Navigation (ION GNSS 2004)*, 21-24 September, Long Beach, CA, , pp. 579-583.

[56] Farrell, Jay, and Matthew Barth (1999) *The global positioning system and inertial navigation*, New York, McGraw-Hill.

[57] Feldman, D. D. and L. J. Griffiths (1991) “A constraint projection approach for robust adaptive beamforming,” *Acoustics, Speech, and Signal Processing, IEEE International Conference on ICASSP 91*, 14-17 April, Toronto ON, pp.1381–1384.

[58] Feldman, D. D. and L. J. Griffiths (1994) “A projection approach for robust adaptive beamforming,” *IEEE Transactions on Signal Processing*, vol 42, no 4, April, pp. 867– 876.

[59] Fernández-Prades, Carles, Pau Closas, and Javier Arribas. (2011) "Eigenbeamforming for interference mitigation in GNSS receivers," *Localization and GNSS (ICL-GNSS) International Conference*, pp.138–148.

[60] Friedlander, B. (1988) "A signal subspace method for adaptive interference cancellation," *IEEE Transactions on Acoustic, Speech, Signal Processing*, vol 36, no 12, December, pp. 1835–1845.

[61] Frost, O. L. (1972) "An Algorithm For Linearly Constrained Adaptive Array Processing," *proceedings of the IEEE*, vol 60, no 8, August, pp. 926-935.

[62] Garin, L. and J. M. Rousseau (1997) "Enhanced strobe correlator multipath rejection for code & carrier," *in Proceedings of the 10th International Technical Meeting of the Satellite Division of the Institute of Navigation (ION GPS '97)*, 16-19 September, Kansas City MO, USA, pp. 559–568.

[63] Godara, L. C. (1990) "Beamforming in the presence of correlated arrivals using structured correlation matrix" *IEEE Transactions on Acoustic, Speech, Signal Processing*, vol 38, no 1, January, pp. 1-15.

[64] Grabowski, J. C. (2012) "Personal Privacy Jammers," *in GPS World Magazine*, April, vol.23, no. 4, pp. 28-37.

[65] Gupta, I. J. and T. D. Moore (2004) "Space-Frequency Adaptive Processing (SFAP) for Radio Frequency Interference Mitigation in Spread-Spectrum

Receivers," *IEEE Transactions on Antennas and Propagation*, vol 52, no 6, June, pp. 1611-1615.

[66] Gupta, I. J., J. R. Baxter, S. W. Ellingson, H. G. Park, H. S. Oh, and M. G. Kyeong (2003) "An experimental study of antenna array calibration," *in IEEE Transactions on Antennas and Propagation*, vol 51, no 3, March, pp. 664-667.

[67] Haber, F. and M. Zoltowski (1986) "Spatial spectrum estimation in a coherent signal environment using an array in motion," *Transactions on Antennas and Propagation*, vol 34, no 3, March, pp. 301–310.

[68] Haimovich, A. M. and Y. Bar-Ness (1988) "Adaptive antenna arrays using eigenvector methods," *In IEEE Antennas and Propagation Society International Symposium*, 6-10 June, Syracuse NY, pp. 980-983.

[69] Haimovich, A. M. and Y. Bar-Ness (1991) "An eigen analysis interference canceller," *IEEE Transactions on Acoustic, Speech, Signal Processing*, vol 39, no 1, January, pp. 76–84.

[70] Hartman, R. G. (1995) *Spoofing detection system for a satellite positioning system* US Patent 5557284, 13 pages.

[71] Hatke, G. F. (1998) "Adaptive array processing for wideband nulling in GPS systems," *in Proceedings of 32th Asilomar Conference Signals, Systems & Computers*, 1-4 November, Pacific Grove CA, pp. 1332–1336.

[72] Humphreys, T. E., B. M. Ledvina, M. L. Psiaki, B. W. O'Hanlon and P. M. Kintner (2008) “Assessing the Spoofing Threat: Development of a Portable GPS Civilian Spoofer,” *ION GNSS 21st. International Technical Meeting of the Satellite Division*, 16- 19 September, Savannah, GA, pp. 2314-2325.

[73] Hung, E. K. L. and R. M. Turner (1983) “A fast beamforming algorithm for large arrays,” *IEEE Transactions on Aerospace Electronic Systems*, vol 19, no 4, July, pp. 598-607.

[74] Hobiger, T., Gotoh, T., Amagai, J., Koyama, Y., & Kondo, T. (2010) “A GPU based real-time GPS software receiver,” *GPS solutions*, vol 14, pp. 207-216.

[75] Hwang S. S., and J. J. Shynk (2006) “Multicomponent receiver architectures for GPS interference suppression,” *IEEE Transactions on Aerospace and Electronic Systems*, vol 42, no 2, April, pp. 489-502.

[76] H. Kim, J. Kim, JH. Kim, H. Wang, and I. Lee(2010) “RF Band-Pass Sampling Frontend for Multiband Access CR/SDR Receiver,” *ETRI Journal*, vol.32, no.2, Apr. 2010, pp.214-221.

[77] Irsigler, M. and B. Eissfeller (2003) “Comparison of multipath mitigation techniques with consideration of future signal structures,” *in Proceedings of the 16th International Technical Meeting of the Satellite Division of the Institute of Navigation*, 9-12 September, Portland OR, USA pp. 2584–2592.

[78] Jafarnia-Jahromi, A., A. Broumandan, J. Nielsen and G. Lachapelle (2012) “GPS Vulnerability to Spoofing Threats and a Review of Antispoofing Techniques,” *in the International Journal of Navigation and Observation*, vol 2012, 16 pages.

[79] Jahn, A., H. Bischl and G. Heiss (1996) “Channel Characterisation for Spread Spectrum Satellite Communications, Spread Spectrum Techniques and Applications,” *in Spread Spectrum Techniques and Applications Proceedings IEEE 4th International Symposium*, 22-25 September, Mainz, pp. 1221-1226.

[80] Jang, J., M. Paonni, and B. Eissfeller (2012) “CW Interference Effects on Tracking Performance of GNSS Receivers,” *IEEE Transactions on Aerospace and Electronic Systems*, vol 48, no 1, January, pp. 243–258.

[81] James Bao-Yen Tsui (2005) *Fundamentals of Global Positioning System Receivers, A Software Approach* , John Wiley & Sons, pp.133-159.

[82] J. Thor and D.M. Akos (2002) “A direct RF sampling multifrequency GPS receiver,” *in Proc. IEEE Position Location and Navigation Symp*. Apr, pp. 44–51.

[83] Kalyanaraman, S. K., M. S. Braasch and J.M Kelly (2006), “Code tracking architecture influence on GPS carrier multipath,” *IEEE Transactions on Aerospace and Electronic Systems*, vol 42, no 2, April, pp. 548-561.

[84] Kaplan, E. D. and C. J. Hegarty (2006) *Understanding GPS Principles and applications 2nd edition*, Artech House, Boston, London.

[85] Kappen, G., C. Haettich and M. Meurer (2012) "Towards a robust multi-antenna mass market GNSS receiver," *in Position Location and Navigation Symposium (PLANS), IEEE/ION*, 23-26 April, Myrtle Beach, SC, pp. 291-300.

[86] Kelly, J. M., M. S. Braasch (1999) "Mitigation of GPS Multipath via Exploitation of Signal Dynamics," *Proceedings of the 55th Annual Meeting of The Institute of Navigation*, 27-30 June, Cambridge, MA, pp. 619-624.

[87] Kim, S. J. and R. A. Iltis (2004) "STAP for GPS receiver synchronization," *IEEE Transactions on Aerospace and Electronic Systems*, vol 40, no 1, January, pp. 132-144.

[88] Kirsteins, I. P. and D. W. Tufts (1985) "On the probability density of signal-to-noise ratio in an improved adaptive detector," *In Proceedings of the IEEE International Conference on Acoustics, Speech, and Signal Processing (IEEE ICASSP 1985)*, April, Tampa, Florida, pp. 572-575.

[89] Konovaltsev, A., D. S. De Lorenzo, A. Hornbostel and P. Enge (2008) "Mitigation of Continuous and Pulsed Radio Interference with GNSS Antenna Arrays," *Proceedings of the 21st International Technical Meeting of the Satellite Division of The Institute of Navigation (ION GNSS 2008)*, 16-19 September, Savannah, GA, pp. 2786-2795.

[90] Korniyenko, Oleksiy V., and Mohammad S. Sharawi (2007) "GPS software receiver implementations," *Potentials*, vol 26, pp. 42-46.

[91] Krim, H. and M. Viberg (1996) “Two Decades of Array Signal Processing Research,” *IEEE Signal Processing Magazine*, vol 13, no 4, July, pp. 67-94.

[92] Ledvina, B. M., W. J. Bencze, B. Galusha and I. Miller (2010) “An In-Line Anti-Spoofing Device for Legacy Civil GPS Receivers,” *Institute of Navigation ITM*, January, San Deigo, CA, pp. 698-712.

[93] Lee, H. K. (2002) Time-propagated measurement fusion and its application to GPS multipath detection and isolation, Department of Electrical and Computer Engineering, Seoul National University

[94] Liberti, Joseph C., and Theodore S. Rappaport (1999) *Smart antennas for wireless communications: IS-95 and third generation CDMA applications*, Prentice Hall PTR.

[95] Lu, D., Q. Feng and R. B. Wu (2006) “Survey on Interference Mitigation via Adaptive Array Processing in GPS,” *in Electromagnetics Research Symposium 2006*, 26-29 March, Cambridge, USA, pp.722-727.

[96] Madhani, P., H., P. Axelrad, K. Krumvieda and J. Thomas (2003) “Application of successive interference cancellation to the GPS pseudolite near-far problem,” *IEEE Transactions on Aerospace and Electronic Systems*, vol 39, no 2, April, pp. 481-488.

[97] McDonald, K. F., P. J. Costa and R. L. Fante (2006) “Insights into Jammer Mitigation Via Space-Time Adaptive Processing,” *Proceedings of IEEE/ION PLANS 2006*, 25-27 April, San Diego, CA, pp. 213-217.

[98] McDonald, K. F., R. Raghavan, and R. Fante (2004) “Lessons Learned Through the Implementation of Space-Time Adaptive Processing Algorithms for GPS Reception in Jammed Environments,” *IEEE PLANS Conference Proceedings*, 26-29 April, pp. 418-428.

[99] McDowell, C. E. (2007) GPS *Spoofer and Repeater Mitigation System using Digital Spatial Nulling*, US Patent 7250903 B1, 7 pages.

[100] McGraw, G. A. and M. S. Braasch (1999) “GNSS multipath mitigation using gated and high resolution correlator concepts,” *in Proceedings of The National Technical Meeting of the Satellite Division of the Institute of Navigation*, 25-27 January, San Diego CA, USA, pp. 333-342.

[101] McGraw, G. A., C. McDowell, J. M. Kelly (2006) “GPS Anti-Jam Antenna System Measurement Error Characterization and Compensation,” *In Proceedings of the 19th International Technical Meeting of the Satellite Division of the Institute of Navigation (ION GNSS 2006)*, 26-29 September, Fort Worth, TX, pp. 705-714.

[102] McGraw, G.A., S. Y. Ryan Young, and K. Reichenauer (2004) “Evaluation of GPS Anti-Jam System Effects on Pseudorange and Carrier Phase Measurements

for Precision Approach and Landing," *In Proceedings of the 17th International Technical Meeting of the Satellite Division of the Institute of Navigation (ION GNSS 2004)*, 21-24 September, Long Beach, CA, pp. 2742-2751.

[103] Melvin, W. L. (2004) "A STAP Overview," *IEEE Aerospace and Electronic Systems Magazine*, vol 19, no 1, January, pp. 19-35.

[104] Moelker, D. J. (1997) "Multiple antennas for advanced GNSS multipath mitigation and multipath direction finding," in Proceedings of ION GPS 1997, 16-19 September, Kansas City MO, pp. 541-550.

[105] Moelker, D. J., E. van der Pol and Y. Bar-Ness (1996) "Adaptive antenna arrays for interference cancellation in GPS and GLONASS receivers," *In IEEE Position Location and Navigation Symposium*, 22-26 April, Atlanta, GA, pp. 191-198.

[106] Montgomery, P. Y., T. E. Humphreys and B. M. Ledvina (2009) "Receiver-Autonomous Spoofing Detection: Experimental Results of a Multi-antenna Receiver Defense against a Portable Civil GPS Spoofer" *ION 2009 International Technical Meeting*, 26-28 January, Anaheim, CA, pp. 124-130.

[107] Motella, B., S. Savasta, D. Margaria, and F. Dovis (2011) "Method for Assessing the Interference Impact on GNSS Receivers", *IEEE Transactions on Aerospace and Electronic Systems*, vol. 47, no 2, April, pp. 1416–1432.

[108] Myrick, W. L., J. S. Goldstein, and M. D. Zoltowski (2001)"Low Complexity Anti-jam Space-Time Processing for GPS," " *In Proceedings of the IEEE International Conference on Acoustics, Speech, and Signal Processing*, 7-11 May, Salt Lake City, UT, pp. 2233-2236.

[109] Myrick, W. L., M. Zoltowski, and J. S. Goldstein (2000) "Exploiting conjugate symmetry in power minimization based pre-processing for GPS: reduced complexity and smoothness," *in Acoustics, Speech, and Signal Processing, IEEE International Conference on ICASSP 2000*, 5-9 June, Istanbul, Turkey, pp. 2833-2836.

[110] Ng, B. C. and C. M. S. See (1996) "Sensor-array calibration using a maximum-likelihood approach," *in IEEE Transactions on Antennas and Propagation*, vol 44, no 6, June, pp. 827-835.

[111] Nielsen, J., A. Broumandan and G. Lachapelle (2011) "GNSS Spoofing Detection for Single Antenna Handheld Receivers" *Journal of Navigation*, vol 58, no 4, Winter, pp. 335-344.

[112] Nielsen, J., A. Broumandan and G. Lachapelle, (2010) "Spoofing Detection and Mitigation with a Moving Handheld Receiver," *in GPS World magazine*, vol 21, no 9, September, pp. 27-33.

[113] Nik, S. A., & Petovello, M. G. (2010) “Implementation of a Dual-Frequency GLONASS and GPS L1 C/A Software Receiver,” *Journal of Navigation*, vol 63), pp. 269-287.

[114] Obst, Marcus, Sven Bauer, and Gerd Wanielik(2012) "Urban multipath detection and mitigation with dynamic 3D maps for reliable land vehicle localization," *Position Location and Navigation Symposium (PLANS)*, 2012.

[115] O’Brien, A. J. and I. J. Gupta (2011) “Mitigation of adaptive antenna induced bias errors in GNSS receivers,” *IEEE Transactions on Aerospace and Electronic Systems*, vol 47, no 1, January,pp. 524-538.

[116] Paulraj, A. J. and C. B. Papadias (1997) “Space-time processing for wireless communications,” *IEEE Signal Processing Magazine*, vol 49, no 6, November, pp. 49-83.

[117] Petovello M., C. O’Driscoll, G. Lachapelle, D. Borio, and H. Murtaza (2008) “Architecture and Benefits of an Advanced GNSS Software Receiver,” *Journal of Global Positioning Systems*, vol 7, no 2, December, pp. 156–168.

[118] Pickholtz, R. L., D. L. Schilling, and L. B. Milstein (1982) “Theory of spread-spectrum communications-a tutorial,” *IEEE Transaction on Communication*, vol. 30, no. 5, May, pp. 855-884.

[119] Pillai, S. U. and B. H. Kwon (1989) “Forward/backward spatial smoothing techniques for coherent signal identification,” *IEEE Transactions on Acoustic, Speech, Signal Processing*, vol 37, no 1, January, pp. 8-15.

[120] Poisel, R. (2004) *Modern communications jamming principles and techniques*, 1st ed.,Artech House, Boston, Massachusetts.

[121] Petovello, M. G., O’Driscoll, C., Lachapelle, G., Borio, D., & Murtaza, H. (2008). “Architecture and benefits of an advanced GNSS software receiver,” *Journal of Global Positioning Systems*, vol 7, pp. 156-168.

[122] Raghunath, K. J., and V. U. Reddy (1992) “Finite data performance analysis of MVDR beamformer with and without spatial smoothing,” *IEEE Transactions on Signal Processing*, vol 40, no 11, November, pp. 2726-2736.

[123] Ramos, J. and M. Zoltowski and M. Urgos (1996) “Robust blind adaptive array, a prototype for GPS,” IEEE International Symposium on Phased Array Systems and Technology, 15-18 October, Boston, MA, pp. 406-410.

[124] Ray, Jayanta Kumar, (2000) *Mitigation of GPS code and carrier phase multipath effects using a multi-antenna system*, University of Calgary.

[125] Rensburg, C. V., and B. Friedlander (2004) “The Performance of a Null-Steering Beamforming in Correlated Rayleigh Fading,” *IEEE Transaction on Signal Processing*, vol. 52, no. 11, November, pp. 3117-3125.

[126] Sahmoudi, M. and M. G. Amin (2007) “Optimal Robust Beamforming for Interference and Multipath Mitigation in GNSS Arrays,” *in Acoustics, Speech, and Signal Processing, IEEE International Conference on ICASSP 2007*, 15-20 April, Honolulu HI , pp. 693-696.

[127] Sahmoudi, M., and M. G. Amin (2008) “Fast Iterative Maximum-Likelihood Algorithm (FIMLA) for Multipath Mitigation in the Next Generation of GNSS Receivers,” *IEEE Transaction on Wireless Communication*, vol 7, no 1, November, pp. 4362-4373.

[128] Seco-Granados G., J. A. Fernández-Rubio, and C. Fernández-Prades (2005) “ML estimator and hybrid beamformer for multipath and interference mitigation in GNSS receivers,” *IEEE Transactions on Signal Processing*, vol 53, no 10, March, pp. 1194-1208.

[129] Shan, T. J. and T. Kailath (1985) “adaptive beamforming for coherent signals and interference,” *IEEE Transactions on Acoustic, Speech, Signal Processing*, vol 33, no 3, June, pp. 527–534.

[130] Shin, J. H., Jun, H. E. O., & KIM, S. Y. (2008) “Interference Cancellation and Multipath Mitigation Algorithm for GPS Using Subspace Projection Algorithms,” *IEICE Transactions on Fundamentals of Electronics, Communications and Computer Sciences*, vol. 3, pp. 905-908.

[131] Slock, D. (1994) “Blind fractionally-spaced equalization, perfect reconstruction filter banks and multichannel linear prediction,” *In Proceedings of the IEEE International Conference on Acoustics, Speech, and Signal Processing (IEEE ICASSP 1994)*, 19-22 April, pp. 585-588.

[132] Steingass, A. and A. Lehner (2004) “Measuring the Navigation Multipath Channel A Statistical Analysis,” in Proceedings of the 17th International Technical Meeting of the Satellite Division of The Institute of Navigation (ION GNSS 2004), Long Beach, CA, 21- 24 September 2004, pp. 1157-1164.

[133] Strang, Gilbert, and Kai Borre (1997) *Linear algebra, geodesy, and GPS*, Siam.

[134] Sun, W. and M. G. Amin (2005a) “A self-coherence anti-jamming GPS receiver,” *IEEE Transactions on Signal Processing*, vol 53, no 10, October, pp. 3910–3915.

[135] Sun, W. and M. G. Amin (2005b) “Maximum signal-to-noise ratio GPS anti-jam receiver with subspace tracking,” *Acoustics, Speech, and Signal Processing, IEEE International Conference on ICASSP 2005*, 18-23 March, Philadelphia, PA, USA, pp. 1085–1088.

[136] Tong, L. and Q. Zhao (1998) “Blind channel estimation by least squares smoothing,” *In Proceedings of the IEEE International Conference on Acoustics, Speech, and Signal Processing (IEEE ICASSP 1998)*, 12-15 May, Seattle, WA, pp. 2121-2124.

[137] Townsend, B. R. and P. Fenton (1994) “A Practical approach to the reduction of pseudorange multipath errors in a L1 GPS receiver,” *in Proceedings of the 7th International Technical Meeting of the Satellite Division of the Institute of Navigation (ION-GPS ’94)*, 20-23 September, Salt Lake City, Utah, USA, pp. 143–148.

[138] Townsend, B., D. J. R. Van Nee, P. C. Fenton, and K. J. Van Dierendonck (1995) “Performance evaluation of the multipath estimating delay lock loop,” *Navigation Journal of the Institute of Navigation*, vol 42, no 3, Fall, pp. 503-514.

[139] Tsai, C. J., J. F. Yang, and T. H. Shiu (1995) “Performance analyses of beamformers using effective SINR on array parameters,” *IEEE Transactions on Signal Processing*, vol 43, no 1, January, pp. 300-303.

[140] Tsatsanis, M. K. and Z. Xu (1999) “Constrained Optimization Methods for Direct Blind Equalization,” *IEEE Journal on selected areas in communications*, vol 17, no 3, March, pp. 424-433.

[141] Van Dierendonck, A. J., P. J. Fenton, and T. Ford (1992) “Theory and performance of narrow correlator spacing in a GPS receiver,” *Journal of the Institute of Navigation*, vol 39, no 3, Fall,pp. 265–283.

[142] Van Nee, D. J. V. (1992) “The Multipath Estimating Delay Lock Loop,” *in Proceedings of the IEEE 2nd International Symposium on Spread Spectrum*

Techniques and Applications, November 29- December 2, Yokohama, Japan, pp. 39-42.

[143] Van Trees, H. L. (1966) "Optimum Processing for passive sonar arrays," *in Processing of IEEE Ocean Electronics symposium*, August 29-31, Honolulu, Hawaii, pp. 41-65.

[144] Van Trees, H. L. (2002) *Optimum Array Processing, Detection, Estimation, and Modulation Theory Part IV*, John Wiley & Sons, New York, pp. 428-699.

[145] Van Veen, B. D. and K. M. Buckley (1988) "Beamforming: a versatile approach to spatial filtering," *IEEE ASSP Magazine*, vol 5, no 2, April, pp.4-24.

[146] Wen, H., P. Y. Huang, J. Dyer, A. Archinal and J. Fagan (2005) "Countermeasures for GPS Signal Spoofing," *ION GNSS 18th International Technical Meeting of the Satellite Division*, 13-16 September, Long Beach, CA, pp. 1285-1290.

[147] Wei, Z., Ke, Z., Bin, W., & Heejong, S. (2010) "Simulation and analysis of GPS software receiver," *In Computer Modeling and Simulation, 2010. ICCMS'10. Second International Conference*, January, vol. 2, pp. 314-317.

[148] Widrow, B., K. M. Duvall, R. P. Gooch, and W. C. Newman (1982) "Signal cancellation phenomena in adaptive antennas: Causes and cures," *IEEE Transactions on Antennas and Propagation*, vol 30, no 4, May, pp. 469-478.

[149] Won, Jong-Hoon, Thomas Pany, and GüNTeR W. HeiN (2006) "GNSS software defined radio," *Inside GNSS* ,vo5,pp. 48-56.

[150] Yang, J. H. (2013) *GNSS Interference Simulator Design for RFI Impact Assessment and Detection Algorithm Development*, Department of Aerospance Engineering, Seoul National University

[151] Youn, W. S. and C. K. Un (1994) “Robust adaptive beamforming based on the eigen structure method,” *IEEE Transactions on Signal Processing*, vol 42, no 6, June, pp. 1543-1547.

[152] Yu, J. L. and C. C. Yeh (1995) “Generalized eigenspace-based beamformers,” *IEEE Transactions on Signal Processing*, vol 43, no 11, November, pp. 2453-2461.

[153] Zoltowski, M. D. (1988) “On the performance analysis of the MVDR beamformer in the presence of correlated interference,” *IEEE Transactions on Acoustic, Speech, Signal Processing*, vol 36, no 6, June, pp. 945-947.

[154] Zoltowski, M. D., and Gecan, A. S (1995) “Advanced adaptive null steering concepts for GPS,” *Military Communications Conference, MILCOM 95, IEEE*, 5-8 November, San Diego, CA, USA, pp. 1214-1218.

Appendix

A. Lagrangian Method

The method of Lagrange multipliers is employed to solve the following linear constraint optimization problem (Van Trees 2002, Frost 1972)

$$\underset{\mathbf{w}}{Min}\, \mathbf{w}^H \mathbf{R}\mathbf{w}, \qquad \mathbf{C}^H \mathbf{w} = \mathbf{f} \tag{A.1}$$

where $\mathbf{R}$ is an $N \times N$ positive definite matrix. $\mathbf{w}$ is a desired gain vector. $\mathbf{C}$ is an $N \times M$ constraint full column rank matrix ($N > M$) and $\mathbf{f}$ is an $M \times 1$ vector. In this minimization, the Lagrangian is formed as (Van Trees 2002)

$$L\left(\underset{M\times 1}{\mathbf{w}, \boldsymbol{\lambda}_L}\right) = \mathbf{w}^H \mathbf{R}\mathbf{w} + \boldsymbol{\lambda}_L^H \left(\mathbf{C}^H \mathbf{w} - \mathbf{f}\right) + \left(\mathbf{w}^H \mathbf{C} - \mathbf{f}^H\right)\boldsymbol{\lambda}_L \tag{A.2}$$

where $\boldsymbol{\lambda}_L$ is the Lagrange multiplier vector. Taking the complex gradient of $L(\mathbf{w}, \boldsymbol{\lambda}_L)$ with respect to $\mathbf{w}$ and setting the result equal to zero results in

$$\mathbf{w}^H \mathbf{R} + \boldsymbol{\lambda}^H \mathbf{C}^H = \underset{1\times N}{\mathbf{0}} \tag{A.3}$$

which is a least-squares problem. The solution is obtained as

$$\mathbf{w}^H = -\boldsymbol{\lambda}_L^H \mathbf{C}^H \mathbf{R}^{-1} \tag{A.4}$$

By substituting $\mathbf{w}$ in constraint in (A.1), the Lagrange multiplier is obtained as

$$\boldsymbol{\lambda}_L^H = -\mathbf{f}^H \left(\mathbf{C}^H \mathbf{R}^{-1} \mathbf{C} \right)^{-1} \tag{A.5}$$

Hence the optimal gain vector is obtained as

$$\mathbf{w} = \mathbf{R}^{-1} \mathbf{C} \left(\mathbf{C}^H \mathbf{R}^{-1} \mathbf{C} \right)^{-1} \mathbf{f} \tag{A.6}$$

국문초록

여러 응용분야에서 수 억대의 GPS(Global Positioning System) 수신기가 사용되고 있지만, GPS을 기반으로 하는 위치기반 서비스(LBS: Location Based Services)에서는 여전히 다중경로 오차와 같은 전파 방해가 발생하고 있으며, 이러한 오차들로 인하여 상관함수의 왜곡은 거리 오차가 발생에 영향을 미치고 있다. 이러한 이유로 인하여 GPS을 이용한 항법 시스템에서의 위치 정확도 향상을 위하여, 다중경로 오차를 효과 적으로 줄이기 위한 강인하고 현실적인 방법이 요구된다.

다중경로는 GPS 신호가 장애물에 의해 반사나 회절 되어 수신기에 도착할 때 잘 일어난다. 가시경로 신호에 결합된 다중경로 신호는 GPS 수신기의 상관함수의 변형을 일으키며 궁극적으로 차별함수에 영향을 미치므로 거리오차를 발생시킨다. 그러므로 다중경로 오차는 위성항법 시스템에서의 위치정확도 향상을 위해 해결 되어야 될 문제로 쟁점이 되어왔다.

최근에는 이러한 전파 간섭신호를 줄이기 위하여 다중개의 안테나(Multiple Antenna)를 이용하는 방법이 GPS 항법 시스템에서 이용되고 있다. 현 시점에서, 다중개의 안테나를 사용하는 응용분야는 주로 학술적인 연구 및 복잡한 군사용 연구로 주로 진행 되었다. 그러나 안테나 제작 방법 및 전기적 시스템의 급격한 발전으로 인해 이전의 하드웨어 및 소프웨어적인 문제를 쉽게 해결 됨에 따라 가까운 미래에는 다중 안테나 기반의 수신기가

민간 상용분야로 확대 될 것으로 예상이 된다. 또한 안테나 수신기 RF단의 소형화로 인하여 다중 안테나 시스템에서의 안테나 크기 문제점 또한 해결 가능하다.

그러므로 본 논문에서는 다중 GPS 안테나를 이용하여 GPS 항법에서의 전파 간섭 및 다중경로 오차 감쇄에 대한 연구를 목적으로 한다. 본 연구는 강한 전파 간섭 및 다중경로 신호에 대하여 공간 처리 기법을 적용한다. 제안된 새로운 방법은 다중 안테나를 기반의 코드 케리어 정보를 이용한 공간 처리 기법으로 전파 간섭 및 다중경로 오차를 완화시키며, 또한 빔형성 기법을 이용하여 신호 대 잡음 비율을 최대로 한다. 제안된 성능을 검증하기 위하여 소프트웨어 GPS 수신기를 사용된다. 소프트웨어 GPS 수신기를 이용한 신호처리 기법은 새로운 장비의 제품화 및 GPS 신호 분석에 장점을 가지고 있다. 또한 GPS 알고리즘 분석 및 수신기 성능 향상 검증 등 여러 연구분야에서 널리 이용되고 있다.

본 논문에서는 제안된 방법의 성능 검증을 위하여 컴퓨터 시뮬레이션 및 가공 IF 데이터를 이용한 소프트웨어 수신기 결과를 제시한다. 그 결과 제안된 방법은 전파 간섭 및 다중경로 오차 감쇄에 강인하며, GPS 항법시스템에서의 위치정확도 향상에 가능성을 보여준다. 그로므로 제안된 방법은 차량 항법 응용분야에서 방해신호 감쇄에 사용될 것으로 예상된다.

주요어: 위성항법시스템, 다중경로, 전파 간섭, 다중수신기, 코드 케리어 정보, 소프트웨어 수신기

이 름: 김 진 익

학 번: 2008-30220